Fisheries and Oceans Science | Pêches et Océans Sciences

CSAS

Canadian Science Advisory Secretariat

Research Document 2001/138

Not to be cited without permission of the authors *

SCCS

Secrétariat canadien de consultation scientifique

Document de recherche 2001/138

Ne pas citer sans autorisation des auteurs *

Pacific Ocean Perch Assessment for the West Coast of Canada in 2001

J. T. Schnute, R. Haigh, B. A. Krishka, and P. Starr[1]

Fisheries and Oceans Canada
Science Branch, Pacific Region
Pacific Biological Station
Nanaimo, B.C. V9R 5K6

[1] Canadian Groundfish Research and Conservation Society
1406 Rose Ann Drive
Nanaimo, B.C. V9T 4K8

* This series documents the scientific basis for the evaluation of fisheries resources in Canada. As such, it addresses the issues of the day in the time frames required and the documents it contains are not intended as definitive statements on the subjects addressed but rather as progress reports on ongoing investigations.

Research documents are produced in the official language in which they are provided to the Secretariat.

This document is available on the Internet at:

* La présente série documente les bases scientifiques des évaluations des ressources halieutiques du Canada. Elle traite des problèmes courants selon les échéanciers dictés. Les documents qu'elle contient ne doivent pas être considérés comme des énoncés définitifs sur les sujets traités, mais plutôt comme des rapports d'étape sur les études en cours.

Les documents de recherche sont publiés dans la langue officielle utilisée dans le manuscrit envoyé au Secrétariat.

Ce document est disponible sur l'Internet à:

http://www.dfo-mpo.gc.ca/csas/

ISSN 1480-4883
Ottawa, 2001

Canada

Abstract

Pacific ocean perch (*Sebastes alutus*, commonly called POP) dominate the rockfish catch in Canada's Pacific groundfish trawl fishery. The species belongs to a larger community of slope rockfish species that inhabit the sloping walls of marine canyons along the coast of British Columbia. This report compiles the scientific data currently available for POP and evaluates its relevance to setting quotas. Following the rationale in the 1997 assessment, we present an updated catch-age analysis for the Goose Island Gully (GIG) stock and extend these results to the rest of the coast. Our analyses take account of spatial distributions and other biological features investigated in slope rockfish stock assessments since 1998.

Our catch-age analysis indicates that the GIG stock currently experiences low recruitment at age 7, probably associated with an ocean climate regime starting in 1988. We urge caution in setting quotas, so that adequate biomass remains for the future when productivity improves. Our coastwide analysis suggests that the current quota distributions among management areas match available biomass levels fairly well, although we find possible opportunities for quota redistribution.

Our models contain many debatable elements, but we are constrained by available data. We have relatively few research surveys, and most data come from the fishery itself. We use graphics and intuitive discussion to engage stakeholders in thinking actively about the current state of our knowledge. Final decisions depend on human judgement, given the facts available. We suggest various options for setting quotas, including maintenance of the status quo.

We also highlight opportunities for future data collection, standardization, and quality control. In particular, we recommend fishery-independent surveys to obtain age distributions that include young fish aged 3–5. Data from such surveys would provide leading indicators of recruitment to the fishery at age 7.

Résumé

Le sébaste à longue mâchoire (*Sebastes alutus*) domine les prises de sébastes dans la pêche canadienne du poisson de fond du Pacifique. Cette espèce fait partie de la grande communauté des sébastes qui habitent les parois inclinées des canyons marins situés le long de la côte de la Colombie-Britannique. Ce rapport rassemble les données scientifiques actuellement disponibles sur le sébaste à longue mâchoire et évalue leur pertinence pour l'établissement de quotas. Suivant la logique de l'évaluation de 1997, nous présentons une analyse à jour des prises selon l'âge pour le stock du goulet de l'île Goose (GIG) et étendons ces résultats au reste de la côte. Nos analyses tiennent compte des répartitions spatiales et d'autres caractéristiques biologiques étudiées depuis 1998 dans le cadre des évaluations des stocks de sébastes de la pente continentale.

Notre analyse des prises selon l'âge indique que le stock du GIG présente actuellement un faible recrutement des poissons de 7 ans, sans doute associé à un régime de climat océanique en place depuis 1988. Nous recommandons fortement d'user de prudence dans l'établissement des quotas, afin de garder suffisamment de biomasse en vue d'une amélioration future de la productivité. Notre analyse portant sur toute la côte porte à croire que la répartition des quotas entre les secteurs de gestion correspond assez bien à la répartition de la biomasse, bien que nous ayons relevé des possibilités de redistribution de quotas.

Nos modèles comportent de nombreux éléments discutables, mais les données disponibles restreignent notre marge de manœuvre. Assez peu de relevés de recherche ont été effectués, et la plupart des données proviennent de la pêche elle-même. À l'aide de documents graphiques et de discussions intuitives, nous encourageons les intervenants à réfléchir sur nos connaissances actuelles. Étant donné les faits connus, les décisions finales reposent sur le jugement humain. Nous suggérons diverses options de quotas, y compris le statu quo.

En outre, nous présentons des possibilités de collecte de données ainsi que de normalisation et de contrôle de la qualité des données. En particulier, nous recommandons d'effectuer des relevés indépendants de la pêche pour déterminer les répartitions par âge comprenant les jeunes poissons âgés de 3 à 5 ans. Les données de tels relevés fourniraient des indicateurs avancés du recrutement à la pêche des poissons de 7 ans.

Table of Contents

1. Introduction....1
2. Data sources....2
3. Spatial distribution of stocks and fisheries....3
4. Catch-age analysis in Goose Island Gully....6
5. Swept area biomass estimates....9
6. Model-based CPUE analysis....11
7. Coastwide extensions....12
8. Discussion, summary, and recommendations....13
Acknowledgements....15
References....16
Appendix A. Survey cruise summary....18
Cruise report references for Appendix A....20
Appendix B. Model for catch-age data....23

List of Tables

Table 1.1. Commercial trawl catches and quotas for POP stocks....30
Table 2.1. Survey cruises for POP abundance and biological data collection....31
Table 2.2. Other GFBio surveys capturing POP using bottom trawls....32
Table 2.3. GFBio catch and sample summary for non-POP surveys using other gear....33
Table 3.1. Major areas with corresponding PMFC names and minor subareas....33
Table 3.2. Locality codes within each minor area....34
Table 3.3. Definitions of historical areas for slope rockfish assessment and management....35
Table 3.4. Historical POP gully definitions....35
Table 4.1. Parameter estimates from the catch-age model for Goose Island Gully....36
Table 6.1. Summary table for GLM analyses....37
Table 7.1. Relationships among SRF areas and newly defined POP areas....38
Table 7.2. Coastwide quota allocations....39

List of Figures

Fig. 1.1. Catch history of POP in SRF areas by DFO fishing year (1954-2000)....40
Fig. 2.1. Catch history of POP in SRF area 5AB by DFO fishing year (1954-2000)....41
Fig. 2.2. Number of survey and commercial POP samples and specimens in GFBio....42
Fig. 2.3. Number of commercial specimens in GFBio with length, sex, and age data....43
Fig. 2.4. Bubble plots of proportion-at-age for POP in SRF areas by calendar year....44
Fig. 3.1. INPFC and PMFC catch reporting areas....45
Fig. 3.2. Polygons outlining major areas, minor areas, and fishing localities....46
Fig. 3.3. Slope rockfish assessment polygons and newly-defined POP polygons....47

Fig. 3.4. Historical SRF gully polygons with total catch from Jan 1994 to Mar 2001 48
Fig. 3.5. Newly-defined POP polygons with bottom bathymetry 49
Fig. 3.6. Newly-defined POP polygons with mean CPUE 50
Fig. 3.7. Newly-defined POP polygons with total catch 51
Fig. 3.8. Survey designed to estimate POP abundance along northwest QCI 52
Fig. 3.9. Survey designed to estimate POP abundance along central B.C. 53
Fig. 3.10. Survey designed to estimate POP abundance along WCVI 54
Fig. 4.1. Analysis of length, weight, and age 55
Fig. 4.2. Maturity vs. age 56
Fig. 4.3. Selectivity, maturity, and weight 57
Fig. 4.4. Annual biomass estimates 58
Fig. 4.5. Observed and predicted age data 59
Fig. 4.6. Recruitment and productivity 60
Fig. 4.7. Fishing mortality vs. biomass 61
Fig. 4.8. Forward simulation with $r = 0.10$ 62
Fig. 4.9. Forward simulation with $r = 0.12$ 63
Fig. 4.10. Risk plot for catch in relation to productivity 64
Fig. 5.1. Distribution of CPUE in GIG 65
Fig. 5.2. Annual biomass estimates and catches in GIG 66
Fig. 5.3. Comparisons of annual biomass estimates and catches in the three gullies 67
Fig. 5.4. Annual biomass estimates and catches in POP-QCI 68
Fig. 5.5. Annual biomass estimates and catches in POP-MR 69
Fig. 5.6. Annual biomass estimates and catches in combined POP-GS + POP-MI 70
Fig. 5.7. Annual biomass estimates and catches in combined POP-NVI + POP-SVI 71
Fig. 5.8. Comparisons of annual biomass estimates and catches in four POP areas 72
Fig. 5.9. Comparisons of annual biomass estimates and catches in six SRF areas and GIG 73
Fig. 5.10. Biomass estimates for POP in U.S. PMFC areas 74
Fig. 6.1. Box plots showing CPUE and related variables for POP-QCI 75
Fig. 6.2. GLM coefficients for POP-QCI 76
Fig. 6.3. Box plots showing CPUE and related variables for POP-MR 77
Fig. 6.4. GLM coefficients for POP-MR 78
Fig. 6.5. Box plots showing CPUE and related variables for combined POP-GS + POP-MI 79
Fig. 6.6. GLM coefficients for combined POP-GS + POP-MI 80
Fig. 6.7. Box plots showing CPUE and related variables for combined POP-SVI + POP-NVI 81
Fig. 6.8. GLM coefficients for combined POP-SVI + POP-NVI 82
Fig. 6.9. Box plots showing CPUE and related variables for historical GIG 83
Fig. 6.10. GLM coefficients for historical GIG 85
Fig. 6.11. Box plots showing CPUE and related variables for coastal B.C. 85
Fig. 6.12. GLM coefficients for coastal B.C. 86
Fig. 7.1. Pairs plot comparing various biomass indices in POP-QCI 87
Fig. 7.2. Pairs plot comparing various biomass indices in POP-MR 88
Fig. 7.3. Pairs plot comparing various biomass indices in POP-GSMI 89
Fig. 7.4. Pairs plot comparing various biomass indices in POP-WCVI 90

1. Introduction

Pacific ocean perch (*Sebastes alutus*) dominate the rockfish catch in Canada's Pacific groundfish trawl fishery. This long-lived species, commonly called POP, inhabits the sloping walls of marine canyons along the coast of British Columbia. It belongs to a larger community of other slope rockfish species. A web site in Prince Rupert:

http://www.princerupert.com/economy/ground_sebastes_alutus.htm

highlights the economic and cultural importance of POP. This report compiles the scientific data currently available for the species and evaluates its relevance to setting quotas.

Recent stock assessments describe the difficulties and opportunities for a rational assessment of POP stocks. Catch-age analyses for a stock in Goose Island Gully (Richards and Olsen 1996, Richards et al. 1997b) were extended coastwide to produce yield recommendations in the six slope rockfish management areas (SRF areas). Limited data on relative abundance constrained these analyses, and subsequent assessments investigated new information available in a database on individual commercial tows from 1996 to the present. Schnute et al. (1998, 1999) produced detailed spatial analyses of stocks and fisheries by latitude, longitude, depth, and time. Schnute and Haigh (2000) carried this analysis one step further by examining biomass estimates obtained from commercial fishery tow data. Although they emphasized limitations to their methods, no alternative information source is available. Few fishery-independent surveys have been conducted for this species.

This report follows the logic of the last assessment for quota purposes (Richards et al. 1997b). We present an updated catch-age analysis for the Goose Island Gully stock and extend the results to the rest of the coast. Our analyses, however, take account of spatial effects and other details described by Schnute et al. (1998, 1999) and Schnute and Haigh (2000). We also describe the current status of available data and make recommendations for future data collection and compilation.

Table 1.1 and Figure 1.1 present historical catch data and regulatory quotas for SRF areas 3C, 3D, 5AB, 5CD, 5ES, and 5EN. In some years, quotas were set for combined areas. To obtain a consistent format, we have post-allocated each combined quota in proportion to catches from areas in the combination. The red marks and green bars in Fig. 1.1 represent a long history of regulation and removal for POP. To some readers, the dominant question is: "What are the quotas for the 2002 fishing year? That is, where should the six red marks for 2002 be placed on the graphs?" The answer to this question involves an assessment of risk and reward. This report outlines rationales for setting quotas, with an emphasis on data limitations and risks to the fish stocks. A final decision depends on human judgement, given the facts available.

Our assessment necessarily includes a great amount of technical detail. We use extensive graphics and tabular formats to render this information comprehensible. Colour images greatly improve the impact of our work. For the first time in our stock assessments, we drop the requirement that all graphics must be adequately represented in black and white print. If a colour printout is not available, readers can obtain this report as an Acrobat PDF file and view this in conjunction with a conventional printed copy.

2. Data sources

We obtain fishery data primarily from two databases maintained by the Groundfish Section at the Pacific Biological Station. The 'GFCatch' database (Rutherford 1999) archives catch records from the historical fishery (1954-1995) on a spatial scale defined by 'localities', which we discuss further in Section 3 below. Fishermen logbook records further identify the longitude-latitude coordinates for most tows in 1994-1995. A second database 'PacHarvTrawl' contains detailed records (1996-present) on individual tows, including:

- the weight of each species captured, both kept and discarded,
- longitude-latitude coordinates,
- tow duration and depth.

Schnute et al. (1998, 1999) give a more complete description of the database. All trawl trips, except those directed at hake or conducted by small vessels in the Strait of Georgia, must employ onboard observers to collect these data. We also obtain historic foreign catch data from Ketchen (1981). As illustrated in Fig. 2.1, foreign fleets removed large quantities of POP from the Goose Island Gully area prior to 1980.

The Groundfish Section conducts numerous surveys, some of which have used bottom trawl gear to study POP (Table 2.1, Appendix A). Surveys for other purposes (Table 2.2) and surveys with other gear types (Table 2.3) also collect POP information. Surveys use research vessels owned by the Department or charter vessels hired from industry. For example, the catch-age analysis in Section 4 incorporates biomass estimates from 10 research and 4 charter surveys. A third database 'GFBio' maintains records from all surveys, including individual tow data similar to that in PacHarvTrawl. This database was constructed long after many of the surveys took place, and the trail has grown cold on data records from older surveys. In 2001, a major effort in data archeology made it possible to add 10 historic POP surveys to GFBio, but others remain to be archived (Appendix A).

In addition to tow data from surveys, GFBio contains individual fish specimen data from commercial and survey samples. Conceptually, each specimen record is linked to a sample record, which in turn is linked to a fishing event, that is, a context in which the sample was collected. For example, Tables 2.1–2.3 show the numbers of POP samples obtained during various research cruises. More generally, Fig. 2.2 portrays annual numbers of POP samples and specimens collected from commercial and research sources, as currently recorded in GFBio. Fig. 2.3 adds details about the commercial sampling program. Fish lengths are recorded for almost every specimen, so that the number of length measurements also reflects the number of specimens. The sex is determined for many specimens, but age measurements from otoliths occur much less frequently. Furthermore, at the time of writing this report, the database shows available age data in many instances when another field indicates that no otoliths have been collected. The 'otolith' field can be important when selecting old samples for additional age reading in support of a modern analysis.

Figures 2.2–2.3 show a spotty record of commercial fishery sampling. The situation has improved somewhat in recent years, due to a port monitoring program initiated in 1994 and the onboard observer program that started in 1996. Figure 2.4 portrays the POP age structure information available from each of the six SRF areas. Within each area and year, proportions at age represent an average of available sample proportions. Richards and Olsen (1996) provide

reasons for stratifying by sample. The most extensive data come from areas 5AB and 5CD, which show a coherent pattern of strong year classes. Unfortunately, historical samples in areas 3C and 3D are too sparse to show such patterns clearly. Because POP live for many years, monitoring them requires a consistent long-term sampling program spread broadly throughout the entire fishery. The data compiled here show opportunities for future improvement in sampling practices.

Our analyses depend on ocean bathymetry data. For this purpose, we have compiled a database of mean depths associated with 1 km × 1 km blocks in Canadian coastal waters. This tabulation requires a relatively flat projection of the earth's surface. We locate grid blocks using Universal Transverse Mercator coordinates that describe distances in km relative to a local origin in zone 9 with central meridian at longitude 123°W. This zone covers a longitude range appropriate for B.C. coastal waters. Schnute et al. (1999, Section 5.1) provide a complete description. In 2001, our summer student Chris Grandin developed computer code in S-Plus, Microsoft Access Basic, Python, and C to perform conversions between longitude-latitude coordinates and UTM easting and northing coordinates.

Other useful data come from external sources. This report makes significant use of studies showing evidence of recent climate regimes in the north Pacific (McFarlane et al. 2000). A change occurred during the fall and winter of 1976 that began a period of relatively high productivity for many species. Another shift occurred in 1989-1990 that caused a productivity reduction, including a high profile decline in Pacific salmon. Oceanic evidence suggests another shift in 1998-1999, although its effect on fish stocks remains largely unknown. Some preliminary data suggest that productivity may improve in this new regime (Sandy McFarlane, Pacific Biological Station, Nanaimo, B.C., pers. comm.).

Recent fish disease investigations (Kent et al. 2001) have identified a surprisingly high infection rate by *Ichthyophonus* in POP and other commercial rockfish. For example, small samples from northern B.C. showed the following infection rates:

- 35 infected from 45 fish in Queen Charlotte Sound (78%);
- 4 infected from 11 fish in Hecate Strait (36%) in Hecate Strait.

This issue has stimulated concern in the U.S., where significant research programs have started to investigate *Ichthyophonus* infections in wild fish populations.

Although Canadian POP surveys have been irregular in recent years, the U.S. has maintained a series of triennial surveys since 1977 along the coasts of California, Oregon, and Washington, with some additional work in area 3C. We report the results of this work in Section 5 below.

3. Spatial distribution of stocks and fisheries

We have alluded to the SRF areas for POP management, but these comprise only one method of subdividing the coast. Spatial standardization has posed a significant problem for this assessment. Complex historical reasons have produced the subdivisions currently in use, and we attempt to summarize them here. The international Pacific Marine Fisheries Commission (PMFC) established areas along the North American Pacific coast from California to Alaska (Fig. 3.1, from Tagart 1991). These correspond roughly to reporting regions for the U.S. triennial

surveys. They also fit into a Canadian scheme of dividing the coast into major areas, where Canadian areas 3–9 correspond to PMFC areas 3C, 3D, 5A, 5B, 5C, 5D, and 5E (Table 3.1). The major areas have hierarchical breakdowns into minor areas and localities (Table 3.2, Fig. 3.2). The major areas cover the B.C. coast, and the minor areas similarly cover the coast with a larger number of subdivisions. Based on historic fishing grounds, each minor area contains localities. These typically leave holes, so that a minor area can consist of various defined localities plus other regions. Each locality has a code number within the minor area, where '9' always means 'other', that is, outside the identified localities. Another code '0' denotes an unknown locality, different than '9'. The current PacHarvTrawl database may incorrectly place tows in locality '0', rather than '9'. If this seems confusing, just remember that *majors cover the coast, so do minors, but localities don't.*

Localities are important for POP analysis, because they constitute the finest spatial resolution available in the historical GFCatch database. Furthermore, the SRF areas differ from the major areas by definitions that depend on minor areas and localities (Table 3.3). Blue boundaries in the map of Fig. 3.3 show how these definitions carve up the coast, with a particularly curvilinear boundary separating 5AB and 5CD. The yellow region identifies another complexity. Prior to 2000, the northwest boundary of 5AB extended along a single line touching the southern tip of the Queen Charlotte Islands. As documented by Schnute et al. (1999, Section 8.3), the industry requested a boundary change to include a fishing ground called 'Flamingo' (Major Area 5E, Minor Area 34, Locality 5; see Rutherford 1999, p. 49) in SRF area 5CD. When the change was implemented in 2000, the yellow region was added to 5CD by removing the corresponding pieces from 5ES and 5AB. Thus, the precise definitions of SRF areas change between 1999 and 2000. Most analyses in this paper use the new 2000 definitions, although Table 3.3 gives the historical definition up to 1999.

Figure 3.3 uses the UTM projection, which, as describe above, preserves distances better than the usual longitude-latitude projection. Consequently, the blue straight-line boundaries in longitude-latitude polygons appear curvilinear in the UTM coordinates of this figure. By contrast, the red boundaries define new polygons discussed below relative to UTM coordinates, so that these have straight-line boundaries in Fig. 3.3.

Localities have also been used to identify three marine canyons: Goose Island Gully, Mitchell's Gully, and Moresby Gully (Table 3.4). The sloping bathymetry of these gullies provide the prime POP habitats in 5AB and 5CD that have supported the majority of the POP fishery (Fig. 1.1) and produced the greatest amount of available data (Figs. 2.2–2.4). Tables 3.3-3.4 show that SRF area 5AB consists of Goose Island and Mitchell's Gullies combined. Moresby Gully coincides with SRF area 5CD. Blue boundaries in Fig. 3.4 show the classical gully definitions. Again we use UTM coordinates, which make it possible to show 5 km × 5 km grid blocks in which POP have been captured during the 1994–2001 period with known tow locations from GFCatch and PacHarvTrawl. Block shadings indicate total removals during the time period. Again, red lines denote UTM polygons, and we come to their definitions shortly.

In summary, coastal strata have various definitions for various purposes. PMFC areas 3C, 3D, 5AB, 5CD, and 5E differ somewhat from SRF areas with the same names. Furthermore, the definitions of SRF areas vary with year. The gullies capture some of the marine bathymetry, but

with some imperfections, as we show below. Historical data constrain our analysis, because GFCatch data prior to 1994 are primarily identified only by localities. After 1994, however, almost every tow record has longitude-latitude coordinates, which determine corresponding UTM coordinates. The databases store polygon coordinates as ancillary tables, and an algorithm (again coded by our student Chris Grandin) locates tows within polygons. The same algorithm identifies polygons for 1 km × 1 km blocks in the bathymetry table. Thus, in the modern databases, we have some flexibility in dealing with polygons. But consider the number of possible sets of polygons:

- PMFC major areas;
- PMFC minor areas;
- localities within PMFC minor areas;
- SRF areas before 2000;
- SRF areas after 2000;
- historical gullies.

While conducting analyses for this assessment, we discovered that our current databases have incorrect definitions for some of the above polygons. Furthermore, our definitions of SRF areas come from a historical context within the science group. These may differ in some respects from the areas actually used for POP management, based on Pacific Fishery Management (PFM) areas – yet another scheme for coastal stratification. These issues need to be addressed in future work.

Differing stratification schemes pose a problem somewhat analogous to currency conversion. How can we convert lire to dollars or francs? How do we translate from one scheme to another? Section 7 below deals with this problem. In the light of current data and technology, however, we can ask a fresh question. What coastal subdivisions make sense for POP stocks and the POP fishery? Because UTM coordinates allow uniform grid patterns, such as that portrayed in Fig. 3.4, a modern scheme requires UTM polygons. Figure 3.5 shows a reasonable possibility that we investigate here. The bathymetry database enables us to portray the ocean floor in a manner that reveals the marine canyons and other features that define the POP fishery. Figure 3.6 adds 5 km × 5 km grid blocks in which POP have been captured by the fishery since 1994. Shading indicates the associated level of CPUE. The structure of the fishery in Fig. 3.6 clearly relates closely to the bathymetry in Fig. 3.5. Similarly, Fig. 3.7 represents the amount of catch removed from each block. This correlates positively with the CPUE, that is, high catches tend to come from blocks with high CPUE.

The red boundaries in Figs. 3.5–3.7 match those shown earlier in Figs. 3.3–3.4. Our northern POP-QCI region includes both the northwest and northern coasts of the Queen Charlotte Islands. A fairly contiguous fishery runs along this coastline, starting north of a section of the west coast that is almost unfishable due to a rocky bottom. Our POP-MR region includes the Flamingo ground off the southwest corner of the islands, plus all of Moresby Gully to the point that it runs into shallower waters in northern Hecate Strait. POP-MI captures Mitchell's Gully, with natural shallow boundaries between Moresby in the north and Goose in the south. The POP-GS area includes all of Goose Island Gully and runs south to the northwest tip of Vancouver Island. Brooks Peninsula on Vancouver Island provides a natural break between northern POP-NVI and southern POP-SVI stocks off the west coast of Vancouver Island. Historical surveys have investigated some of the same fishing grounds discussed here (Figs. 3.8-3.10).

If CPUE acts as an index of fish density and fishermen take them in relation to availability, then Fig. 3.6 conveys a sense of the coastwide POP distribution. We examine this possibility further in Section 5 below.

4. Catch-age analysis in Goose Island Gully

We confine our catch-age analysis to Goose Island Gully (GIG), the only area along the B.C. coast with adequate historical data. To match the spatial resolution available in GFCatch for fishery data prior to 1996, we use the historical GIG definition in Table 3.4. Where possible, we supplement information from the current databases with external data, such as the large historical foreign catches (Fig. 2.1). Previous catch-age analyses used data from surveys not yet available in GFBio, particularly two surveys by the G. B. Reed (August 23 to September 25, 1965; October 21 to November 9, 1985; see Appendix A).

To circumvent current data limitations, we start with the data compiled by Richards et al. (1997b) and supplement it with data extracted from the modern databases. We also use queries to test that the historical data are consistent with current results from the databases, wherever a comparison is possible. In summary, we

- accept all catch data from the previous analysis up to 1990;
- add our catch data (1991-2000) by extracting from GFCatch and PacHarvTrawl the catch records relevant to GIG;
- accept all age proportion data from the previous analysis up to 1990;
- add commercial age proportion data (1991-2000) from GFBio, stratifying by samples taken from the historical Goose Island and Mitchell's gullies;
- accept all survey data compiled in the previous analysis;
- obtain new estimates of growth and maturity data by methods described below.

Richards and Olsen (1996) and Richards et al. (1997b) completely document the procedures used to compile data for the previous analysis. In some cases, age data from surveys supplement commercial age data, but the available survey data are too sparse to offer an independent time series of age proportions.

Appendix B presents the detailed catch-age model used here. Table B.2 lists the data requirements (M.3)–(M.8):

1. commercial catch weight D_t for each year t;
2. the proportion p_{at} of fish caught in age class a during year t;
3. survey indices I_{it} in various years t conducted at a time that represents the fraction f_{it} of the year, where subscripts $i = 1,2$ denote research and charter surveys, respectively;
4. mean weight w_a and maturity proportion m_a of age class a.

Items 1–3 come from the data compilation above, and we deal with 4 below. Notation for the model uses age class a starting with $a = 1$ at true age $k = 7$, the youngest age that appears significantly in the catch. Thus, the true age $a' = a + 6$ corresponds to age class a.

Figure 4.1 summarizes the new weight analysis, based on a sample of 400 fish from SRF area 5AB collected in 1995. Data from this sample includes length, weight, and age information for each specimen. Although length data are collected extensively (Fig. 2.3), GFBio contains a much smaller number of specimen weights. Fortunately, Fig. 4.1A shows a remarkably tight linear relationship between logged weights and lengths, and a slope 3 through the origin captures this relationship almost perfectly. Thus, POP appear to grow in a manner that preserves their shape, so that weight w (kg) is proportional to the length l (m) cubed (Fig. 4.1B):

$$(4.1) \quad w = (14.7\,\mathrm{kg\,m^{-3}})\, l^3,$$

where we use kg rather than g and m rather than mm, as in Fig. 4.1. Much greater scatter occurs in the relationships with age (Figs. 4.1C–4.1D), but the von Bertalanffy models:

$$(4.2) \quad l_a = l_\infty - (l_\infty - l_1)\lambda_l^{a-1}, \qquad (l_\infty, l_1, \lambda_l) = (0.440\ \mathrm{m}, 0.317\ \mathrm{m}, 0.872);$$

$$(4.3) \quad w_a = w_\infty - (w_\infty - w_1)\lambda_w^{a-1}, \qquad (w_\infty, w_1, \lambda_w) = (1.298\ \mathrm{kg}, 0.498\ \mathrm{kg}, 0.909);$$

fit the average values reasonably well. Furthermore, combining the weight-length relationship (4.1) with the length-age relationship (4.2) gives an excellent approximation to the direct weight-age relationship (4.3). These models correspond, respectively, to the red and green curves in Fig. 4.1D. The catch-age analysis uses (4.3), i.e., the green curve, where w_∞ is the asymptotic weight and w_1 is the weight of a 7-year-old fish.

Our maturity analysis (Fig 4.2) uses over 10,000 specimens collected from SRF area 5AB, with hundreds of specimens available annually for most years 1979–2000. After compiling the data by age and rejecting an outlier (Fig. 4.2A), we obtain the maturity model (Fig. 4.2B):

$$(4.4) \quad m_{a'} = (1 - \lambda_m^{a'})^{1/b}, \qquad (\lambda_m, b) = (0.529, 0.0252);$$

where $m_{a'}$ is the proportion mature at true age $a' = a + 6$ corresponding to age class a. All models (4.1)–(4.4) use samples with males and females combined, consistent with a catch-age model that does not discriminate between the sexes.

Table 4.1 and Figs. 4.3–4.6 summarize the model results. Equation (M.6) in Table B.2 modifies the weight relationship (4.3) to deal with accumulator age classes (Fig. 4.3B). POP mature more rapidly than the fishery selects them (Fig. 4.3A). The biomass trajectory (Fig. 4.4) tracks the available survey data and follows a pattern found earlier by Richards and Olsen (1996), Richards et al. (1997a), and Richards et al. (1997b). Previous analyses found a slow decline in abundance after 1994, and our results indicate that this decline has continued to the end of 2000. The model matches the observed age data reasonably well (Fig. 4.5), where the mean age is increasing in both observations and predictions. This has occurred because of relatively low recruitment in recent years (Fig. 4.6). Recruitment patterns are consistent with the north Pacific regimes discussed above in Section 2. Note the time lag between the year of maximum productivity (1976 in Fig. 4.6B) and the years of maximum recruitment to the fishery at ages 7 and 9 (1983 and 1985 in Fig. 4.6A). The fishery is slowly cropping down large

recruitments from the productive 1976–1988 regime, while new recruitment comes from the less productive regime starting in 1988. If a new regime in 1998 brings better recruitment, the resulting age 7 fish won't appear in the fishery until 2005.

Following a precautionary approach to management (Richards et al. 1999; e.g., Fig. 5.2.1), we can track the progress of biomass and fishing mortality for POP in Goose Island Gully. Figure 4.7 shows a pattern that moves through three phases: high biomass with high fishing mortality (1963–1975), low biomass with low fishing mortality (1976–1988), and moderate biomass with low fishing mortality (1989–2000). Both reduced fishing mortality and improved recruitment productivity allowed the biomass to increase from second to third phase. Theoretically, the next step would be to show reference lines for fishing mortality and biomass on Fig. 4.7, but this would require some knowledge of a stock recruitment relationship. Instead, we deal directly with the primary uncertainty: future recruitment.

Figure 4.6B focuses on recruitment productivity, that is, the ratio of age-7 recruitment biomass to the spawning stock biomass 7 years earlier. In model notation (Appendix B), this definition becomes

$$(4.5) \quad r_t = w_1 R_{t+7} / \sum_{a=1}^{A} (m_a w_a N_{at}),$$

where t is the spawning year. The history of recruitment productivity shows values ranging from 0.01 to 0.26 (Fig. 4.6B). POP population dynamics depends on these rates just as the economy depends on interest rates. We can compare ocean climate regimes to phases of the economy. Right now, POP are living through a period of low interest rates.

Given a growth curve (4.3), maturity curve (4.4), natural mortality M, current population structure $N_{a,38}$, a constant productivity rate r, and hypothetical catch weight D, the model equations in Table B.2 allow projection into the future. Because recruitment occurs at a constant rate r, the model is essentially linear and the population eventually grows or dies. Figures 4.8–4.9 shows projections 30 years into the future with $r = 0.10$ and $r = 0.12$. In each case, the population biomass grows or declines, depending on the sustained catch. The overall growth rate

$$(4.6) \quad \left(\frac{\text{initial biomass}}{\text{final biomass in year 30}} \right)^{1/30}$$

depends on the catch biomass, as shown in the lower panels of Figs. 4.8–4.9. At a certain critical catch level, the growth rate is 1; higher catches cause the population to decline.

Figure 4.10 allows an assessment of risk in relation to future productivity r. Just as a financial investment can sustain withdrawals in an amount that depends on the interest rate, the GIG POP stock can sustain catches depending on the future recruitment rate. Because POP have a natural mortality, a certain recruitment rate is necessary even if the catch is 0. The curve in Fig. 4.10A allows no catch with $r < 0.076$; consequently, with the parameters estimated here, POP require a recruitment productivity near 7% or 8% to survive. This conclusion depends only on

the biological parameters M, m_a, and w_a; it does not depend on the estimated current biomass. For example, a larger current biomass in GIG would cause the curve in Fig. 4.10A to rise more steeply from 0, but it would not change the critical point at $r = 0.076$. Figure 4.10B shows the historical record of rates r and allows an assessment of risk with regard to levels of catch.

5. Swept area biomass estimates

Figure 3.9 shows the locations reached by one of the larger surveys of Goose and Mitchell's gullies. By contrast, Fig. 3.4 shows the coverage of the commercial fishery since 1994. Obviously, the large number of commercial tows provides much better coverage and raises the possibility that the commercial fishery itself might provide a useful survey. In last year's assessment, Schnute and Haigh (2000) investigated this possibility for POP and other species. They recognized from previous assessments (Schnute et al. 1998, 1999) that population density depends on depth and that the fishery experiences seasonal patterns. Consequently, they investigated quarterly biomass estimates stratified by depth.

We recognize many problems associated with using commercial CPUE data to derive biomass indices. Unlike a planned survey, market conditions and management regulations influence commercial fishing behaviour. For example, low POP catch quotas can produce avoidance fishing, in which vessel masters try to avoid catching POP while targeting another species. We attempt to mitigate such effects by selecting fishing events associated with prime POP habitat and minimal spawning aggregation. Schnute and Haigh (2000) explore these possibilities more completely than we can here, and they illustrate conditions in which surveys and commercial fisheries give similar or different results.

Conceptually, a single tow gives an estimate of biomass density. Suppose that a vessel tows a net of width w at speed v. If the tow lasts for the duration E, then the net moves a distance vE and sweeps an area vwE. Furthermore, if this tow captures a biomass C of POP, then the observed biomass density is

$$\text{(5.1)} \qquad \delta = \frac{C}{vwE} = \frac{1}{vw} U ,$$

where $U = C / E$ is the catch per unit effort (CPUE). A set of tows i $(i = 1,\ldots,m)$ gives a mean density estimate

$$\text{(5.2)} \qquad \bar{\delta} = \frac{1}{m} \sum_{i=1}^{m} \delta_i ,$$

where we assume a constant vessel speed v and net width w among tows. In particular, $\delta_i = 0$ if tow i fails to catch the designated species $(C_i = 0)$.

Suppose that a region is divided into n depth strata

$$\text{(5.3)} \qquad S_j = \{d \mid D_{j-1} < d \le D_j\};\ j = 1,\ldots,n;,$$

specified by given depths $D_0 < D_1 < D_2 < \cdots < D_n$, where stratum j has area A_j of each depth stratum j. Then from the logic that

density × area = biomass,

we obtain the total biomass estimate

$$B = \sum_{j=1}^{n} A_j \bar{\delta}_j . \tag{5.4}$$

Even though (5.4) theoretically represents an absolute biomass estimate, we use the results here only as relative abundance indices. Thus, vessels may fail to capture all fish available on the path, introducing an unknown catchability factor into (5.1). Similarly, we are concerned only with the relative sizes of areas A_j.

In a realistic analysis, the measurements δ have high variability and the areas A_j may be poorly known. For the work here, we use $v = 2.9$ nmi h^{-1} = 5.371 km h^{-1}, $w = 43$ m, and $n = 5$ depth strata in the range 150-400 m, each covering a 50 m range. Because commercial fishermen do not choose random sites, extrapolating densities to non-fished areas can be misleading. Therefore, we use two estimates of A_j:

- total area of the depth stratum computed from the bathymetry database (the 'upper' estimate);
- the area within the depth stratum that produced a positive POP catch since 1994, computed by counting the 1 km × 1 km blocks in a figure similar to Fig. 3.4 (the 'lower' estimate).

We further restrict our analyses by considering only tows that

- are conducted by vessels that fished in the region of interest for at least 5 years (not necessarily consecutive) during the period 1994–2000;
- occur during the 5-month period June to October (to reduce the effects of spawning migrations);
- use bottom trawl gear (gear code 1);
- are successful (success codes 0 or 1);
- have positive effort recorded in the database.

Figure 5.1A illustrates the data used for applying (5.4) to the historical GIG area. Bubbles show the mean CPUE in each depth stratum and coloured bars on the left represent relative sizes of the upper (blue) and lower (red) area estimates. Note that the red and blue bars have different scales, where the red bars represent less than 1/3 the area of the blue bars. The fact that the blue and red bars look similar indicates that the upper and lower estimates (5.4) use areas A_j with similar relative sizes.

Bubbles in Fig. 5.1A represent means for all tows, including those that catch no POP. Figure 5.1B segregates the tows that catch POP from those that don't. The mean μ of CPUE

from positive catches is plotted against the proportion p of tows with no catch for each stratum in panel A. The figure shows some negative correlation between μ and p.

Figure 5.2A shows swept area estimates for the historical GIG computed from the data portrayed in Fig. 5.1A. We use a simple bootstrap, with random sampling of tows in each depth stratum, to assess uncertainty. Upper and lower biomass estimates follow a similar time pattern that reflects the factor of about 1/3 mentioned earlier between upper and lower area estimates. In Fig. 5.2B, we examine the running 365-day catch, taking particular note of annual catches between the midpoint (August 15) of our 5-month base period. Similarly, we obtain biomass estimates for the other two historical gullies (Table 3.4, Fig. 3.4) and compare the lower biomass estimates and annual catches in Fig. 5.3.

Figures 5.4–5.7 show similar biomass estimates in four regions defined by our new POP areas (Fig. 3.5):

- POP-QCI, where the query admits tows from vessels with only 4 years fishing;
- POP-MR;
- POP-MI and POP-GS combined;
- POP-NVI and POP-SVI combined.

Figure 5.8 pulls these analyses together by comparing the lower biomass estimates and annual catches. Similarly, Fig. 5.9 shows the results of a second complete analysis for the SRF areas, where we use the new 2000 definitions that take account of the yellow boundary change in Fig. 3.3. Readers can speculate on the relative sizes of biomass and catch. For example, it appears that the biomass in 3C has increased while the catch has been reduced.

Data from triennial U.S. National Oceanic and Atmospheric Administration (NOAA) surveys (Fig. 5.10) give these analyses a coastwide perspective (Fig. 3.1) over a longer time period from 1977, where 2001 data are preliminary (Mark Wilkins, National Marine Fisheries Service, Seattle, WA, pers. comm.).

6. Model-based CPUE analysis

The preceding section relates CPUE measurements directly to biomass. The analyses stratify tows by depth and adopt a standard time period (June-October). To investigate relationships between CPUE and various factors in the fishery, we use generalized linear models (GLMs; McCullagh and Nelder 1989). We are interested in effects on tow h that can be attributed to year i, depth j, month k, vessel l, and grid block m. A deterministic version of the model has the form

$$(6.1) \quad f(U_{hijklm}) = \mu + Y_i + D_j + M_k + V_l + G_m,$$

where f is a suitable transformation of U called the 'link function'. The right-hand side of (6.1), called the 'linear predictor', expresses the assumption that effects due to various factors are additive. Here μ acts as an overall mean and the remaining terms express effects due to year, depth, month, vessel, and grid block, respectively. Please don't confuse the meaning of D_j here with its meaning as a depth stratum boundary in Section 5 above.

As it stands, model (6.1) obviously is not unique, because a constant could be added to one set of effects (say, year) and subtracted from another (say, depths) without changing the value of the linear predictor. We impose the usual constraints that

$$(6.2) \quad \sum Y_i = \sum D_j = \sum M_k = \sum V_l = \sum G_m = 0,$$

so that factor levels sum to 0. If n_y, n_d, n_m, n_v, and n_g denote the numbers of years, depths, months, vessels, and grid blocks, then a short calculation shows that the linear predictor has $n_y + n_d + n_m + n_v + n_g - 4$ independent parameters. The extra index h on the left-hand side of (6.1) corresponds to an individual tow within cell (i,j,k,l,m), so that we typically have many more data values than predictors. A statistical version of the model requires suitable error assumptions. We consider two cases. In the first, we use only positive CPUE measurements; in the second we use all CPUE measurements, but consider them in a binomial sense: 0 if no POP are caught and 1 if they are. For the first case we use a log link function with additive normal error; thus, the model gives a lognormal prediction for U. For the second case we use a standard GLM binomial model with the canonical link function $\log[p/(1-p)]$, where p is the proportion of nonzero tows.

We restrict tows by the same criteria identified in Section 5, and conduct analyses for the same four POP area combinations, plus historical Goose Island Gully. Finally, we combine all data to obtain a coastwide analysis. Figures 6.1–6.12 present the results, where we also use boxplots to portray distributions of the input data. As in Fig. 6.2, we consistently use the left column of panels for the positive catch model and the right column for the binomial model. Table 6.1 summarizes the model results, showing factors that entered the model significantly after starting with the year effect Y_i.

Years $i = 1,\ldots,7$ correspond to 1994–2000, and month 1 corresponds to April, the beginning of the fishing year for the Canadian trawl fishery since 1997. Model results generally show noticeable depth effects and indicate a positive influence to the fishery during months 3–7 (June–October), consistent with the choices of time period and depth strata adopted in Section 5.

7. Coastwide extensions

We can now return to the problem of 'currency conversion' mentioned in the spatial analysis of Section 3. What's the relationship between new POP areas and old SRF areas? Table 7.1 shows at least one route to addressing this question. The upper third of this table shows the area in common between these two coastal stratifications. The two schemes together divide the coast into 12 pieces, corresponding to the 12 positive area entries in the table. (See also Fig. 3.3.) These areas define proportions that might be used to allocate quantities from one system to another. The table also shows accumulated catch and effort. Swept area biomass estimates in the 12 regions (not derived here) might also be used to obtain a set of relative proportions.

For the four combined POP regions, we have obtained annual swept area biomass estimates (upper and lower), as well as annual effects Y_i from two GLMs (positive catch and

binomial). Figures 7.1–7.4 compare these index measurements. The two swept area methods show very consistent agreement, so that our biomass indices appear robust to the choice of upper or lower area measurements. The two GLM indices do not show such consistency, and can be negatively correlated. (For example, see the opposing time trends in the upper left and right panels of Fig. 6.8). Although GLMs provide useful exploratory data analysis, we do not expect them to produce meaningful abundance indices. They capture only CPUE effects, which reflect densities as described in (5.1). Furthermore, the model (6.1) fails to consider interactions among factors, such as those illustrated Fig. 5.1 by a noticeable change in CPUE patterns among depth zones in 2000. These data appear not to fit the additive model (6.1) with a log link function. This is not an issue for the estimator (5.4), which combines data from zero and nonzero tows with stratum areas to produce a composite result.

The introduction cites the most important conversion problem for this assessment. Given a catch quota for Goose Island Gully from the catch-age analysis, how do we translate this to quotas for SRF areas? We're pressing the limits of the available data here, but the biomass estimates provide an approach illustrated in Table 7.2. Figure 5.9 shows relatively stable biomass patterns in the last three years (1998-2000). The table lists these estimates and their three-year averages (labeled B3). These averages have fairly consistent ratios to the current quotas, although the 3C quota appears low relative to the estimated biomass. If the current coastwide quota were redistributed in proportion to our average biomass estimates, the effective quota in historical GIG would be 1525 t. Additional columns in Table 7.2 illustrate calculations based on GIG quotas of 1000 t, 1500 t, and 2000 t.

8. Discussion, summary, and recommendations

Many other scenarios could be explored beyond the analyses presented here, which are constrained by available data and time. Our spatial analysis (Section 3) lacks any biological basis, other than the existence of segregated fishing grounds associated with bathymetric characteristics of the sea floor. While these features appear to influence the conduct of the fishery, they may or may not indicate biologically distinct stocks. Future work could focus more precisely on the association of biological characteristics, such as length, age, and sex ratio, with geographic features. Genetic stock identification might also provide insights into POP population structure (Withler et al. 2001), although we found the existing information difficult to apply in the current context.

Our catch-age analysis (Section 4) examines a relatively simply scenario. Natural mortality remains independent of age a and year t. Similarly, we assume that length, weight, maturity, and catchability depend only on a, but not t. Although we generally lack the data to weaken such assumptions, we have not explored all reasonable alternatives. Furthermore, our risk analysis doesn't account for all sources of parameter uncertainty, and we have not investigated optimal control policies for fishing stocks with episodic recruitment patterns, like POP in Goose Island Gully.

A precise mechanism for linking climate change to fish stocks remains largely unknown. Various researchers have suggested that ocean conditions can alter a stock's productivity, carrying capacity, or both. For example, the regimes starting in 1977 and 1988 experienced increasing and declining primary productivity, respectively, off the B.C. coast (Robinson and Ware 1999). These changes could potentially influence recruitment through the survival of

pelagic POP larvae. Our model focuses on this issue, and we have not explored possible changes in the adult carrying capacity.

To produce swept area biomass estimates, we need to make numerous assumptions about commercial CPUE discussed in Section 5. The existing CPUE data fail to fit simple generalized linear models (Section 6), although we use models without factor interactions as tools for exploratory data analysis. Despite their limitations, our biomass index estimates follow an intuitive logic from Fig. 3.6: catch rates indicate biomass density; highlighted blocks show known habitat area; and biomass equals area times density. The results in Figs. 5.8–5.9 match the relative abundances implicit in Fig. 3.6 reasonably well for new POP areas and historical SRF areas. Furthermore, current catches and quotas reflect these relative sizes fairly well, except possibly for SRF areas 3C and 3D off the west coast of Vancouver Island.

In applying the GIG quota coastwide (Section 7), based on relative biomass proportions, we make the implicit assumption that stocks move together and share common reference points. Shifting quota among the areas, as in Table 7.2, might be compared with redistribution in a diversified investment portfolio to keep investments balanced. Revised quotas would keep the various POP stocks synchronized. Skeptics (we include ourselves in this group) could argue, however, that this entire analysis merely reflects current management practices. Quotas determine the catches, which then determine the apparent biomass levels in the swept area calculations. For this reason, we avoid putting too much faith in any single approach. Instead, we look broadly at all available indicators. The GIG analysis suggests a recruitment problem, supported by research into climate regimes. On the other hand, our biomass estimates (Fig. 5.2) suggest a slight upturn in 2001. Furthermore, the U.S. triennial surveys (Fig. 5.10) show an upturn in the Vancouver areas (Fig. 3.1) since 1995, although with large reported errors. Limited age data from area 3C (Fig. 2.4) suggest a young cohort present there. So, we have mixed signals from various indicators.

Although numerous potential analyses remain unexplored, we don't think that the available evidence would justify a conclusion much different from the essential message of this stock assessment. The GIG stock currently experiences low recruitment, probably associated with an ocean climate regime starting in 1988 (McFarlane et al. 2000). The age data (Fig. 4.5) reflect this situation, where the mean age increases as cohorts from the 1980s grow older. The risk analysis in Fig. 4.10 suggests caution in setting quotas. With current low productivity, the stock can't maintain itself, even in the absence of fishing. On the other hand, Figs. 4.8–4.9 show that population growth and decline happens slowly. This long-lived species takes advantage of recruitment opportunities, such as the period of high productivity starting in 1976. Similarly, stock market investors take advantage of unpredictable periods of market growth by staying invested for the long term. We don't think it's a time for panic about GIG stock status, but a conservative fishery will maintain a biomass investment for the future when productivity improves. We need to adopt a long-term strategy similar to that of the fish.

We present our recommendations in the spirit described by Schnute and Richards (2001). Through extensive graphics and intuitive discussion, we hope to engage stakeholders in thinking actively about the current state of our knowledge. Every analysis here contains debatable elements, but we are constrained by available data. We have relatively few research surveys, and most data come from the fishery itself. As stated in the introduction, a final decision depends on human judgement, given the facts available. We can suggest three quota options:

1. Maintain the current quotas for each SRF area.
2. Maintain the coastwide quota, but redistribute among areas as shown in Table 7.2.
3. Lower or raise the GIG quota, and distribute among areas as in Table 7.2. On balance, we think that the evidence available does not justify an increased quota.

Our analyses also indicate needs and opportunities for future POP analysis and management, such as:

A. Conduct fishery-independent surveys, particularly to obtain age distributions back to young ages in the range 3–5. The surveys should also provide more complete coverage of the B.C. coast to allow comparison of stocks in the major gullies with others in outlying areas.
B. Resolve issues associated with area definitions, as described in Section 2.
C. Ensure synoptic sampling of all fisheries to obtain fully representative samples. Obtain more weight samples to verify the temporal and spatial consistency of the relationships portrayed in Fig. 4.1.
D. Collaborate with research into *Ichthyophonus* infections in Pacific rockfish populations. This may prove important to understanding the reproductive capacity of POP stocks.
E. Add more historical surveys to GFBio and devise a strategy for embedding metadata, such as the descriptions and references in Appendix A.
F. Resolve other quality control issues, such as the 'otolith' field mentioned in conjunction with Fig. 5.3.

We particularly highlight the opportunity suggested in item A. Reliable, fishery-independent age distributions back to age 4 would provide leading indicators of future recruitment. Because POP don't enter the fishery until age 7, this information would enable stakeholders to foresee recruitment three years in advance. Imagine what investment analysts would pay for a reliable market forecast three years in advance!

Acknowledgements

We thank Brian Mose, Kelly Anderson, Brian Dickens, and other members of the fishing industry for providing expert knowledge of the POP fishing grounds in B.C. Mark Wilkins supplied valuable data from the U.S. triennial surveys. Jack Tagart kindly agreed to let us use Fig. 3.1. Sandy McFarlane provided a useful summary of extensive research into ocean climate processes. Kate Rutherford and Norm Olsen helped us navigate through the minefield of spatial area stratifications and expedited historical data archival in GFBio. Simon Jones, Mike Kent, and Sheila Dawe alerted us to recent studies of *Ichthyophonus* infections in commercial rockfish. Chris Grandin generated important computer algorithms with youthful flourish and skill. Reviewers John Moore and Noel Cadigan made numerous useful suggestions leading to an improved final draft.

References

Kent, M. L., V. Watral, S. C. Dawe, P. Reno, J. R. Heidel, and S. R. M. Jones. 2001. *Ichthyophonus* and *Mycobacterium*-like bacterial infections in commercially-important rockfish, *Sebastes* spp., in the eastern North Pacific Ocean. Journal of Fish Diseases 24: 427–431.

Ketchen, K. S. 1981. Reconstruction of Pacific ocean perch (*Sebastes alutus*) stock history in Queen Charlotte Sound. Part II. Catch per unit effort as a measure of abundance, 1959-79. Can. Manuscr. Rep. Fish. Aquat. Sci. 1599, 72 p.

McCullagh, P. and J. A. Nelder. 1989. Generalized linear models, 2nd edition. Chapman and Hall, New York, NY.

McFarlane, G. A., J. R. King, and R. J. Beamish. 2000. Have there been recent changes in climate? Ask the fish. Progress in Oceanography 47: 147-169.

Richards, L. J. 1993. Slope rockfish assessments for 1993 and recommended yield options for 1994. PSARC Working Paper G93-8, 63 p.

Richards, L. J. 1994. Slope rockfish assessments for 1994 and recommended yield options for 1995. PSARC Working Paper G94-9, 25 p.

Richards, L. J. 1995. Slope rockfish assessments for 1995 and recommended yield options for 1996. PSARC Working Paper G95-9, 35 p.

Richards, L. J. and N. Olsen. 1996. Slope rockfish stock assessment for the west coast of Canada in 1996 and recommended yields for 1997. Can. Tech. Rep. Fish. Aquat. Sci. 2134, 91 p.

Richards, L. J., J. T. Schnute, and N. Olsen. 1997a. Visualizing catch-age analysis: a case study. Can. J. Fish. Aquat. Sci. 54: 1646-1658.

Richards, L. J., N. Olsen, J. Schnute and R. Haigh. 1997b. Slope rockfish stock assessment for the west coast of Canada in 1997 and recommended yield options for 1998. Can. Stock Assess. Sec. Res. Doc. 97/147, 61 p.

Richards, L. J., J. T. Schnute, R. Haigh, C. Sinclair. 1999. Science strategic project on the precautionary approach in Canada, proceedings of the second workshop. Can Stock Assess. Proc. Series 99/141, 96 p.

Robinson, C. L. K. and D. M. Ware. 1999. Simulated and observed response of the southwest Vancouver Island pelagic ecosystem to oceanic conditions in the 1990s. Can. J. Fish. Aquat. Sci. 56: 2433-2443.

Rutherford, K. L. 1999. A brief history of GFCATCH (1954-1995), the groundfish catch and effort database at the Pacific Biological Station. Can. Tech. Rep. Fish. Aquat. Sci. 2299, 66 p.

Schnute, J. T. 1994. A general framework for developing sequential fisheries models. Can J Fish. Aquat. Sci. 51: 1676-1688.

Schnute, J. T. and R. Haigh. 2000. Estimating stock biomass from tow-by-tow data for Pacific Groundfish. Can. Stock Assess. Sec. Res. Doc. 2000/155, 32 p.

Schnute, J. T., N. Olsen, and R. Haigh. 1998. Slope rockfish assessment for the west coast of Canada in 1998. Can. Stock Assess. Sec. Res. Doc. 99/16, 79 p.

Schnute, J. T., N. Olsen, and R. Haigh. 1999. Slope rockfish assessment for the west coast of Canada in 1999. Can. Stock Assess. Sec. Res. Doc. 99/184, 104 p.

Schnute, J. T. and L. J. Richards. 1995. The influence of error on population estimates from catch-age models. Can J Fish. Aquat. Sci. 52: 2063-2077.

Schnute, J. T. and L. J. Richards. 2001. Use and abuse of fishery models. Can J Fish. Aquat. Sci. 58: 10-17.

Tagart, J. V. 1991. Population dynamics of yellowtail rockfish (*Sebastes flavidus*) stocks in the northern California to southwest Vancouver Island region. Ph.D. thesis (Univ. Washington), 323 p.

Withler, R. E., T .D. Beacham, A. D. Schulze, L.J. Richards, and K. M. Miller. 2001. Co-existing populations of Pacific ocean perch, *Sebastes alutus*, in Queen Charlotte Sound, British Columbia. Marine Biology 139: 1-12.

Appendix A. Survey cruise summary.

This appendix is a list of the research and charter cruises that collected abundance, distribution and/or biological data specifically for Pacific ocean perch or the slope rockfish community. The format for each cruise in this listing includes: GFBio Trip ID, cruise type (research or charter), cruise dates, vessel name, SRF areas surveyed, and the purpose related to Pacific ocean perch. The references for cruise reports are included in brackets.

N/A Research Aug. 23-Sept. 25/65 G. B. REED 3C/5AB
Trawl survey to investigate Pacific ocean perch availability, abundance and biology in Queen Charlotte Sound and along the outer coast from Cape Spencer, Alaska to Cape Blanco, Oregon (Westrheim 1967).

41333 Research Aug. 24-Sept. 15/66 G. B. REED 5AB/5CD/5ES
Trawl survey to estimate distribution and biomass of Pacific ocean perch from Estevan Point to southeast Alaska (Westrheim 1966).

41313 Research Sept. 6-Oct. 4/67 G. B. REED 5AB
Trawl survey to estimate distribution and biomass of Pacific ocean perch from southern Queen Charlotte Sound to southeast Alaska. Also test oval trawl doors and midwater trawl gear (Westrheim et al. 1968).

41133 Research Sept. 9-25/69 G. B. REED 3C/5AB
Trawl survey to investigate distribution and abundance of Pacific ocean perch in southern Queen Charlotte Sound; evaluate of two bottom trawls; collect length-weight data for Pacific ocean perch and determine maturity stages of rockfish gonads from off southwest Vancouver Island and Queen Charlotte Sound (Harling et al. 1969).

N/A Research June 4-18/70 G. B. REED 5AB
Trawl survey to collect estimate bathymetric distribution and abundance of Pacific ocean perch, plus maturation, spawning season and larval rockfish identification off Queen Charlotte Sound (June portion of cruise) (Harling et al. 1970a).

41295 Research Sept. 9-25/70 G. B. REED 3C
Trawl survey of rockfish off the southwest coast of Vancouver Island. Investigate distribution and abundance of Pacific ocean perch. Collect material for systematic studies of rockfish and other species. Determine maturity stages of rockfish gonads (Harling et al. 1970b).

40657 Research Oct. 1-29/71 G. B. REED 5AB
Trawl survey to investigate distribution and abundance of Pacific ocean perch in southern Queen Charlotte Sound. Collect rockfish specimens to determine frozen fillet storage life (Harling et al. 1971).

40537 Research Sept. 5-25/73 G. B. REED 5AB/5CD
Trawl survey for biomass estimates of Pacific ocean perch in two areas of Queen Charlotte Sound (Goose Island Gully, Mitchell's Gully (Harling et al. 1973).

40057 Research Sept. 8-27/76 G. B. REED 5AB/5CD
Trawl survey for biomass estimates of Pacific ocean perch in two areas of Queen Charlotte Sound (Goose Island Gully, Mitchell's Gully). Also conduct trawl calibration studies with two U.S. vessels (Westrheim et al. 1976).

40037 Research Aug. 22-Sept. 8/77 G. B. REED 5AB/5CD
Trawl survey to estimate biomass of Pacific ocean perch in Queen Charlotte Sound and assess catch rate differences using varying lengths of sweepline extensions (Harling and Davenport 1977).

N/A Charter July 7-Aug. 8/79 SCOTIA BAY 5EN
Charter trawl survey to assess rockfish abundance and biology off the west coast of the Queen Charlotte Islands (joint survey with BLUE WATERS) (Lapi and Richards 1981).

N/A Charter July 12-Aug. 1/79 BLUE WATERS 5EN
Trawl survey to assess rockfish abundance and biology off the west coast of the Queen Charlotte Islands (joint survey with SCOTIA BAY) (Lapi and Richards 1981).

N/A Charter Sept. 5-24/79 ARTIC HARVESTER 3C/3D
Trawl survey to estimate biomass and abundance of Pacific ocean perch stocks along the west coast of Vancouver Island (Lapi and Richards 1981).

10921 Charter Sept. 7-27/79 SOUTHWARD HO 5AB
Trawl survey to estimate biomass of all rockfishes and collection biological data and samples from Queen Charlotte Sound (Nagtegaal and Farlinger 1980).

N/A Research July 5-22/83 G. B. REED 5EN
Trawl survey to investigate distribution, abundance and collect biological data from rockfish stocks in the Dixon Entrance – southeast Alaska region. (joint survey with FREE ENTERPRISE) (Leaman and Nagtegaal 1986).

N/A Charter July 8-19/83 FREE ENTERPRISE 5EN
Trawl survey to investigate distribution, abundance and collect biological data from rockfish stocks in the Dixon Entrance – southeast Alaska region. (joint survey with G. B. REED) (Leaman and Nagtegaal 1986).

36864 Research Aug. 14-Sept. 11/84 G. B. REED 5AB
Two-vessel (G. B. Reed and Eastward Ho), swept-area, bottom trawl survey to estimate Pacific ocean perch biomass in area 5AB, plus compare catches from commercial and research vessels (Nagtegaal et al. 1986).

36844 Charter Aug. 25-Sept. 9/84 EASTWARD HO 5AB
Two-vessel (G. B. Reed and Eastward Ho), swept-area, bottom trawl survey to estimate Pacific ocean perch biomass in area 5AB, plus compare catches from commercial and research vessels (Nagtegaal et al. 1986).

41273 Charter Sept. 9-22/85 HOWE BAY 3C
Trawl survey of rockfish stocks off the southwest coast of Vancouver Island (Areas 3C and 3D) and U.S. waters off Cape Flattery (Leaman et al. 1988).

N/A Research Oct. 21-Nov. 9/85 G. B. REED 3C/3D/5AB/5CD/5ES/5EN
Research cruise to collect reproductive biology, genetic, and gill parasite data from five stocks of Pacific ocean perch in British Columbia waters (Leaman and Nagtegaal 1988).

10378 Charter July 12-30/89 OCEAN SELECTOR 3C/3D/5AB/5CD/5ES/5EN
Charter cruise to collect biological samples of commercially important rockfish species and provide population data primarily for Pacific ocean perch (Gillespie and Leaman 1990).

N/A Research June 19-30/93 W. E. RICKER 5EN
Pacific ocean perch monitoring cruise to assess impacts due to seven years of unrestricted fishing on rockfish stocks in the experimental fishing area off Langara Island. This is the first year of monitoring (Leaman et al. 1996).

30744 Charter June 20-July 7/94 OCEAN SELECTOR 5AB
Swept-area trawl survey to update series of biomass estimates for Pacific ocean perch in Area 5AB. W.E. Ricker carried out a hydroacoustic survey in conjunction with this trawl survey (Hand et al. 1995).

31244 Charter Sept. 11-22/95 OCEAN SELECTOR 5AB
Trawl survey to estimate relative biomass of the Goose Island Gully Pacific ocean perch stock and compare catch rates between two commercial vessels (Ocean Selector and Frosti) (Yamanaka et al. 1995).

31245 Charter Sept. 11-22/95 FROSTI 5AB
Trawl survey to estimate relative biomass of the Goose Island Gully Pacific ocean perch stock and compare catch rates between two commercial vessels (Ocean Selector and Frosti) (Yamanaka et al. 1995).

30864 Research June 2-14/96 W. E. RICKER 5EN
Pacific ocean perch monitoring cruise to assess impacts due to seven years of unrestricted fishing on rockfish stocks in the experimental fishing area off Langara Island. This is the second year of monitoring (Leaman et al. 1997).

30624 Charter Sept. 10-27/96 CALEDONIAN 3C
Charter cruise to estimate relative biomass of Pacific ocean perch in Statistical Area 3C and part of 3D, and collect biological samples of several rockfish species (Olsen et al. 1997).

29804 Charter Sept. 5-23/97 OCEAN SELECTOR 5ES/5EN
Charter cruise to conduct a random, depth-stratified biomass survey of Pacific ocean perch and three other commercial rockfish species off the west coast of the Queen Charlotte Islands (Workman et al. 1998).

Cruise report references for Appendix A

Gillespie, G. E., and B. M. Leaman. 1990. Rockfish sampling cruise: F/V OCEAN SELECTOR, July 12 to 30, 1989. Can. Manuscr. Rep. Fish. Aquat. Sci. 2061, 89 p.

Hand, C. M., G. D. Workman, L. J. Richards, R. Kieser and R. I. Perry. 1995. Bottom trawl and exploratory hydroacoustic survey for rockfish in Queen Charlotte Sound, June 20 to July 7, 1994. Can. Manuscr. Rep. Fish. Aquat. Sci. 2300, 87 p.

Harling, W. R., and D. Davenport. 1977. G. B. REED Groundfish Cruise No. 77-3, August 22 to September 8, 1977. Fish Mar. Serv. Data Rep. 42, 46 p.

Harling, W. R., D. Davenport, M. S. Smith, U. Kristiansen and S. J. Westrheim. 1970a. G. B. REED Groundfish Cruise No. 70-1 March 5 - June 18, 1970. Fish. Res. Board Can. Tech. Rep. 205, 82 p.

Harling, W. R., D. Davenport, M. S. Smith, A. C. Phillips and S. J. Westrheim. 1973. G. B. REED Groundfish Cruise No. 73-2, September 5-25, 1973. Fish. Res. Board Can. Tech. Rep. 424, 37 p.

Harling, W. R., D. Davenport, M. S. Smith and R. M. Wilson. 1969. G. B. REED Groundfish Cruise No. 69-3, September 8 to 25, 1969. Fish. Res. Board Can. Tech. Rep. 144, 35 p.

Harling, W. R., D. Davenport, M. S. Smith and R. M. Wowchuk. 1970b. G. B. REED Groundfish Cruise No. 70-3, September 9-25, 1970. Fish. Res. Board Can. Tech. Rep. 221, 35 p.

Harling, W. R., D. Davenport, M. S. Smith, A., R. M. Wowchuk and S. J. Westrheim. 1971. G. B. REED Groundfish Cruise No. 71-3, October 1-29, 1971. Fish. Res. Board Can. Tech. Rep. 290, 35 p.

Lapi, L. A., and J. E. Richards. 1981. Data collected during rockfish (Sebastes spp.) assessments of west Langara Island and west coast Vancouver Island fishing grounds in 1979. Can. Data Rep. Fish. Aquat. Sci. 286, 113 p.

Leaman, B. L., A. M. Cornthwaite and R. D. Stanley. 1996. Cruise details and biological information from the Pacific ocean perch monitoring survey, R/R/ W. E. RICKER, June 19-30, 1993. Can. Manuscr. Rep. Fish. Aquat. Sci. 2388, 71 p.

Leaman, B. L., A. M. Cornthwaite and R. D. Stanley. 1997. Cruise details and biological information from the Pacific ocean perch monitoring survey, R/R/ W. E. RICKER, July 2-13, 1996. Can. Manuscr. Rep. Fish. Aquat. Sci. 2436, 91 p.

Leaman, B. M., G. E. Gillespie, D. A. Nagtegaal and R. D. Stanley. 1988. Biomass survey of rockfish stocks off the southwest coast of Vancouver Island, September 7-23, 1985 (M/V HOWE BAY). Can. Tech. Rep. Fish. Aquat. Sci. 1611, 99 p.

Leaman, B. M., and D. A. Nagtegaal. 1986. Biomass survey of rockfish stocks in the Dixon Entrance – southeast Alaska region, July 5-22, 1983 (R/V G. B. REED and M/V FREE ENTERPRISE No. 1). Can. Tech. Rep. Fish. Aquat. Sci. 1510, 63 p.

Leaman, B. M., and D. A. Nagtegaal. 1988. Rockfish reproductive biology cruise (GBR-R85-1) October 21-Novemeber 9, 1985. Can. Data Rep. Fish. Aquat. Sci. 716, 36 p.

Nagtegaal, D. A., and S. P. Farlinger. 1980. Catches and trawl locations of the M/V SOUTHWARD HO during a rockfish exploration and assessment cruise to Queen Charlotte Sound, September 7-27, 1979. Can. Data Rep. Fish. Aquat. Sci. 216, 95 p.

Nagtegaal, D. A., B.M. Leaman and R. D. Stanley. 1986. Catches and trawl locations of R/V G. B. REED and M/V EASTWARD HO during Pacific ocean perch assessment cruise to Queen Charlotte Sound, August-September, 1984. Can. Data Rep. Fish. Aquat. Sci. 611, 109 p.

Olsen, N., G. D. Workman and L. J. Richards. 1997. Bottom trawl survey for rockfish off the southwest coast of Vancouver Island, September 9 to 27, 1996. Can. Manuscr. Rep. Fish. Aquat. Sci. 2409, 83 p.

Westrheim, S. J. 1966. Report of the trawling operations of the Canadian research vessel G. B. REED from Queen Charlotte Sound, British Columbia to Sitka Sound, Alaska, August 24 to September 15, 1966. Fish Res. Board Can. Manuscr. Rep. 891, 27 p.

Westrheim, S. J. 1967. G. B. REED Groundfish cruise reports, 1963-66. Fish Res. Board Can. Tech. Rep. 30

Westrheim, S. J., W. R. Harling and D. Davenport. 1968. G. B. REED Groundfish Cruise No. 67-2, September 6 to October 4, 1967. Fish. Res. Board Can. Tech. Rep. 46, 45 p.

Westrheim, S. J., B. M. Leaman, W. R. Harling, D. Davenport, M. S. Smith and R. M. Wowchuk. 1976. G. B. REED Groundfish Cruise No. 76-3, September 8-27, 1976. Fish. and Marine Serv. Data Record 21, 47 p.

Workman, G. D., N. Olsen and A. R. Kronlund. 1998. Results from a bottom trawl survey of rockfish stocks off the west coast of the Queen Charlotte Islands, September 5 to 23, 1997. Can. Manuscr. Rep. Fish. Aquat. Sci. 2457, 86 p.

Yamanaka, K. L., L. J. Richards and G. D. Workman. 1995. Bottom trawl survey for rockfish in Queen Charlotte Sound, September 11 to 22, 1995. Can. Manuscr. Rep. Fish. Aquat. Sci. 2362, 116 p.

Appendix B. Model for catch-age data

Table B.1 presents notation for a variation of the model proposed by Richards et al. (1997a) to analyse Pacific ocean perch data from Goose Island Gully. Following state space design principles described by Schnute (1994), the model includes a population state vector $\{N_{at}\}_{a=1}^{A_t}$ for each year t. Equations (M.16)–(M.20) in Table B.2 define the biological system dynamics for these states, based on the parameter vector $\mathbf{\Phi}$ in (M.9) and control data (M.3)–(M.6). The controls can be subdivided into human interventions (M.3) and biological characteristics (M.4)–(M.6). In particular, (M.4) corresponds to a von Bertalanffy growth model for w_a in which w_1 is the weight for age class 1, w_∞ is the asymptotic weight, and $K_w = -\log \lambda_w$. The maturity model (M.5) describes a proportion m_a that varies from 0 to 1 as the true age $a + k - 1$ varies from 0 to ∞. The special rule (M.6) defines w_{A_t} and m_{A_t} for the accumulator age class A_t in year t.

The model includes selectivities β_a in (M.10) that vary with age-class a. Moments (M.11)–(M.14) of the state vector, such as the exploitable population P_t and exploitable age proportions u_{at}, depend on these selectivities. The known catch biomass D_t is converted to catch numbers C_t in (M.14), using the average weights w_a. Similarly, age-dependent maturities m_a enter the calculation (M.15) of spawner biomass S_t.

Equations (M.21)–(M.24) in Table B.2 relate observed data to the underlying biological system. Following Schnute and Richards (1995), we indicate an estimated observation with a line over the corresponding symbol. Two biomass indices I_{1t} and I_{2t} correspond to the research and charter vessel surveys conducted in various years $\mathbf{T}_1$ and $\mathbf{T}_2$, respectively. Estimated survey numbers are assumed proportional to the underlying exploitable biomass after a known fraction f_{it} $(i = 1, 2)$ of the catch D_t has been removed. Similarly, the proportions p_{at} are estimated directly from the exploitable proportions u_{at} calculated within the model.

By definition, accumulator age-classes contain all fish with ages equal to or older than the designated age. In the model here, age-class $a = 1$ corresponds to fish that recruit at age $k = 7$ yr. To avoid potential bias from otolith surface readings, we use accumulator age-classes $A' = 11$ and $A = 23$ (actual ages 17 and 29) for fish aged by surface or break

and burn readings, respectively. Consequently, in year t, the observed proportions p_{at} in (M.7) have the accumulator class A'_t, given by (M.1). Internal to the model, we use accumulator classes A_t in (M.2), which begin at age A' in year $t = 1$ and advance to a maximum age A in year $t = 1 + A - A'$. The observation equation (M.24) corrects for this difference between observed data and model dynamics.

Table B.2 defines an algorithm for estimating the observations (M.7)–(M.8). The calculation begins with the control data (M.3)–(M.6) and the parameter vector $\mathbf{\Phi}$ in (M.9), which includes recruitments $\{R_t\}_{t=2-A'}^{T}$. These determine the initial states N_{a1} from (M.16)–(M.17) and the initial moments (M.11)–(M.15). The dynamic equations (M.18)–(M.20) at time $t = 2$ determine N_{a2} from N_{a1}, C_1, and u_{a1}. Following this procedure iteratively gives N_{at} for each time t. Finally, the estimates (M.21)–(M.24) can be computed directly from N_{at}. All quantities produced by these calculations (estimates, underlying states, moments) can be considered functions of the parameter vector $\mathbf{\Phi}$.

The algorithm in Table B.2 is completely deterministic. To render it statistical we impose three sources of error: (1) autoregressive lognormal process error among the recruitments R_t, (2) lognormal measurement error in the indices I_{it} $(i = 1, 2)$, and (3) multivariate logistic measurement error in the observed proportions p_{at}. Schnute and Richards (1995) show that these sources of error introduce the following additional parameters: (1) autoregressive recruitment coefficients R and γ, plus a recruitment standard deviation σ_1; (2) an index standard deviation τ_1; and (3) a standard deviation τ_2 for the multivariate logistic distribution. We make the simplifying assumption that the standard deviation τ_1 applies to both I_{1t} and I_{2t}. We also follow Schnute and Richards (1995) in excluding process error from the dynamics (M.18)–(M.20).

Table B.3 defines the likelihood function $L(\mathbf{\Theta})$ for this stochastic model, where the full parameter vector $\mathbf{\Theta}$ in (L.1) extends $\mathbf{\Theta}$ to include the additional parameters R, γ, σ_1, τ_1, and τ_2. To calculate $L(\mathbf{\Theta})$, first obtain the estimates $\overline{p_{at}}$ and $\overline{I_{it}}$ from Table B.2, and then proceed sequentially through (L.4)–(L.12). Equations (L.2)–(L.3) allow $\mathbf{\Theta}$ to be expressed in terms of either (σ_1, τ_1) or (κ, ρ). In the analyses here, we fix ρ and allow κ to vary.

To simplify mathematical notation, we omit two technical details from the calculations in Tables B.2–B.3. First, missing age data for the years 1986 and 1988 require that two years be dropped from the product (L.11). Second, in our calculations we alter the definition of age-classes to require that $p_{at} \geq 0.02$ for every a and t. We accomplish this by grouping consecutive ages, where necessary, into a single age-class. This grouping reduces the influence on the likelihood of observations (presumably with high measurement error) obtained from only a few fish. In trial runs, we found that grouping produced much smaller residuals overall than those obtained without grouping.

Table B.1. Notation for the Pacific ocean perch model.

Symbol	Description
	Indices and Index Ranges
k	youngest age in the model (k=7); age of recruitment to the fishery
a	age class, where $a = 1$ corresponds to actual age k
t	year, where $t = 1$ corresponds to 1963
A'	accumulator age-class for surface age data ($A' = 11$, age 17)
A	accumulator age-class for break-and-burn age data ($A = 23$, age 29)
A'_t, A_t	accumulator age-classes for the data and model, respectively, in year t
T'	final year 1976 ($T' = 14$) for surface age data
T	final year 1995 ($T = 33$) of data
$\mathbf{T}_1, \mathbf{T}_2$	sets of years with research and charter vessel surveys
	Data
D_t	observed catch biomass in year t
p_{at}	observed proportion of age-class a fish in the catch from year t
w_a	average weight of age-class a fish from parameters $(w_1, w_\infty, \lambda_w)$
m_a	mature proportion of age-class a fish from parameters (λ_m, b)
I_{1t}, I_{2t}	biomass estimates from research and charter vessel surveys in year t
f_{1t}, f_{2t}	fraction of catch taken prior to research and charter vessel surveys
	Parameters
$\boldsymbol{\Theta}, \boldsymbol{\Phi}$	parameter vectors
α, β_1	selectivity parameters
β_a	selectivity for age-class a
M	natural mortality rate
q_1, q_2	catchability for research and charter vessel surveys
R, γ	autoregressive recruitment parameters
σ_1	standard deviation of recruitment process error
τ_1	standard deviation of survey index measurement error
τ_2	standard deviation of age proportion measurement error
κ^2	combined variance $\sigma_1^2 + \tau_1^2$
ρ	variance ratio σ_1^2/κ^2, fixed in the model analysis
	States and State Moments
R_t	age-class 1 recruitment in year t
N_{at}	number of age-class a fish at the start of year t
P_t	exploitable population numbers at the start of year t
B_t	exploitable population biomass at the start of year t
S_t	spawner biomass at the start of year t
C_t	number caught in year t
u_{at}	exploitable proportion of age-class a fish in year t

Table B.2. Deterministic model, where the parameter vector Φ and controls (M.3)–(M.6) iteratively define states N_{at}, moments (M.11)–(M.15), and estimates for the observations (M.7)–(M.8).

Accumulator Age Classes ($1 \le t \le T$)

(M.1) $$A'_t = \begin{cases} A'; & 1 \le t \le T' \\ A; & T' < t \le T \end{cases}$$

(M.2) $$A_t = \min(A' + t - 1, A)$$

Data: Controls and Observations

(M.3) $$D_t; \quad 1 \le t \le T$$

(M.4) $$w_a = w_\infty - (w_\infty - w_1)\,\lambda_w^{a-1}; \quad 1 \le a$$

(M.5) $$m_a = (1 - \lambda_m^{a+k-1})^{1/b}; \quad 1 \le a$$

(M.6) $$w_a = 0.5\,(w_{A_t} + w_\infty), \; m_a = 0.5\,(m_{A_t} + 1); \quad a = A_t$$

(M.7) $$p_{at}; \quad 1 \le a \le A'_t, \; 1 \le t \le T$$

(M.8) $$I_{it}, \; f_{it}; \quad t \in \mathbf{T}_i; \; i = 1, 2$$

Parameters

(M.9) $$\Phi = (\alpha, \beta_1, M, q_1, q_2, \{R_t\}_{t=2-A'}^{T})$$

Selectivity

(M.10) $$\beta_a = 1 - (1 - \beta_1)\left(\frac{A - a}{A - 1}\right)^{\alpha}$$

State Moments ($1 \le t \le T$)

(M.11) $$P_t = \sum_{a=1}^{A_t} \beta_a N_{at}$$

(M.12) $$B_t = \sum_{a=1}^{A_t} \beta_a w_{at} N_{at}$$

(M.13) $$u_{at} = \beta_a N_{at} / P_t; \quad 1 \le a \le A_t$$

(M.14) $$C_t = D_t / \sum_{a=1}^{A_t} u_{at} w_{at}$$

(M.15) $$S_t = \sum_{a=1}^{A_t} m_a w_{at} N_{at}$$

Table B.2 continued on next page

Table B.2 (cont.)

Initial States ($t = 1$)

(M.16) $N_{a1} = R_{2-a}e^{-M(a-1)}; \quad 1 \leq a < A'$

(M.17) $N_{A1} = R_{2-A'}\dfrac{e^{-M(A'-1)}}{1-e^{-M}}$

State Dynamics ($2 \leq t \leq T$)

(M.18) $N_{1t} = R_t$

(M.19) $N_{at} = e^{-M}\left[N_{a-1,t-1} - u_{a-1,t-1}C_{t-1}\right]; \quad 2 \leq a \leq A_t; \; 2 \leq t \leq 1 + A - A'$

(M.20) $N_{At} = e^{-M}\left[N_{A-1,t-1} + N_{A,t-1} - (u_{A-1,t-1} + u_{A,t-1})C_{t-1}\right];$
$1 + A - A' < t \leq T$

Estimated Observations ($1 \leq t \leq T$)

(M.21) $\overline{I_{1t}} = q_1(B_t - f_{1t}D_t); \quad t \in \mathbf{T}_1$

(M.22) $\overline{I_{2t}} = q_2(B_t - f_{2t}D_t); \quad t \in \mathbf{T}_2$

(M.23) $\overline{p_{at}} = u_{at}; \quad 1 \leq a < A'_t$

(M.24) $\overline{p_{A'_t,t}} = \sum_{a=A'}^{A_t} u_{at}$

Table B.3. Likelihood function $L(\boldsymbol{\Theta})$ for a stochastic counterpart to the model in Table B.2.

Parameters

(L.1) $\boldsymbol{\Theta} = (\Phi, R, \gamma, \sigma_1, \tau_1, \tau_2)$

(L.2) $\kappa^2 = \sigma_1^2 + \tau_1^2\,, \quad \rho = \dfrac{\sigma_1^2}{\sigma_1^2 + \tau_1^2}$

(L.3) $\sigma_1^2 = \rho\kappa^2\,, \quad \tau_1^2 = (1-\rho)\kappa^2$

Residuals

(L.4) $\xi_{2-A'} = \log(R_{2-A'}) - \log(R)$

(L.5) $\xi_t = \log(R_t) - (1-\gamma)\log(R) - \gamma\log(R_{t-1})\,; \quad 2 - A' < t \le T$

(L.6) $\zeta_{1t} = \log(I_{1t}) - \log(\overline{I_{1t}})\,; \quad t \in \mathbf{T}_1$

(L.7) $\zeta_{2t} = \log(I_{2t}) - \log(\overline{I_{2t}})\,; \quad t \in \mathbf{T}_2$

(L.8) $\eta_{at} = \log(p_{at}) - \log(\overline{p_{at}}) - \dfrac{1}{A_t'}\displaystyle\sum_{a=1}^{A_t'}[\log(p_{at}) - \log(\overline{p_{at}})]$

Likelihoods

(L.9) $L_1(\boldsymbol{\Theta}) = \sqrt{1-\gamma^2}\,(\sqrt{2\pi}\,\sigma_1)^{2-A'-T}\,\exp\left[-\dfrac{1}{2\sigma_1^2}\left((1-\gamma^2)\xi_{2-A'}^2 + \displaystyle\sum_{t=3-A'}^{T}\xi_t^2\right)\right]$

(L.10) $L_2(\boldsymbol{\Theta}) = \displaystyle\prod_{i=1}^{2}\prod_{t\in\mathbf{T}_i}\left[\frac{1}{\sqrt{2\pi}\,\tau_1}\exp\left(-\frac{1}{2\tau_1^2}\zeta_{it}^2\right)\right]$

(L.11) $L_3(\boldsymbol{\Theta}) = \displaystyle\prod_{t=1}^{T}\left[\frac{\sqrt{A_t'}}{(\sqrt{2\pi}\,\tau_2)^{A_t'-1}}\exp\left(-\frac{1}{2\tau_2^2}\sum_{a=1}^{A_t'}\eta_{at}^2\right)\right]$

(L.12) $L(\boldsymbol{\Theta}) = \displaystyle\prod_{i=1}^{3} L_i(\boldsymbol{\Theta})$

Table 1.1. History of commercial trawl catch (t) and assigned quotas (t) for Pacific ocean perch stocks. Catch includes landed plus discarded catch whenever possible. Area 5ES was managed on the basis of the slope rockfish aggregate (Pacific ocean perch, yellowmouth rockfish, and rougheye rockfish) between 1983-88. An open fishing experiment was conducted in Area 5EN between 1983-90; the area was closed from 1991-97 and yields were given for reference only. In 1986, coastwide aggregate quotas were assigned to the slope aggregate. In 1989-93, species quotas were assigned on a coastwide basis and area-specific quotas reflect the contribution in the coastwide quota. Coastwide aggregate quotas were again assigned in 1994-96, and were post-allocated as area quotas for this table. In 1997-2000, the area 5E quotas for this table were divided into 5ES and 5EN values in proportion to catch. Quotas listed for years in which aggregates were assigned include other species in addition to Pacific ocean perch.

	3C		3D		5AB		5CD		5ES		5EN		Total	
Year	Catch	Quota	Catch	Quota	Catch	Quota	Catch	Quota	Catch	Quota	Catch	Quota	Catch	Quota
1979	136	50	0		1,257	2,000	370		839	600	227		2,830	2,650
1980	430	600	0		1,388	2,200	2,545		877	600	85	200	5,325	3,400
1981	550	500	0		1,623	1,500	2,226	1,800	599	600	109	200	5,108	4,400
1982	508	500	0	250	916	1,000	3,631	2,000	615	600	360	200	6,031	4,350
1983	752	500	86	250	1,485	1,000	2,223	2,000	867	aggr	292	open	5,705	3,750
1984	551	500	193	250	944	800	2,059	2,000	841	aggr	2,186	open	6,774	3,550
1985	256	300	315	350	831	850	1,967	2,000	829	aggr	1,921	open	6,119	3,500
1986	242	100	1,046	350	663	500	629	2,000	642	aggr	2,725	open	5,947	2,950
1987	566	100	450	350	1,661	500	1,914	2,000	661	aggr	1,131	open	6,383	2,950
1988	349	100	503	350	1,222	700	3,107	3,000	766	aggr	1,089	open	7,037	4,150
1989	306	150	996	400	1,187	850	1,526	3,000	586	400	1,527	open	6,127	4,800
1990	280	150	919	400	1,405	850	1,427	2,450	614	400	1,163	open	5,807	4,250
1991	41	0	809	400	872	850	2,042	2,150	644	400	0	0	4,408	3,800
1992	401	0	682	400	974	850	1,703	2,400	380	400	0	0	4,139	4,050
1993	980	150	667	400	900	850	1,557	2,400	501	400	19	0	4,624	4,200
1994	1,374	1,173	243	207	2,550	2,177	1,297	1,107	297	253	28	0	5,788	4,917
1995	810	548	106	72	2,799	1,892	1,742	1,178	805	544	49	0	6,311	4,234
1996	461	491	154	164	1,408	1,500	3,759	4,003	682	726	26	0	6,490	6,884
1997	511	431	168	230	2,270	2,358	2,413	2,818	425	418	230	226	6,016	6,481
1998	400	300	109	230	1,977	2,070	2,695	2,817	623	594	143	136	5,947	6,147
1999	471	300	128	230	2,149	2,070	2,802	2,817	590	641	81	89	6,222	6,147
2000	445	300	118	230	1,926	2,070	2,087	2,818	1,231	646	160	84	5,967	6,148

Table 2.1. Summary of research and assessment cruises for POP biomass estimation and/or collection of biological data. The number of usable bottom tows catching POP is shown by SRF area, along with total POP catch and mean catch/tow for each cruise. Numbers of POP samples currently in GFBio are provided for area 5AB and the other areas combined. N/A indicates the cruise is not archived in GFBio. A statement of purpose for each POP cruise is provided in Appendix A.

		GFBio	Biomass	Number of Usable[3] Bottom Tows by Area								POP Catch (kg)		POP Samples[4]	
Cruise Date	Vessel	Trip ID	Survey[1]	3C	3D	5AB	5CD	5EN	5ES	U.S.	Total	Total	Mean	5AB	Other
Aug. 23-Sept. 25/65	G. B. REED	N/A	QCS	14		8				52	74	60,669	820	N/A	N/A
Aug. 24-Sept. 15/66	G. B. REED	41333	QCS			15	7		1	6	29	18,260	630	N/A	N/A
Sept. 6-Oct. 4/67	G. B. REED	41313	QCS			29				11	40	35,041	876	32	12
Sept. 9-25/69	G. B. REED	41133	QCS	3		28					31	24,569	793	30	3
June 4-18/70	G. B. REED	N/A	QCS			25					25	16,442	658	N/A	0
Sept. 9-25/70	G. B. REED	41295	WCVI[2]	43							43	14,399	335	0	43
Oct. 1-29/71	G. B. REED	40657	QCS			37					37	27,385	740	36	0
Sept. 5-25/73	G. B. REED	40537	QCS			40	2				42	13,842	330	42	2
Sept. 8-27/76	G. B. REED	40057	QCS			52	4				56	62,064	1,108	50	4
Aug. 22-Sept. 8/77	G. B. REED	40037	QCS			56	2				58	16,687	288	55	2
July 7-Aug. 8/79	SCOTIA BAY	N/A	QCI[2]					42			42	62,048	1,477	0	N/A
July 12-Aug. 1/79	BLUE WATERS	N/A	QCI[2]					65			65	29,037	447	0	N/A
Sept. 7-27/79	SOUTHWARD HO	10921	QCS[2]			59					59	9,246	157	13	0
Sept. 5-24/79	ARCTIC HARVESTER	N/A	WCVI[2]	38	17						55	106,601	1,938	0	N/A
July 5-22/83	G. B. REED	N/A	QCI[2]					4			4	3,638	910	0	N/A
July 8-19/83	FREE ENTERPRISE	N/A	QCI[2]					14			14	39,726	2,838	0	N/A
Aug. 14-Sept. 11/84	G. B. REED	36864	QCS			61					61	22,563	370	31	0
Aug. 5-Sept. 9/84	EASTWARD HO	36844	QCS			42					42	31,873	759	9	0
Sept. 9-22/85	HOWE BAY	41273	WCVI[2]	74							74	38,509	520	0	20
Oct. 21-Nov. 9/85	G. B. REED	N/A	N/A	7		5	3	3	2		20	8,671	434	N/A	N/A
July 12-30/89	OCEAN SELECTOR	10378	N/A	7	4	7	11	6	5		40	165,621	4,141	6	27
June 19-30/93	W. E. RICKER	N/A	Langara					42			42	39,211	934	0	N/A
June 20-July 7/94	OCEAN SELECTOR	30744	QCS			50					50	36,376	728	54	0
Sept. 11-22/95	OCEAN SELECTOR	31244	QCS			57					57	42,227	741	62	0
Sept. 11-22/95	FROSTI	31245	QCS			54					54	30,359	562	60	0
July 2-14/96	W. E. RICKER	30864	Langara					38			38	46,897	1,234	0	33
Sept. 10-27/96	CALEDONIAN	30624	WCVI[2]	100							100	34,943	349	0	67
Sept. 5-23/97	OCEAN SELECTOR	29804	QCI[2]					66	33		99	27,768	280	0	59

1. Biomass estimates available for QCS – Queen Charlotte Sound, QCI - west coast Queen Charlotte Islands, WCVI - west coast Vancouver Island
2. Biomass estimates from surveys using different designs than the standard POP swept-area biomass design
3. Usable tows include those where catch was not significantly affected by snags, net damage or other gear failures
4. Values refer to the number of samples currently found in GFBio

Table 2.2. Other GFBio research/assessment cruises capturing POP using bottom trawls, and the number of POP biological samples archived in GFBio.

Cruise Date	Vessel	GFBio Trip ID	POP Tows[1]	POP Catch (kg) Total	POP Catch (kg) Mean	POP Samples	Main Area	Purpose of Cruise
June 9-21/80	NUCLEUS	41112	22	641	29	0	5CD	Turbot biomass survey of Hecate Strait
May 24-June 14/84	G. B. REED	38645	29	172	6	26	5CD	Hecate Strait Assemblage Survey
May 28-June 17/84	ARCTIC OCEAN	39678	5	19	4	5	5CD	Hecate Strait Assemblage Survey
May 27-June 16/87	EASTWARD HO	34426	15	2,748	183	15	5CD	Hecate Strait Assemblage Survey
Oct. 31-Nov. 24/88	EASTWARD HO	10374	5	3,378	676	0	5CD	Shelf rockfish cruise
May 24-June 13/89	EASTWARD HO	33945	23	2,265	98	22	5CD	Hecate Strait Assemblage Survey
Aug. 13-22/89	OCEAN KING	28785	3	518	173	0	3C	Pacific hake cruise
Aug. 15-25/90	HOWE BAY	28743	2	2,077	1,039	0	3C	Pacific hake cruise
May 14-23/91	W. E. RICKER	29119	5	1,664	333	3	3C	Juvenile rockfish survey
June 3-22/91	W. E. RICKER	38644	22	219	10	13	5CD	Hecate Strait Assemblage Survey
May 17-June 3/93	W. E. RICKER	30664	8	45	6	7	5CD	Hecate Strait Assemblage Survey
Aug. 18-Sept. 1/93	W. E. RICKER	24019	1	<1	<1	1	3C	Pacific hake cruise
May 23-June 9/95	W. E. RICKER	28763	13	227	17	2	5CD	Hecate Strait Assemblage Survey
Aug. 12-30/95	W. E. RICKER	25739	1	1,516	1,516	0	5AB	Pacific hake cruise
May 30-June 13/96	W. E. RICKER	27117	7	115	16	0	5CD	Hecate Strait Assemblage Survey
May 30-June7/96	STEADFAST	27118	1	<1	<1	0	5CD	Hecate Strait Assemblage Survey
July 9-15/96	ROYAL FISHER	17473	2	14	7	0	5CD	Pacific cod survey
Aug. 5-9/96	SAVAGE EAGLE	17475	1	5	5	0	5CD	Pacific cod survey
Aug. 6-12/-96	ARCTIC OCEAN	17470	1	7	7	0	5CD	Pacific cod survey
June 5-17/98	W. E. RICKER	33863	7	69	10	3	5CD	Hecate Strait Assemblage Survey
June 2-16/99	W. E. RICKER	31224	75	8,059	107	24	5AB	Queen Charlotte Sound flatfish survey
May 31-June 13/00	W. E. RICKER	34586	5	3	1	0	5CD	Hecate Strait Assemblage Survey

1. Only tows that caught POP are included

Table 2.3. POP catch and sample summary from GFBio for survey gear other than bottom trawls. The purpose of each cruise is not provided here, and was not directed at POP assessment unless noted.

Cruise Date	Vessel	GFBio Trip ID	Gear[1]	POP Tows[2]	POP Catch (kg) Total	Mean	POP Samples	Main Area
Sept. 7-27/79	SOUTHWARD HO[3]	10921	MW	14	1,277	91	26	5AB
Aug. 16-25/88	W. E. RICKER	23048	MW	3	53	18	0	5AB
Aug. 13-24/89	GAIL BERNICE3	23820	MW	5	464	93	0	5AB
Aug. 15-25/90	HOWE BAY	28743	MW	4	2,426	607	0	5AB
Aug. 17-29/90	W. E. RICKER	23976	MW	5	44	9	0	3C
Aug. 15-29/91	W. E. RICKER	24017	MW	5	164	33	0	3C
Aug. 10-31/92	W. E. RICKER	24018	MW	4	1,328	332	0	5AB
Aug. 4-12/93	W. E. RICKER	28670	MW	2	3	2	0	3C
Aug. 18-Sept. 1/93	W. E. RICKER	24019	MW	4	137	34	2	3D
June 20-July 7/94	OCEAN SELECTOR	30744	MW	5	50	10	54	5AB
Aug. 17-31/94	W. E. RICKER	24040	MW	3	162	54	4	5AB
Aug. 12-30/95	W. E. RICKER	25739	MW	4	339	85	0	5AB
July 30-Aug. 5/96	W. E. RICKER	29098	MW	1	18	18	0	3C
Aug. 10-25/97	W. E. RICKER	23717	MW	6	128	21	0	-
Sept. 7-14/97	SEA HUNT	25750	HL	1	1	1	0	5ES
Sept. 9-14/97	OCEAN PARK	25748	HL	1	2	2	0	3D
May 19-30/98	DOUBLE DECKER	25899	HL	1	1	1	0	3D
Sept. 27-Oct. 30/99	OCEAN PEARL	40589	TRAP	26	26	1	0	5AB
Aug. 3-11/00	DOUBLE DECKER	36885	HL	1	0	0	0	5ES
Aug. 8-13/00	W. E. RICKER	36804	MW	3	118	39	0	-
Jan. 11-Feb. 6/01	W. E. RICKER	38524	MW	2	15	7	0	3C

1. Gear types : HL – Hook and Line, MW - mid-water trawl, TRAP – sablefish trap
2. Only tows that caught POP are included
3. Cruise also listed in Table 2.1 using bottom trawl

Table 3.1. Major areas (1-10) with corresponding PMFC names and minor subareas (1-35). Note that minor area 10 is not defined.

Major_Area	PMFC_Area	Description	Minor Areas
1	4B	Strait of Georgia	12-20, 28, 29
2	3B[1]	Washington coast	30[1]
3	3C	Southwest Vancouver Island	21[1], 22[2], 23, 24
4	3D	Northwest Vancouver Island	25, 26, 27
5	5A	South Queen Charlotte Sound	9, 10[3], 11
6	5B	North Queen Charlotte Sound	8
7	5C	South Hecate Strait	2, 6, 7
8	5D	North Hecate Strait	1, 3, 4, 5
9	5E	West coast Queen Charlotte	31, 34, 35
10	6[1]	Alaska	32[1], 33[1]

1. US Waters: Washington (part of minor area 21, minor area 30); Alaska (minor areas 32,33)
2. Minor area 22: Nitnat Lake, not impacted by the B.C. groundfish fishery
3. Minor area 10: Historical significance unknown. Minor areas 9 and 11 span major area 5. Proposed new name: "Queen Charlotte Triangle"

Table 3.2. Locality codes within each minor area. For further details, see p. 41-50 in Rutherford (1999). The localities listed here come from the current GFCatch and PacHarvTrawl databases. These include a few code values not reported by Rutherford (1999). Code 0 denotes an unknown locality within the minor area. Code 9 denotes "other", i.e., a location in the minor area not included in the identified localities. Currently, the PacHarvTrawl database may not properly support code 9.

Major Area	PMFC Area	Description	Minor Area	Localities
1	4B	Strait of Georgia	12	0-11
1	4B	Strait of Georgia	13	0-9
1	4B	Strait of Georgia	14	0-12
1	4B	Strait of Georgia	15	0-4
1	4B	Strait of Georgia	16	0-9
1	4B	Strait of Georgia	17	0-13
1	4B	Strait of Georgia	18	0-11
1	4B	Strait of Georgia	19	0-2
1	4B	Strait of Georgia	20	0-3,6-7
1	4B	Strait of Georgia	20	3-4 (US)
1	4B	Strait of Georgia	28	0-3
1	4B	Strait of Georgia	29	0-7
2	3B	Washington coast	30	0-3
3	3C	Southwest Vancouver Island	21	0-7, 9
3	3C	Southwest Vancouver Island	23	0-19
3	3C	Southwest Vancouver Island	24	0-10
4	3D	Northwest Vancouver Island	25	0-6
4	3D	Northwest Vancouver Island	26	0-11
4	3D	Northwest Vancouver Island	27	0-9
5	5A	South Queen Charlotte Sound	9	0-2
5	5A	South Queen Charlotte Sound	11	0-12
6	5B	North Queen Charlotte Sound	8	0-15
7	5C	South Hecate Strait	2	0-10
7	5C	South Hecate Strait	6	0-10
7	5C	South Hecate Strait	7	0-4
8	5D	North Hecate Strait	1	0-5
8	5D	North Hecate Strait	3	0-6
8	5D	North Hecate Strait	4	0-12
8	5D	North Hecate Strait	5	0-6, 9
9	5E	West coast Queen Charlotte Islands	31	0-15
9	5E	West coast Queen Charlotte Islands	34	0-5
9	5E	West coast Queen Charlotte Islands	35	0-7
10	6	Alaska	32	0-7
10	6	Alaska	33	0-2

Table 3.3. Definitions of historical areas for slope rockfish assessment and management. Multiple rows indicate multiple criteria for a definition. The symbol "*" denotes all possibilities available, given the higher level geographic strata.

Area	Description	Major Area	PMFC	Minor Areas	Localities
SG	Straight of Georgia	1	4B	*	*
3C	Southwest Vancouver Island	3	3C	*	*
		4	3D	25	*
3D	Northwest Vancouver Island	4	3D	26, 27	*
5AB	Queen Charlotte Sound	5	5A		
		6	5B	8	0-5, 7-10, 13
5CD	Hecate Strait	6	5B	8	6, 11-12, 14-15
		7	5C	*	*
		8	5D	*	*
5ES	West QCI	9	5E	31, 34	*
5EN	North QCI	9	5E	35	*

Table 3.4. Definitions of historical POP gullies, used in stock assessments by Leaman and Richards. Multiple rows indicate multiple criteria for a definition. The symbol "*" denotes all possibilities available, given the higher level geographic strata.

Area	Description	Major Area	PMFC	Minor Areas	Localities
GS	Goose Island Gully	5	5A	*	*
		6	5B	8	0-2, 7-10, 13
MI	Mitchell's Gully	6	5B	8	3-5
MR	Moresby Gully	6	5B	8	6, 11-12, 14-15
		7	5C	*	*
		8	5D	*	*

Table 4.1. Parameter estimates from the catch-age model for Goose Island Gully (Appendix B) with a fixed variance ratio ρ. The model uses 23 age classes $a = 1,\ldots,23$ corresponding to true ages $a' = 7,\ldots,29$ and 38 years $t = 1,\ldots,38$ corresponding to the true year $y = 1963,\ldots,2000$.

Parameter	Estimate	Dimensions
ρ	0.9	
σ_1	0.590208	
τ_1	0.196736	
τ_2	0.417091	
M	0.055695	
α	6.16482	
β_1	0.130610	
q_1	0.359749	
q_2	0.553071	
γ	0.745408	
R	4.40088	10^6 fish
R_1	6.38162	10^6 fish
R_{38}	3.64091	10^6 fish
B_1	70.1188	10^6 kg
B_{38}	39.2560	10^6 kg

Table 6.1. Summary output table for POP GLM analysis by area and by model type. Positive catch model is a log-normal model regressing the log(catch/[hours_fished]) against the indicated independent variables and the binomial model is a logit model which uses the presence/absence of POP catch as the dependent variable. The order of acceptance into the final model for each of the five independent variables used is indicated (– means not accepted into the model). The proportion of the total residual deviance explained by each model is shown in the final column.

		Model Independent Variables					
Area	Model	Fishing Year	50 m Depth Band	Month	Vessel	Area Variable	Proportion Deviance Explained
Queen Charlotte Islands[3]	Positive catch	1	2	–	4	3	0.50
	Binomial	1	2	5	4	3	0.34
Moresby	Positive catch[2]	1	5	3	4	2	0.43
	Binomial[3]	1	2	3	5	4	0.46
Goose Island & Mitchell[1]	Positive catch	1	2	4	5	3	0.25
	Binomial	1	4	3	5	2	0.33
Old Goose Definition[1]	Positive catch	1	3	4	5	2	0.25
	Binomial	1	4	3	5	2	0.34
WCVI[1]	Positive catch	1	2	4	5	3	0.35
	Binomial	1	2	3	5	4	0.31
Total B.C.[2]	Positive catch	1	3	5	4	2	0.30
	Binomial	1	2	4	–	3	0.35

1. Area variable: 10 km^2 grid
2. Area variable: 40 km^2 grid
3. Area variable: 25 km^2 grid

Table 7.1. Relationships among the various SRF areas and the newly defined POP areas. Shared area (km²) is defined as the number of 1-km² grid blocks that experienced some POP catch from Jan 1994 to Mar 2001 in both SRF and POP polygons. Shared catch (t) is the total catch of POP from Jan 1994 to Mar 2001 common to both SRF and POP polygons. Shared effort (t) is the total effort of tows catching POP from Jan 1994 to Mar 2001 common to both SRF and POP polygons.

	SRFA	POP-QCI	POP-MR	POP-MI	POP-GS	POP-NVI	POP-SVI	Total
Area (km²)	3C						1,644	**1,644**
	3D					209	73	**282**
	5AB			542	2,508	152		**3,202**
	5CD	629	2,416	219				**3,264**
	5EN	416						**416**
	5ES	423	56					**479**
	Total	**1,468**	**2,472**	**761**	**2,508**	**361**	**1,717**	**9,287**
Catch (t)	3C						3,856	**3,856**
	3D					940	13	**953**
	5AB			2,315	10,893	289		**13,496**
	5CD	772	15,391	424				**16,587**
	5EN	723						**723**
	5ES	3,960	891					**4,852**
	Total	**5,455**	**16,283**	**2,738**	**10,893**	**1,229**	**3,869**	**40,466**
Effort (h)	3C						16,306	**16,306**
	3D					2,804	207	**3,011**
	5AB			2,864	20,039	842		**23,745**
	5CD	2,288	21,397	804				**24,490**
	5EN	2,458						**2,458**
	5ES	4,298	554					**4,852**
	Total	**9,044**	**21,951**	**3,668**	**20,039**	**3,645**	**16,513**	**74,861**

Table 7.2. Coastwide quota allocation based on the relationship of swept-area biomass in Goose Island Gully to swept-area biomass in the SRF areas. We calculate the mean biomass estimate B3 for all SRF areas and GS using the lower biomass estimates from the latter three years (1998-2000). We then re-allocate the coastwide 2000 quota of 6148 t to Qnew using the ratios of SRF B3 to Total B3. GS Qnew is apportioned from 5AB Qnew using the ratio of GS B3 to 5AB B3. Further, using GS B3 as a standard, we can scale any given GS quota (Qlow, Qmid, Qhigh) into SRF quotas using the ratios of SRF B3 to GS B3.

Area	1998	1999	2000	B3	Quota	Qnew	Qlow	Qmid	Qhigh
3C	2,496	1,751	3,041	2,429	300	751	492	738	984
3D	226	194	393	271	230	84	55	82	110
5AB	5,610	5,944	7,333	6,296	2,070	1,945	1,275	1,913	2,551
5CD	9,044	7,372	9,451	8,622	2,818	2,664	1,747	2,620	3,494
5ES	1,852	2,754	795	1,801	563	556	365	547	730
5EN	475	452	504	477	167	147	97	145	193
Total	**19,704**	**18,466**	**21,518**	**19,896**	**6,148**	**6,148**	**4,031**	**6,046**	**8,062**
GS	4,455	4,620	5,733	4,936	1,623	1,525	1,000	1,500	2,000

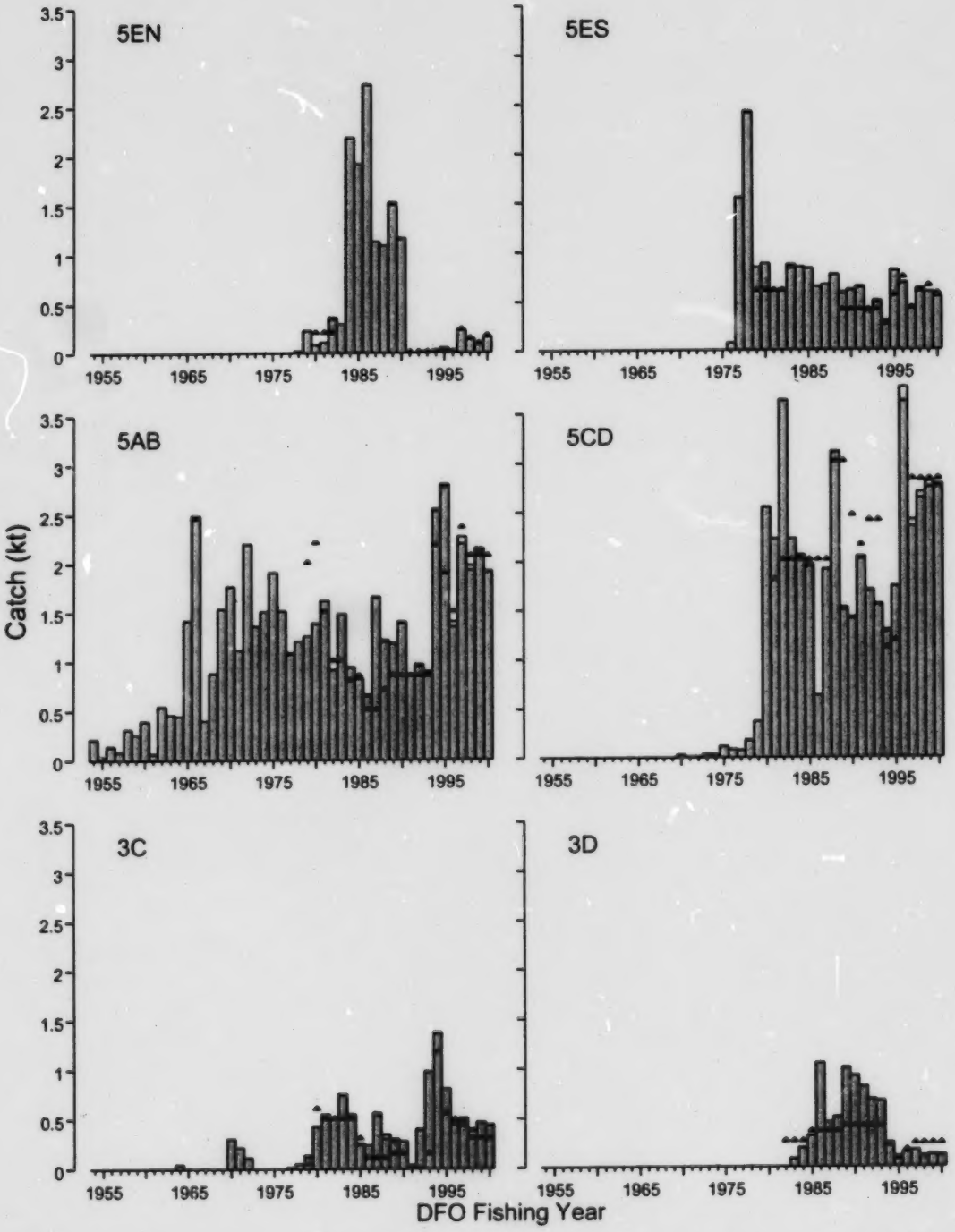

Figure 1.1. POP catch by Canadian groundfish trawlers in specified SRF areas and DFO fishing years (1954-2000). Each year comprises a lower green bar of landed catch (kt) and an upper yellow bar of estimated discarded catch (yellow). Red triangles denote quotas set by DFO management.

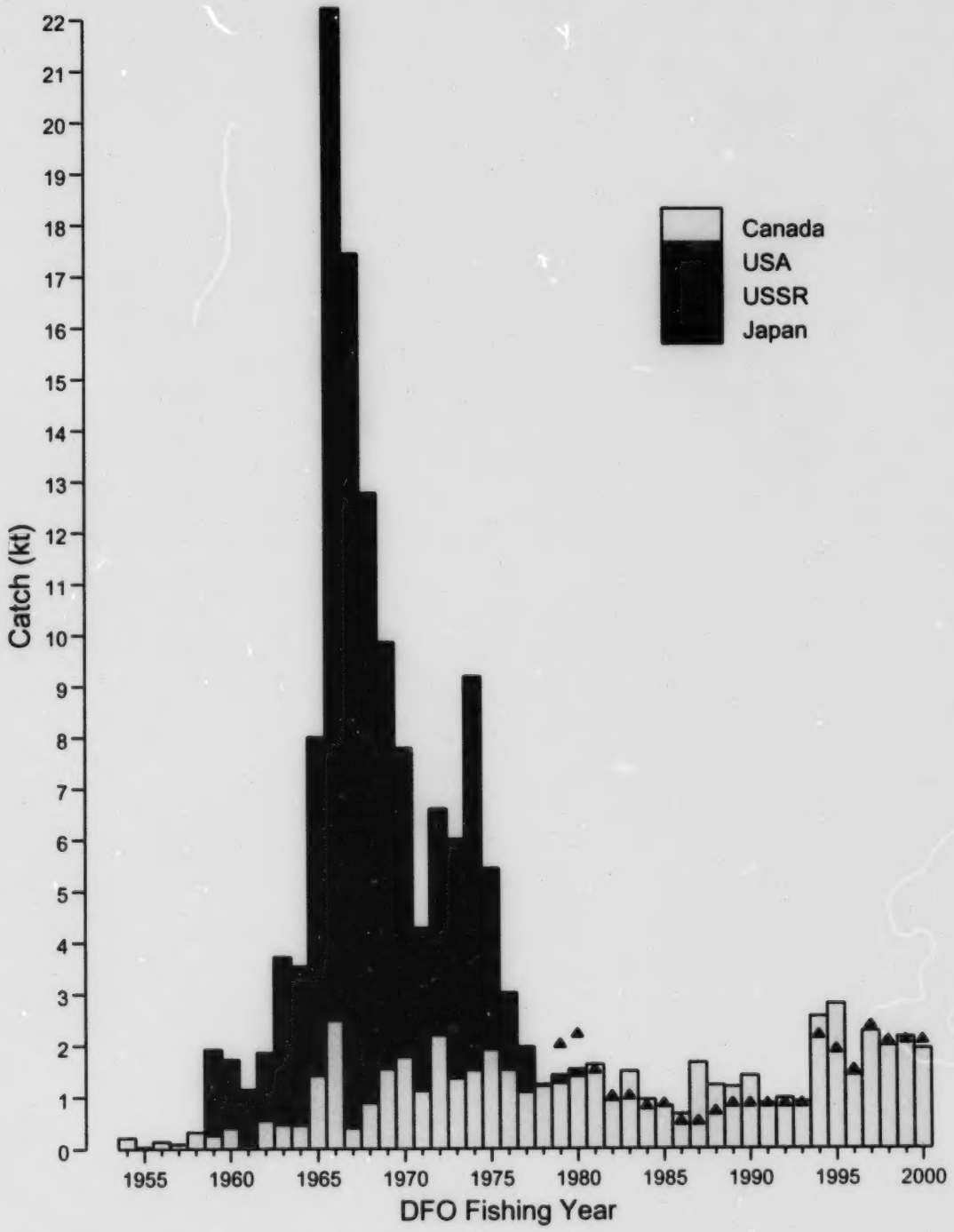

Figure 2.1. Catch history of POP in SRF area 5AB by DFO fishing year (1954-2000). Catches (kt) are broken down by nationality – domestic Canadian (yellow), USA (green), Russia (red), and Japan (blue). Red triangles denote domestic Canadian quotas set by DFO management.

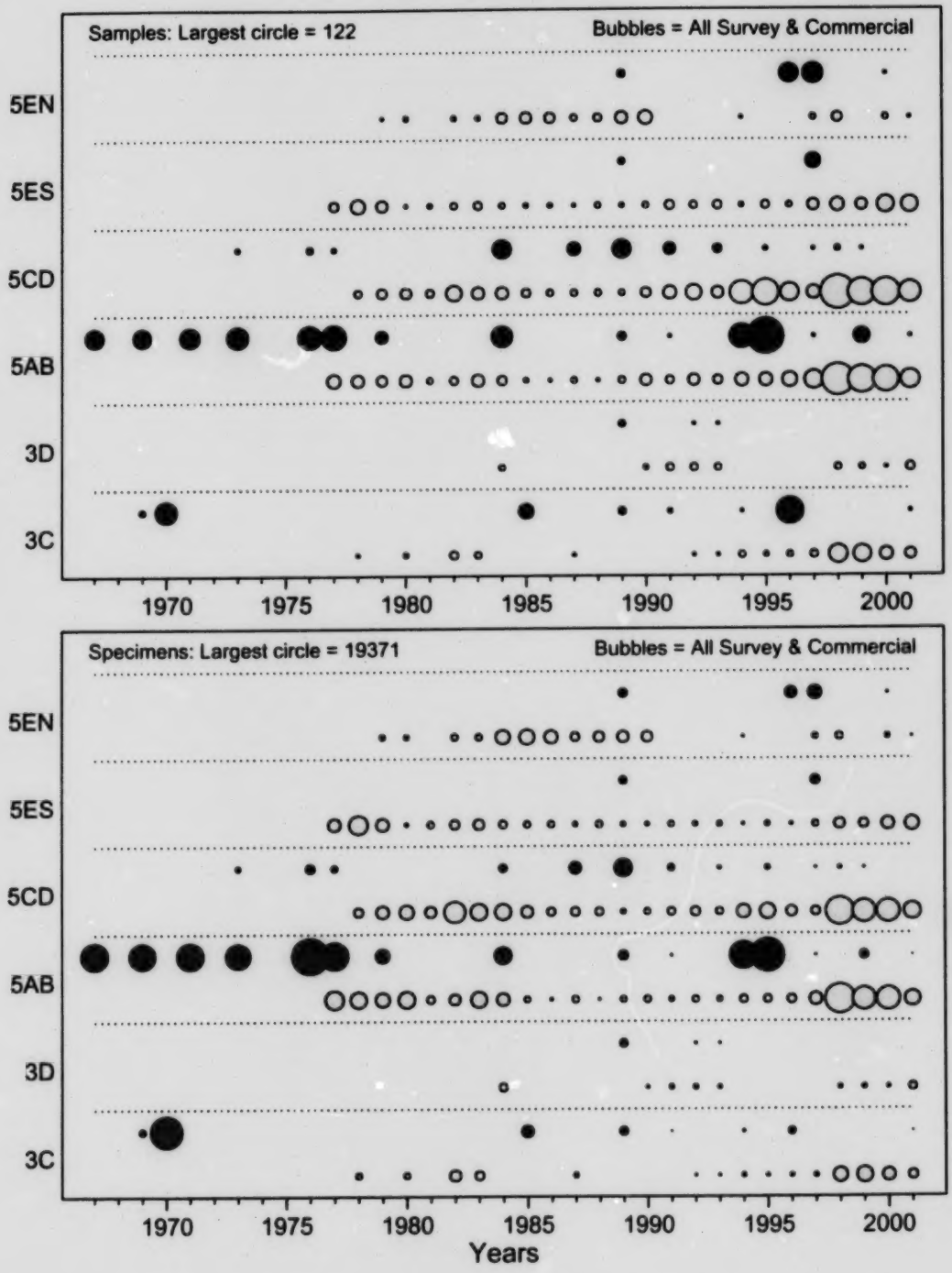

Figure 2.2. Number of survey (blue) and commercial (yellow) samples (upper panel) and specimens (lower panel) recorded in the GFBio database by SRF area and calendar year. Bubble area is proportional to number.

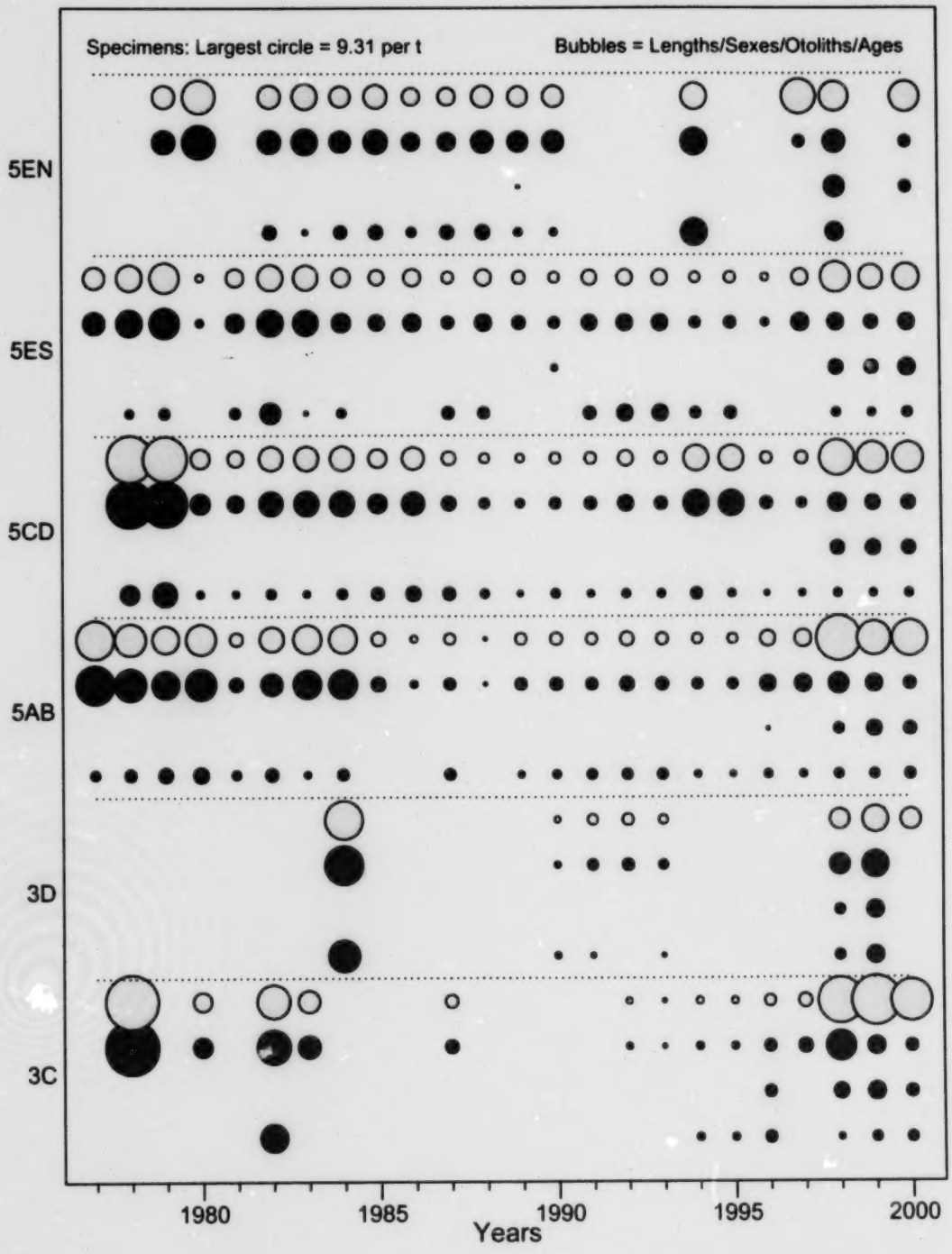

Figure 2.3. Number of commercial specimens indicated in the GFBio database with recorded body length (yellow), sex as male/female (green), otolith pairs extracted (red), and age (blue) by SRF area and calendar year. Bubble area is proportional to number.

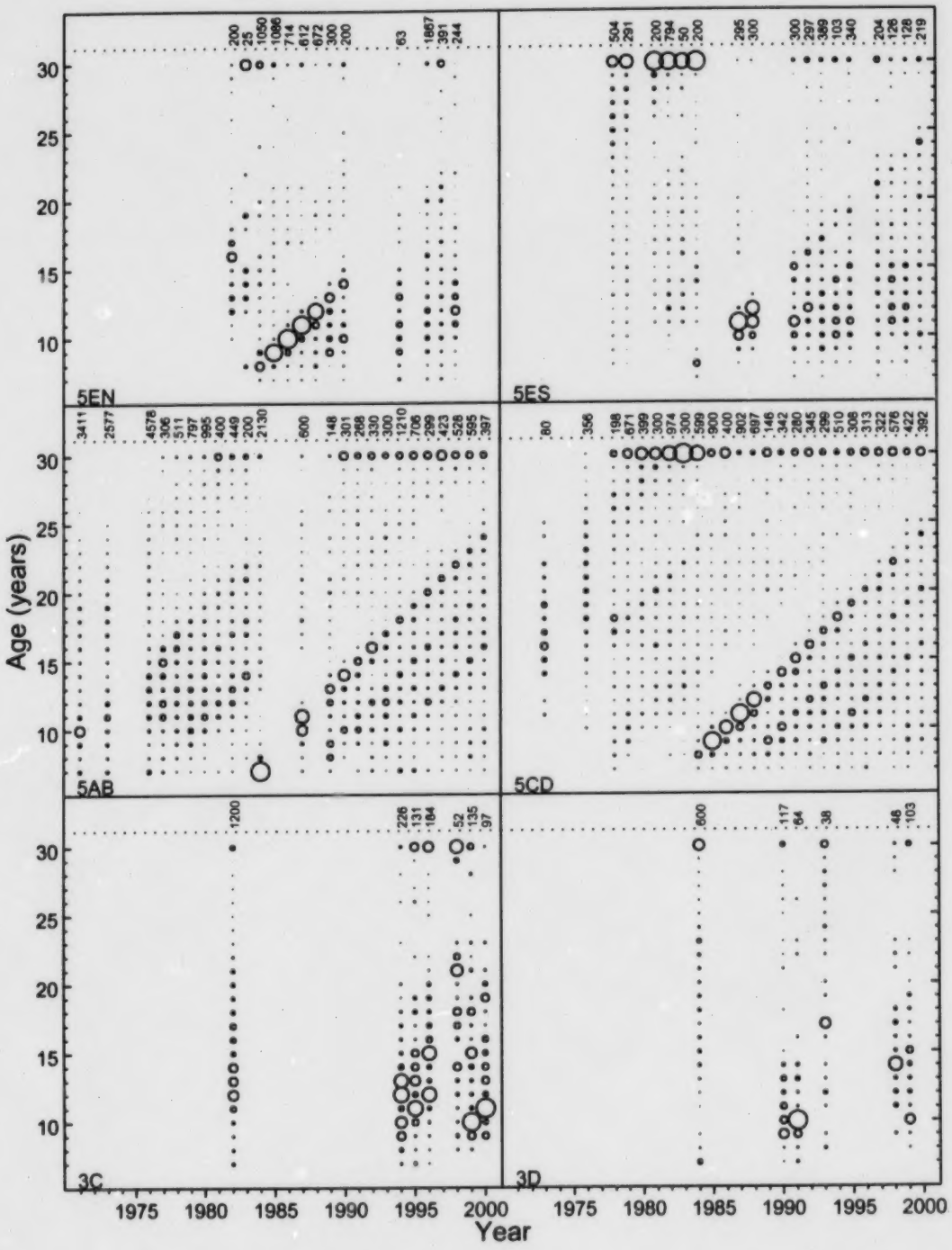

Figure 2.4. Bubble plots of proportion-at-age for POP in SRF areas by calendar year. Proportions are stratified by sample. Samples come from commercial fishery, research cruises and charter surveys. Ages below 7y are excluded. Ages ≥ 30y are aggregated.

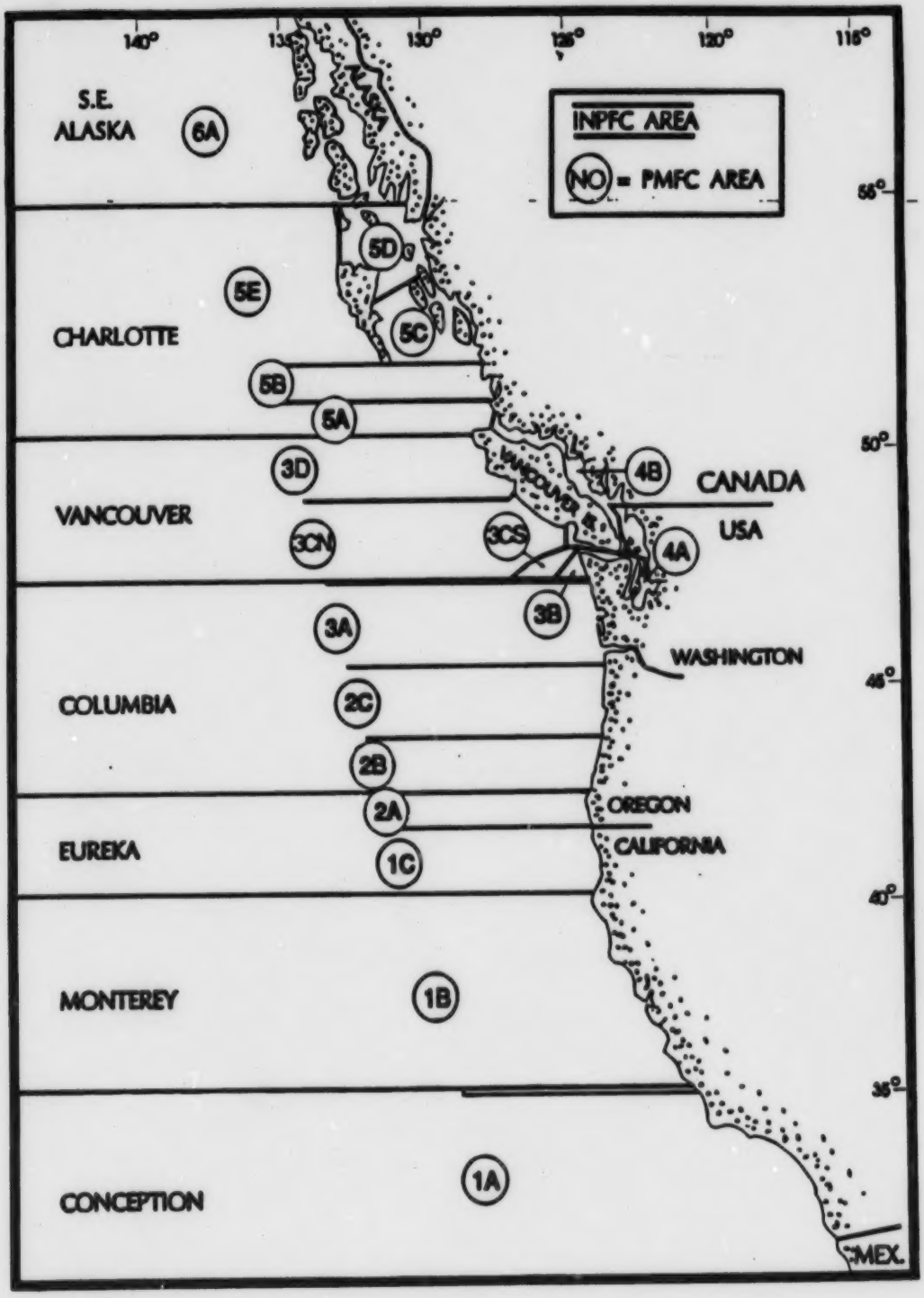

Figure 3.1. International North Pacific Fisheries Commission (INPFC) and Pacific Marine Fisheries Commission (PMFC) catch reporting areas (reproduced from Tagart 1991).

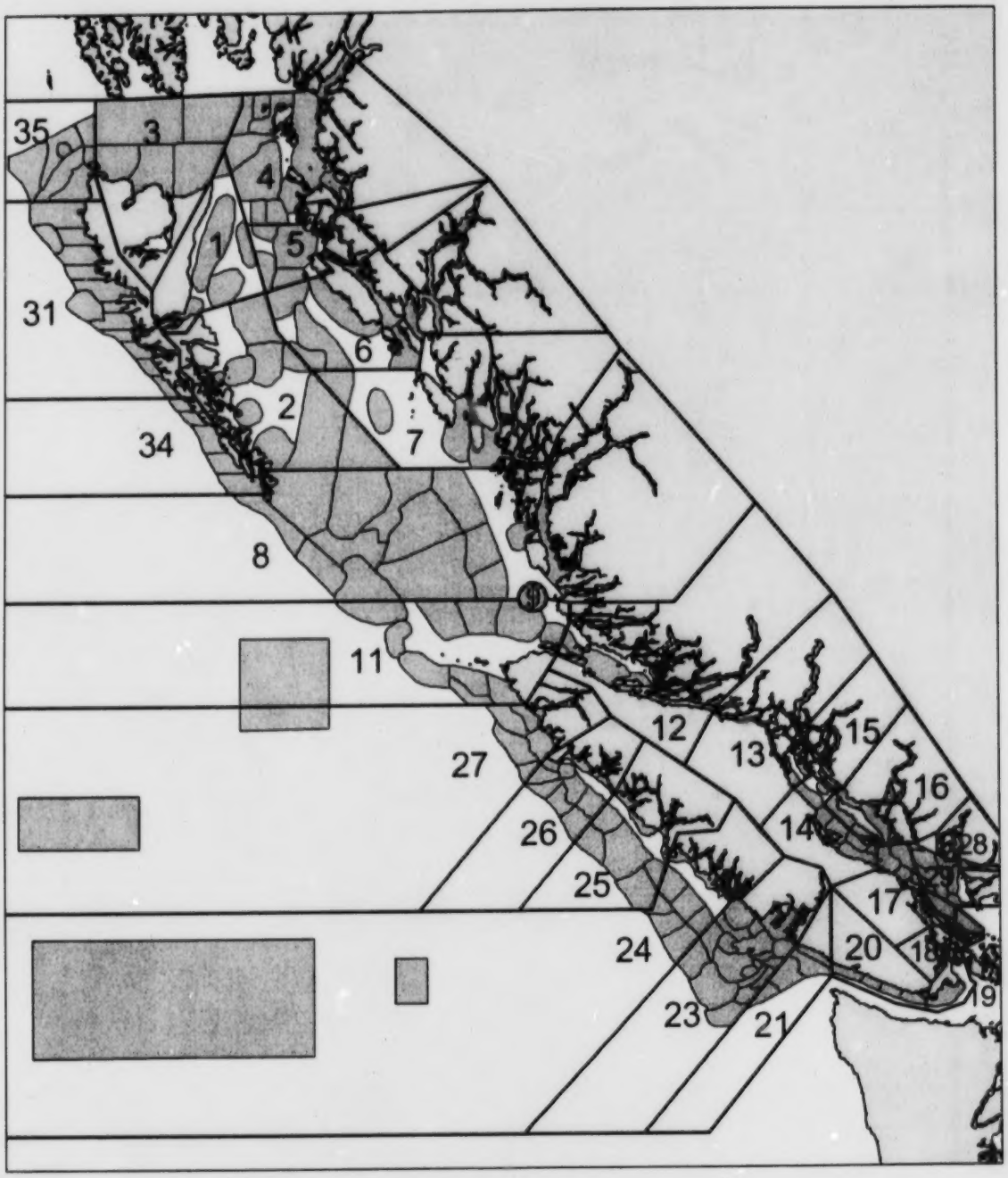

Figure 3.2. Polygons outlining major PMFC areas (blue), minor PMFC areas (red) and fishing localities (grey) along the B.C. coast (see Rutherford 1999 for details). Numbers identify the minor PMFC areas.

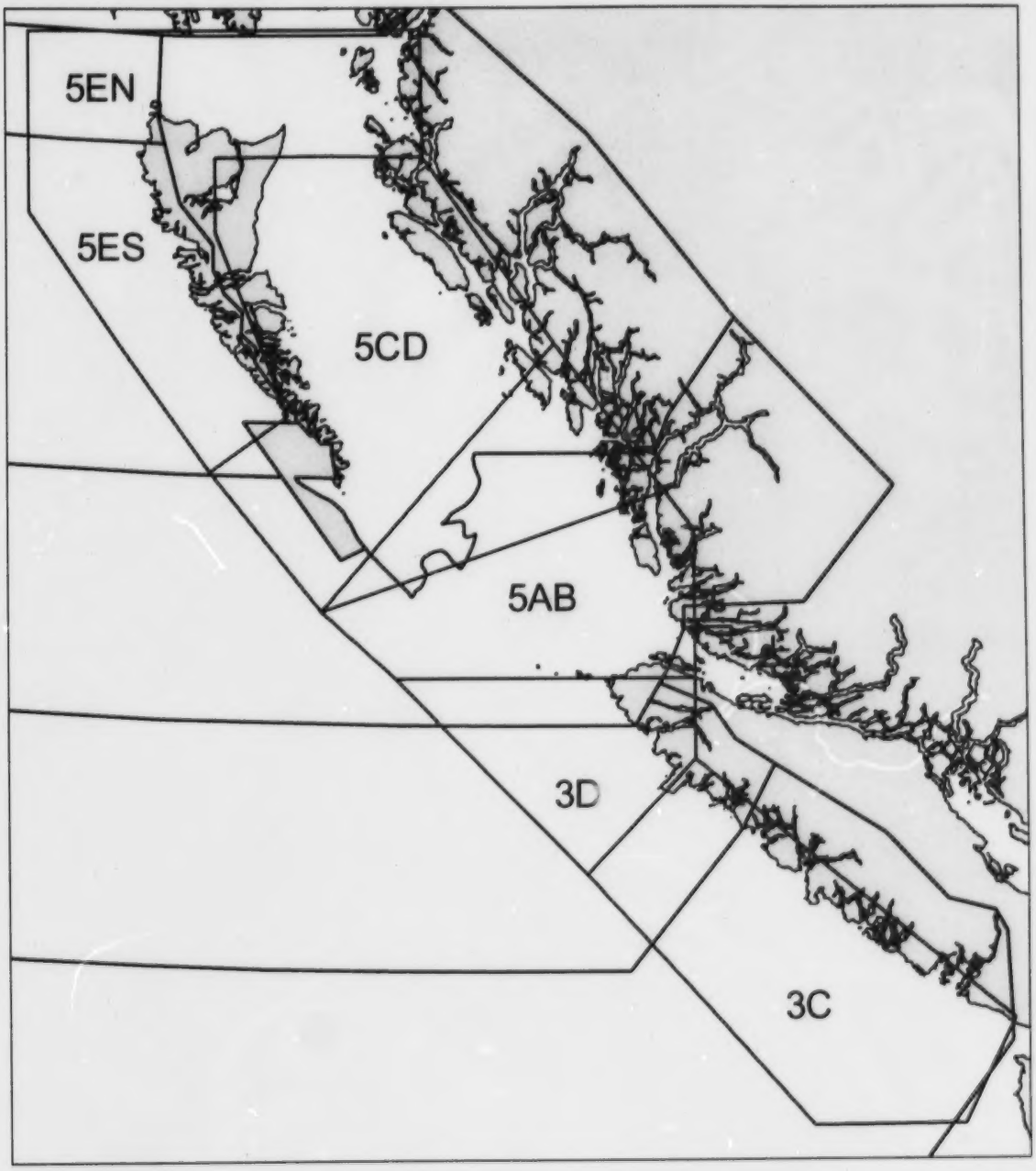

Figure 3.3. Slope rockfish assessment polygons (blue) and newly-defined POP polygons (red). Note the polygon highlighted in yellow is a recent DFO management change that allocates parts of 5AB and 5ES to 5CD. The new 5CD boundary became effective April 1, 2000.

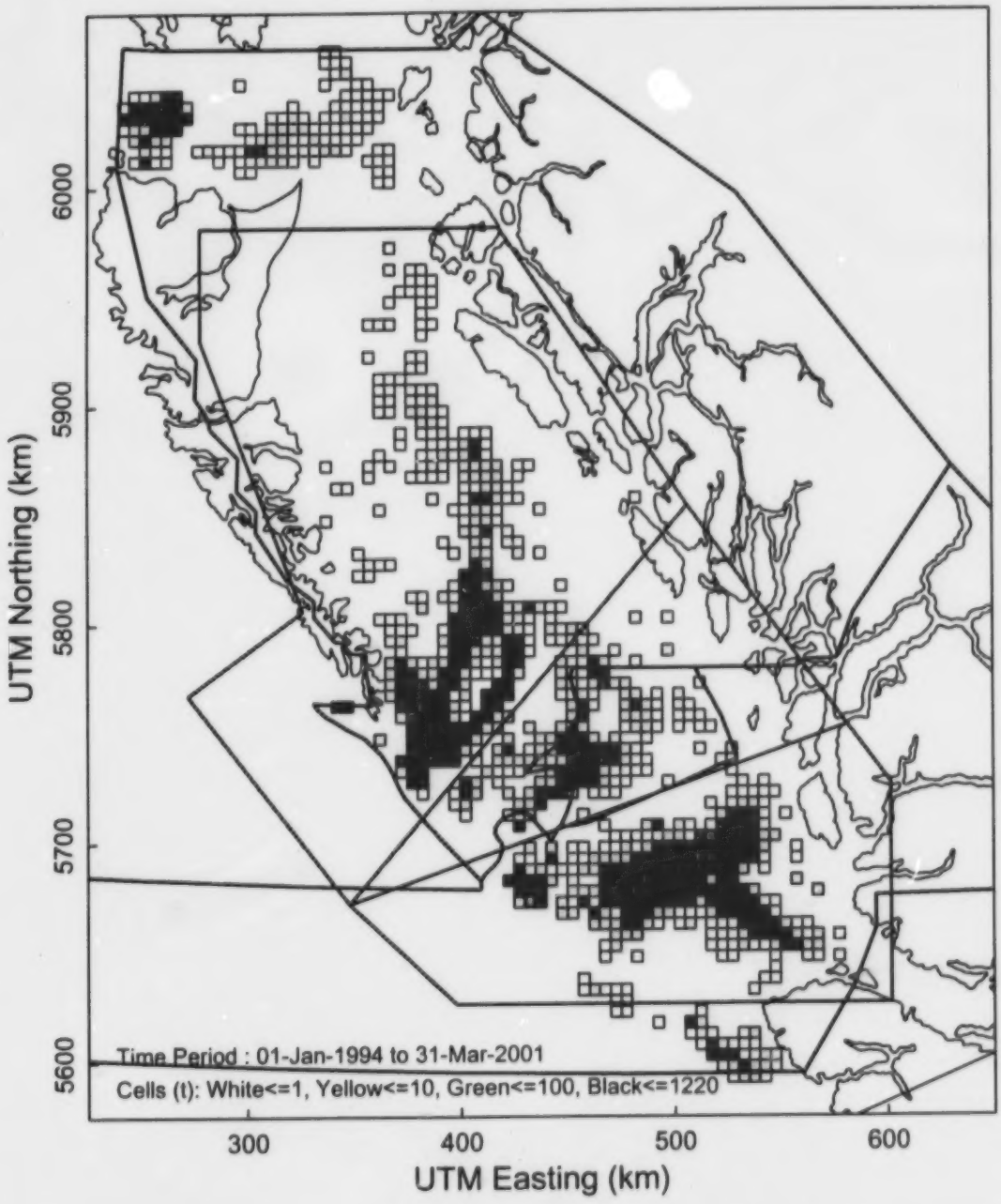

Figure 3.4. Historical SRF gully polygons (outlined in blue – MR = Moresby, MI = Mitchell's, GS = Goose Island) with total catch C in 5 km² UTM grid cells from Jan 1994 to Mar 2001. Coloured grid cells denote the following catch – White: $C \leq 1$ t, Yellow: $1 \text{ t} < C \leq 10$ t, Green: $10 \text{ t} < C \leq 100$ t, and Black: $C > 100$ t. Superimposed are the three corresponding POP polygons (outlined in red – POP-MR, POP-MI, POP-GS).

Figure 3.5. Newly-defined POP polygons based partly on bottom bathymetry.

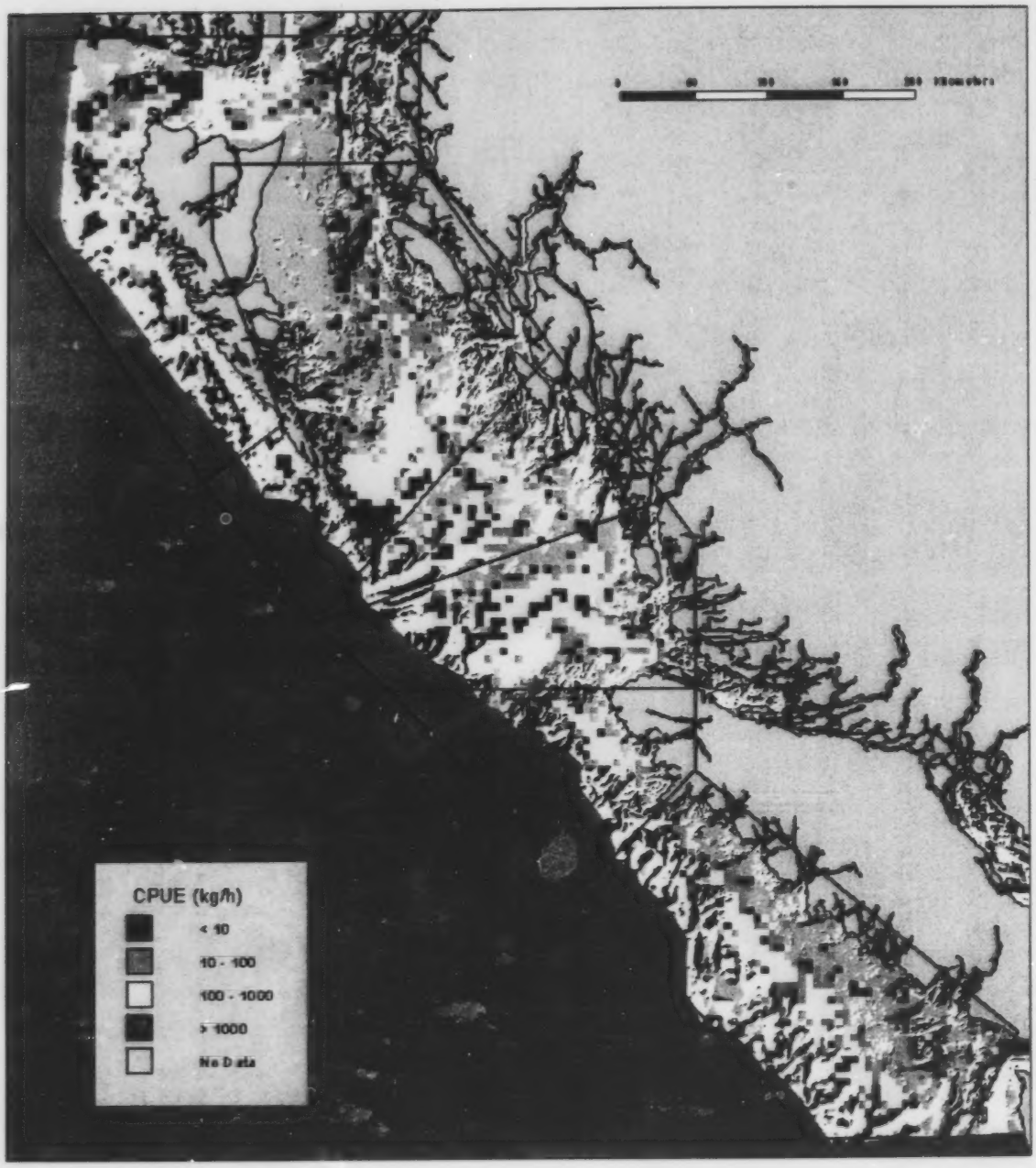

Figure 3.6. Newly-defined POP polygons based chiefly on patterns of mean CPUE (kg/h) from Jan 1994 to Mar 2001 in 5 km^2 grid cells. Grid colours depict POP density, where red cells denote areas of high density.

Figure 3.7. Newly-defined POP polygons and their relation to patterns of total catch (t) from Jan 1994 to Mar 2001 in 5 km² grid cells. Grid colours depict POP catch abundance, where red cells denote areas of high catch.

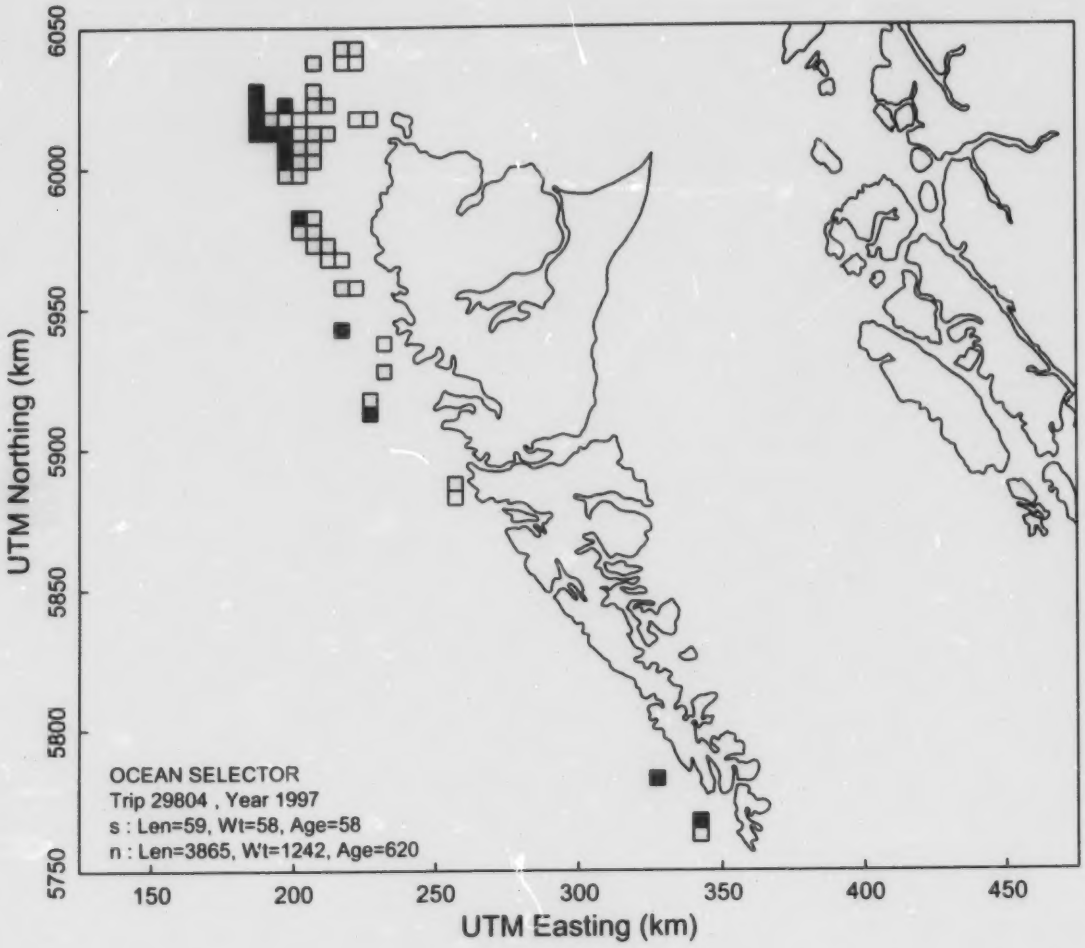

Figure 3.8. Example of a survey cruise designed to estimate POP abundance along the NW coast of Queen Charlotte Islands. Catch from the 1997 charter trip aboard the Ocean Selector is presented in 5 km² grid cells. Colours denote the following catch – White: $C \leq 50$ kg, Yellow: 50 kg $< C \leq 500$ kg, Green: 500 kg $< C \leq 5000$ kg, and Black: $C > 5000$ kg. From this cruise, researchers obtained 58 age samples, comprising 620 specimens.

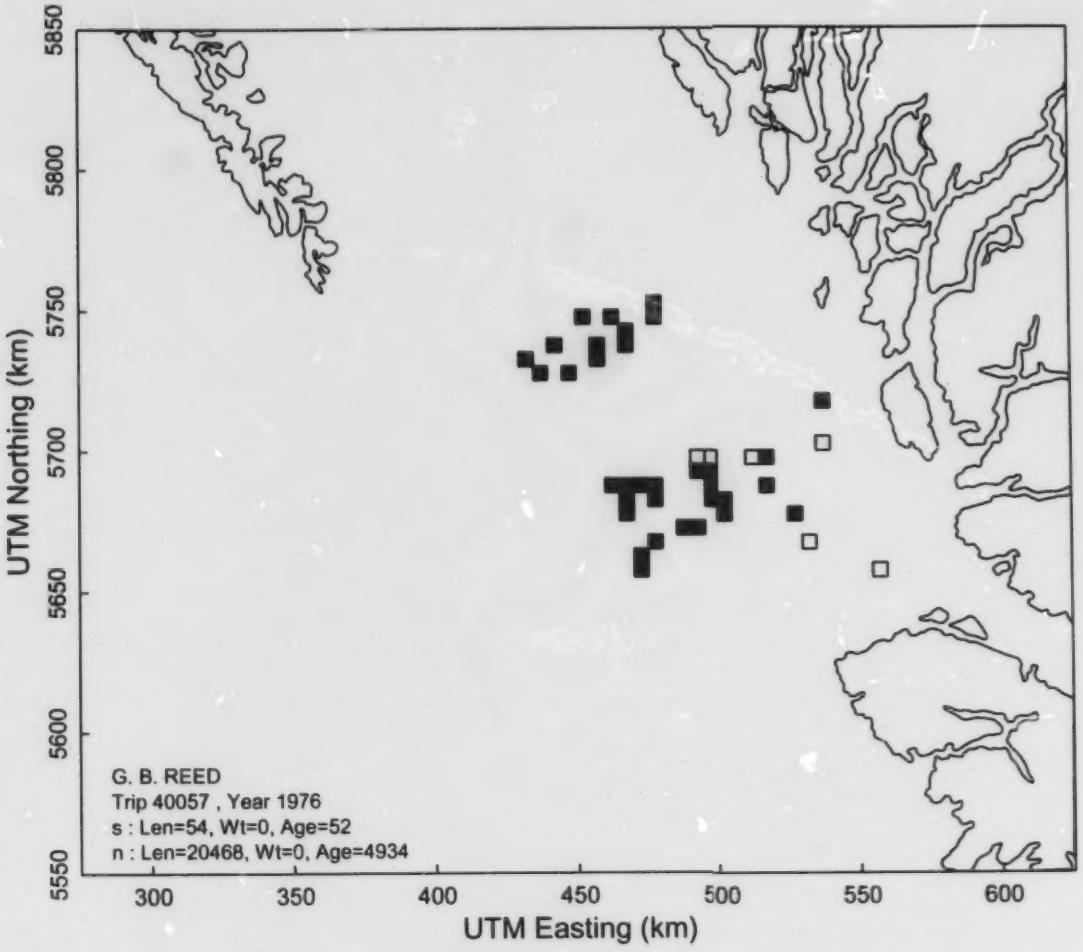

Figure 3.9. Example of a survey cruise designed to estimate POP abundance along the central coast of B.C. Catch from the 1976 research trip aboard the G. B. Reed is presented in 5 km² grid cells. Colours denote the following catch – White: $C \leq 50$ kg, Yellow: 50 kg $< C \leq 500$ kg, Green: 500 kg $< C \leq 5000$ kg, and Black: $C > 5000$ kg. From this cruise, researchers obtained 52 age samples, comprising 4934 specimens.

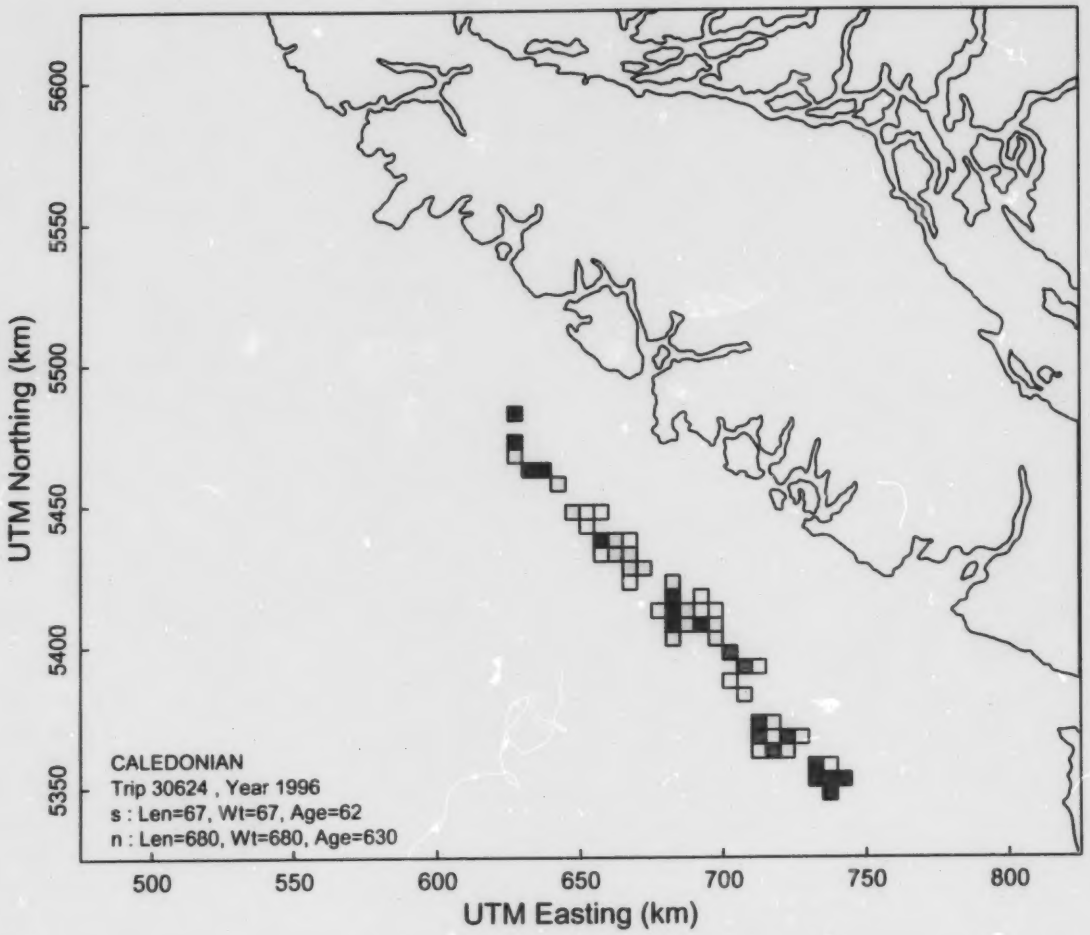

Figure 3.10. Example of a survey cruise designed to estimate POP abundance along the west coast of Vancouver Island. Catch from the 1996 charter trip aboard the Caledonian is presented in 5 km² grid cells. Colours denote the following catch – White: $C \leq 50$ kg, Yellow: $50 \text{ kg} < C \leq 500$ kg, Green: $500 \text{ kg} < C \leq 5000$ kg, and Black: $C > 5000$ kg. From this cruise, researchers obtained 62 age samples, comprising 630 specimens.

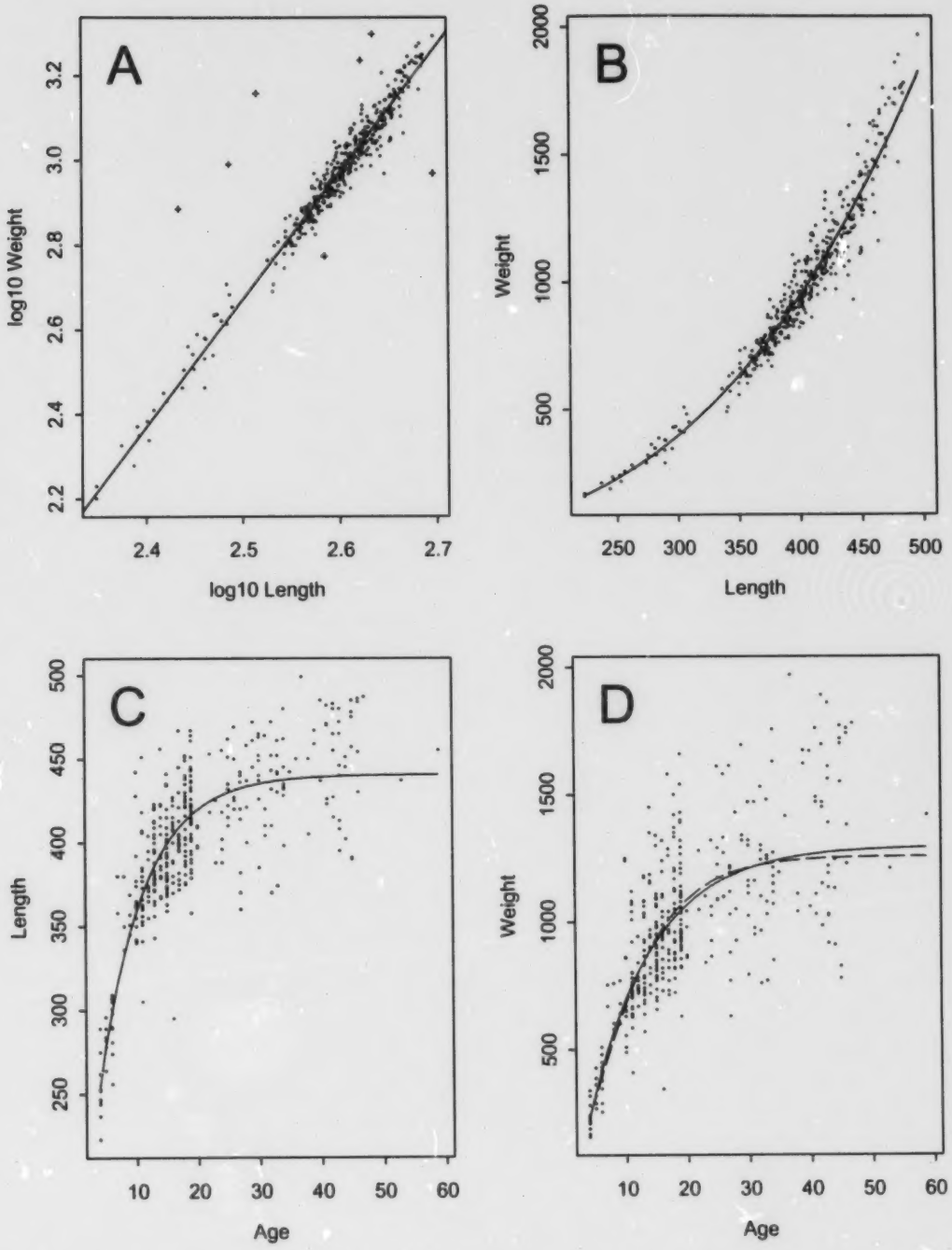

Figure 4.1. Analysis of length (mm), weight (g), and age. (A) The indicated line has slope 3 and passes through the data means. (B) The cubic curve is defined by (4.1). (C) The asymptotic curve satisfies the von Bertalanffy relationship (4.2). (D) The dashed red curve combines (4.2) and (4.1), The solid green curve satisfies (4.3). Seven outliers marked + in panel A are excluded from the remaining analyses.

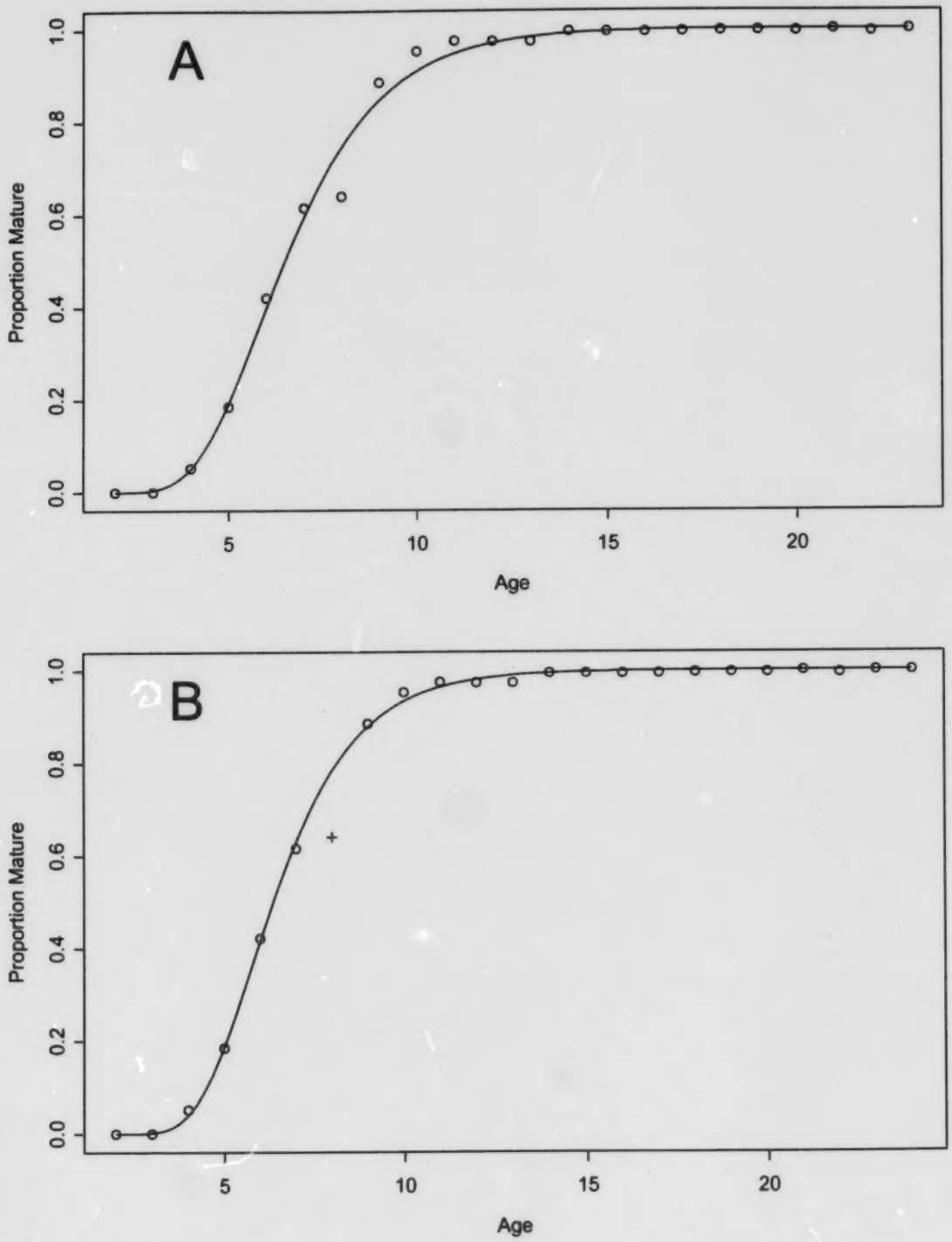

Figure 4.2. Maturity vs. age. (A) A fit through all data. (B) The curve (4.4), which fits all data except an outlier at age 8.

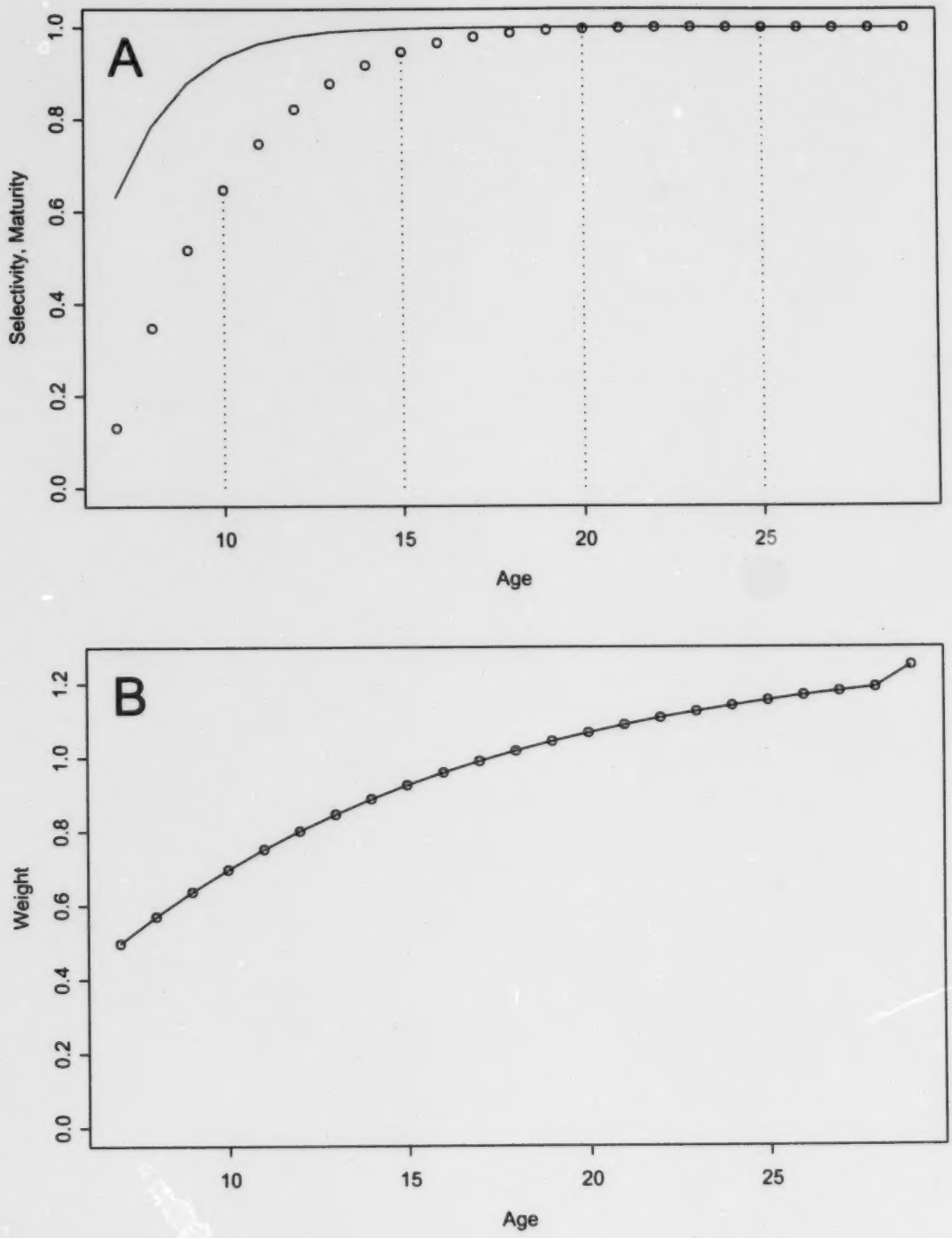

Figure 4.3. (A) Estimated selectivity (points) compared with maturity (red curve). (B) Weight (kg) vs. age, showing the correction (M.6) in Table B.2 for a plus class at age 29.

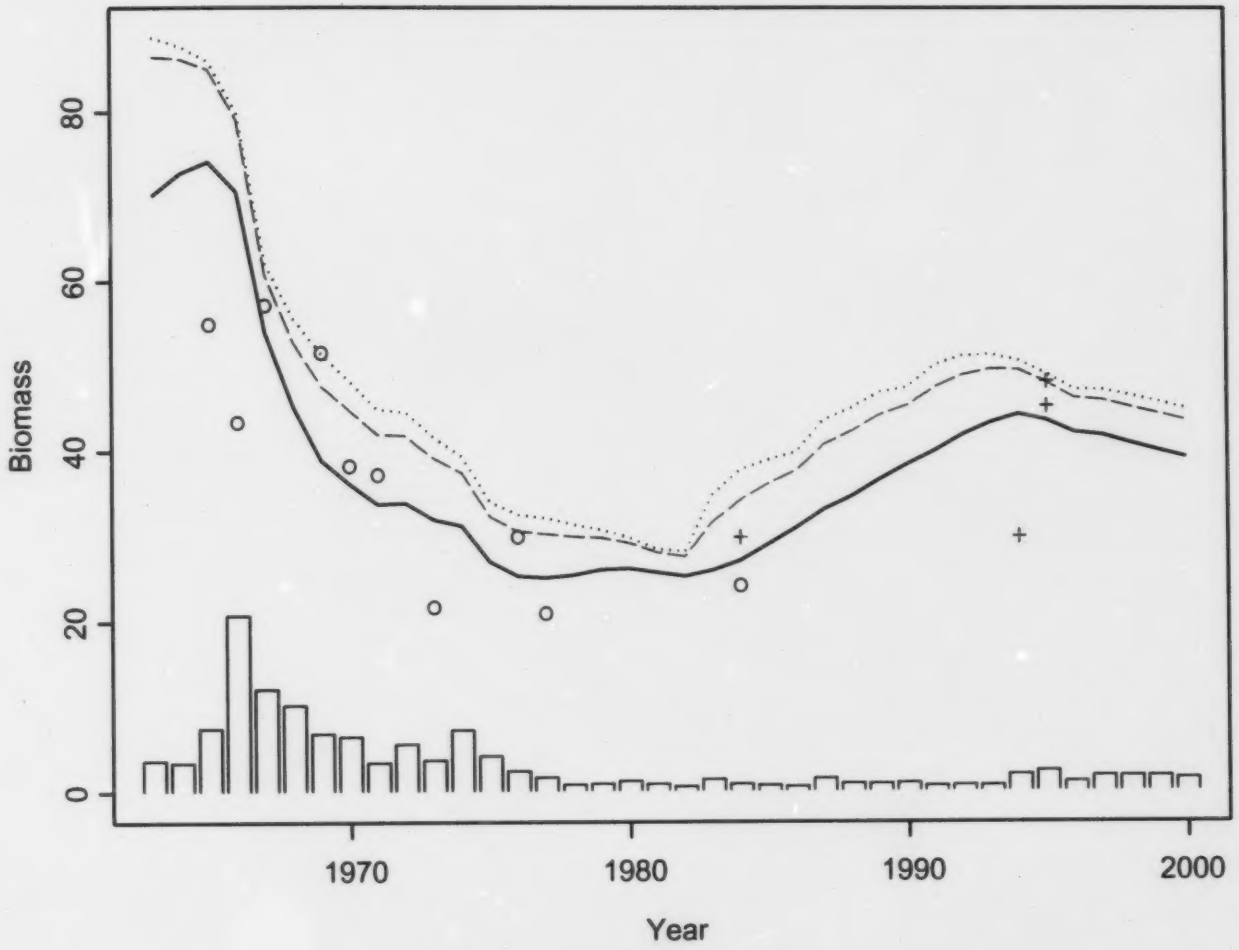

Figure 4.4. Annual biomass estimates: available to the fishery (solid black line); mature (dashed red line); total (dotted green line). Circles indicate research survey estimates, scaled to available biomass by q_1. Plus symbols indicate charter survey estimates, scaled with q_2. The blue bar plot represents annual catches, as in Fig. 2.1.

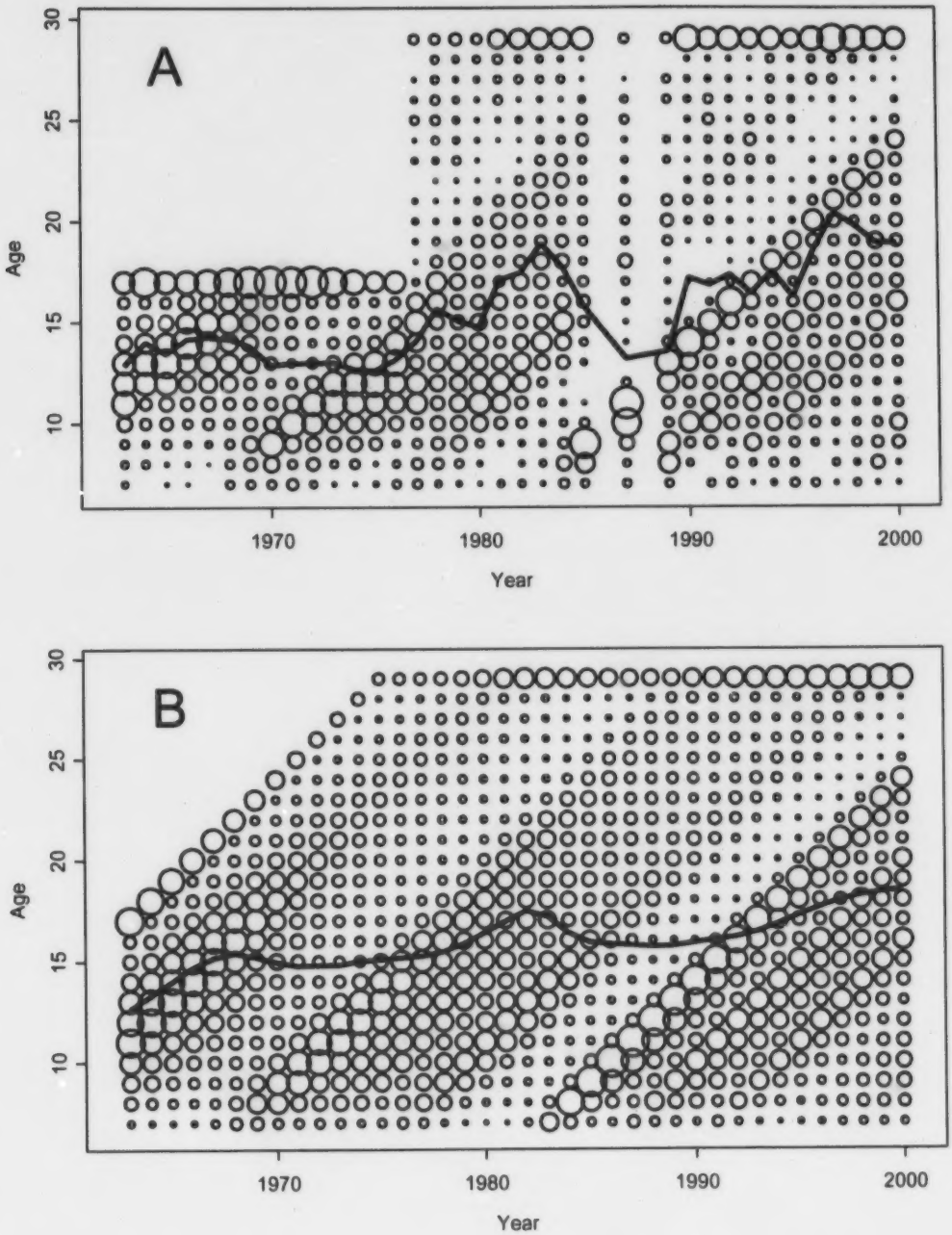

Figure 4.5. (A) Bubble plot representing observed ages in the historical GIG fishery, where values from 1985 come from a survey by the G. B. Reed (Richards and Olsen 1996). No age data are available for 1986 or 1988; see also SRF area 5AB in Fig. 2.4. Plus classes at ages 17 and 29 correspond to surface and break-and-burn ageing methods. (B) Predicted ages from the model, with a graduated plus class between ages 17 and 29. Red lines in the two panels represent the annual mean age.

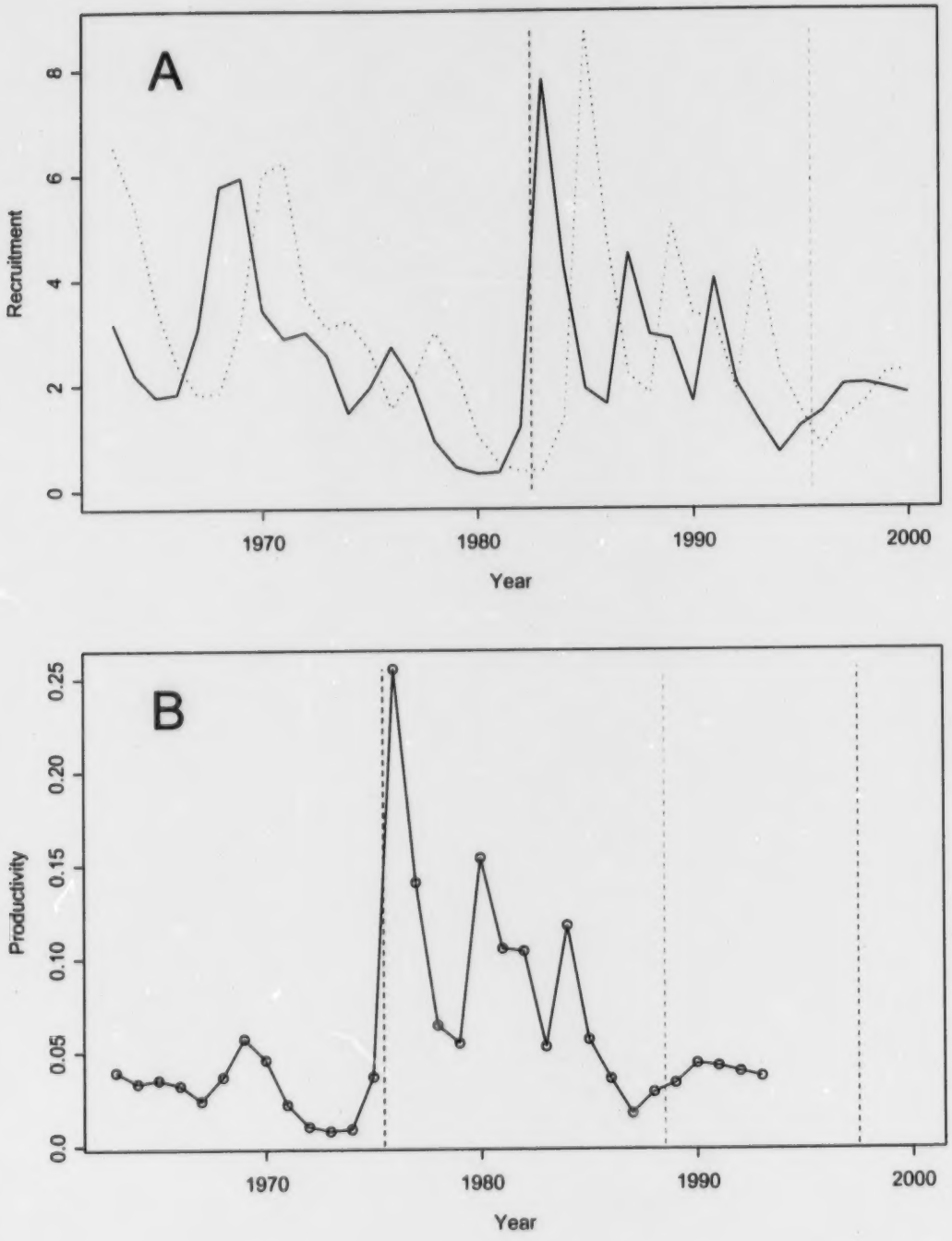

Figure 4.6. (A) Recruitment (10^6 fish) at ages 7 (solid black line) and 9 (dotted blue line). (B) Productivity computed from (4.5), with regime shifts indicated by vertical green, red, and blue lines from left to right. These translate 7 years forward in panel A to represent their influence on age 7 recruitment.

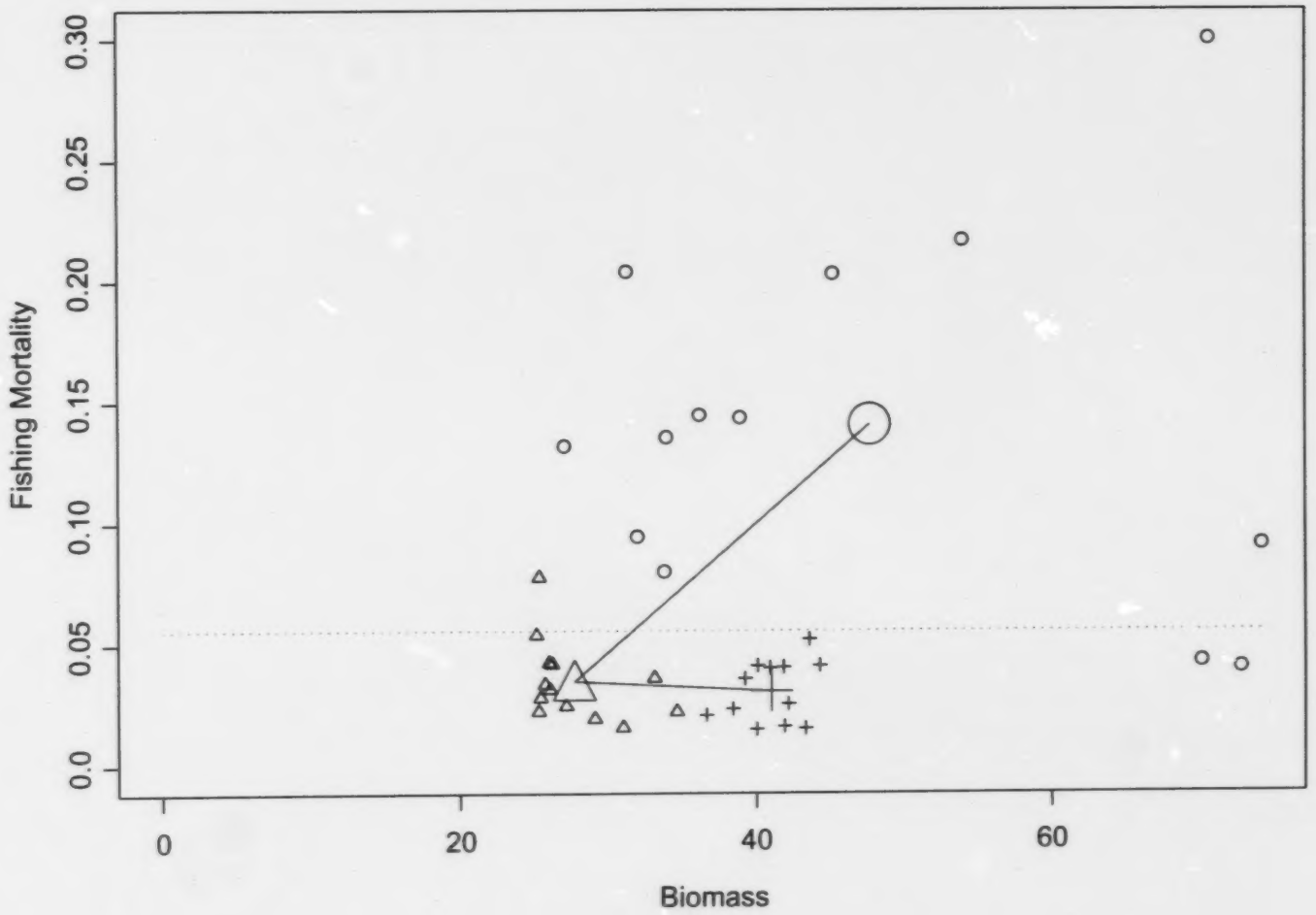

Figure 4.7. Fishing mortality vs. biomass (kt), showing progress through three regimes: 1963–1975 (circles); 1976–1988 (triangles); 1989–2000 (plus symbols). Large red symbols denote means for each period, as tracked by a red line. A dotted blue line indicates the estimated natural mortality $M = 0.056$.

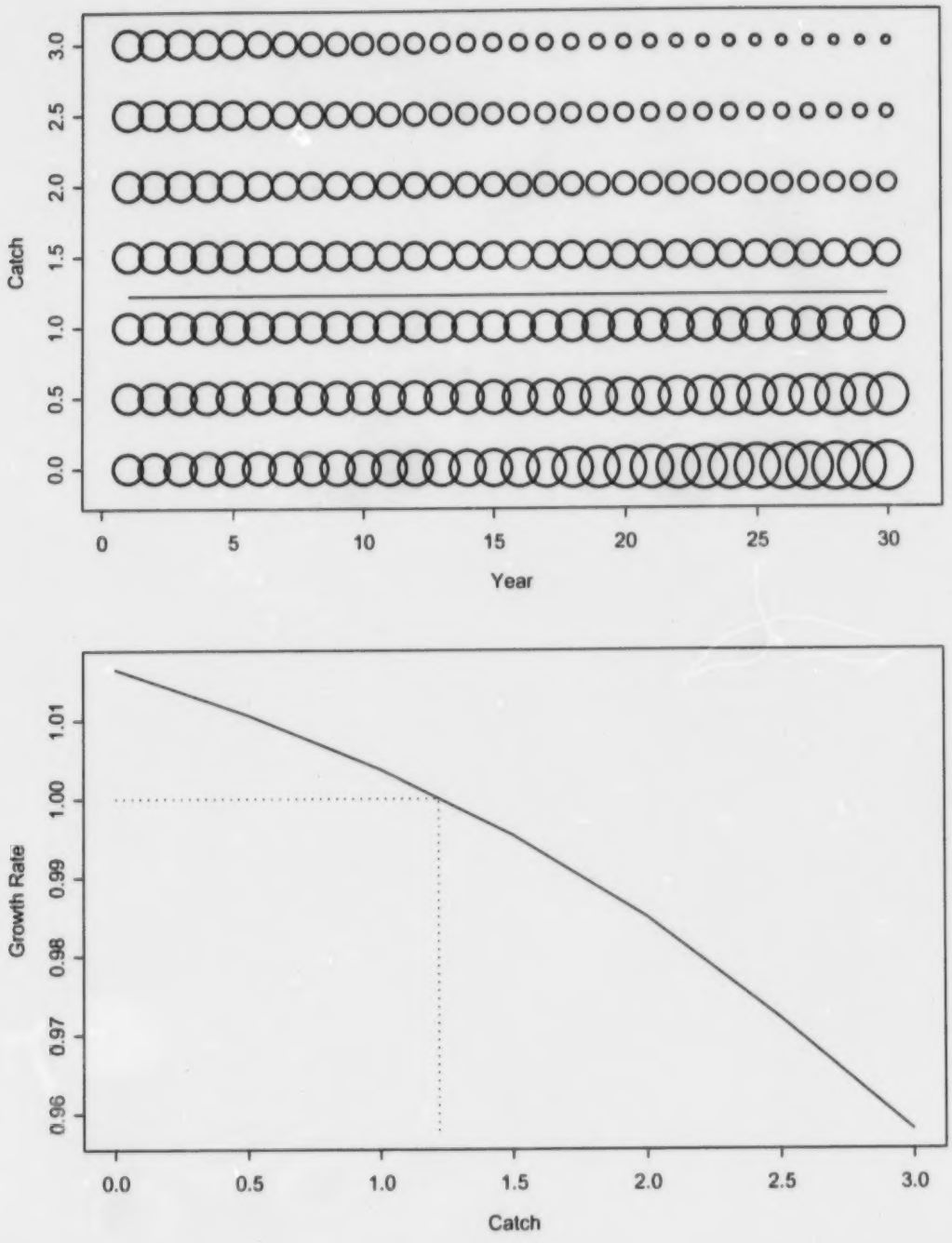

Figure 4.8. Forward simulation for 30 years with $r = 0.10$, starting from the population estimated in 2000. (Upper panel) Bubbles indicate relative biomass sizes, given a fixed catch level (10^3 t). (Lower panel) The annual growth rate (4.6) as a function of catch, with lines showing the catch biomass that allows no growth or decay.

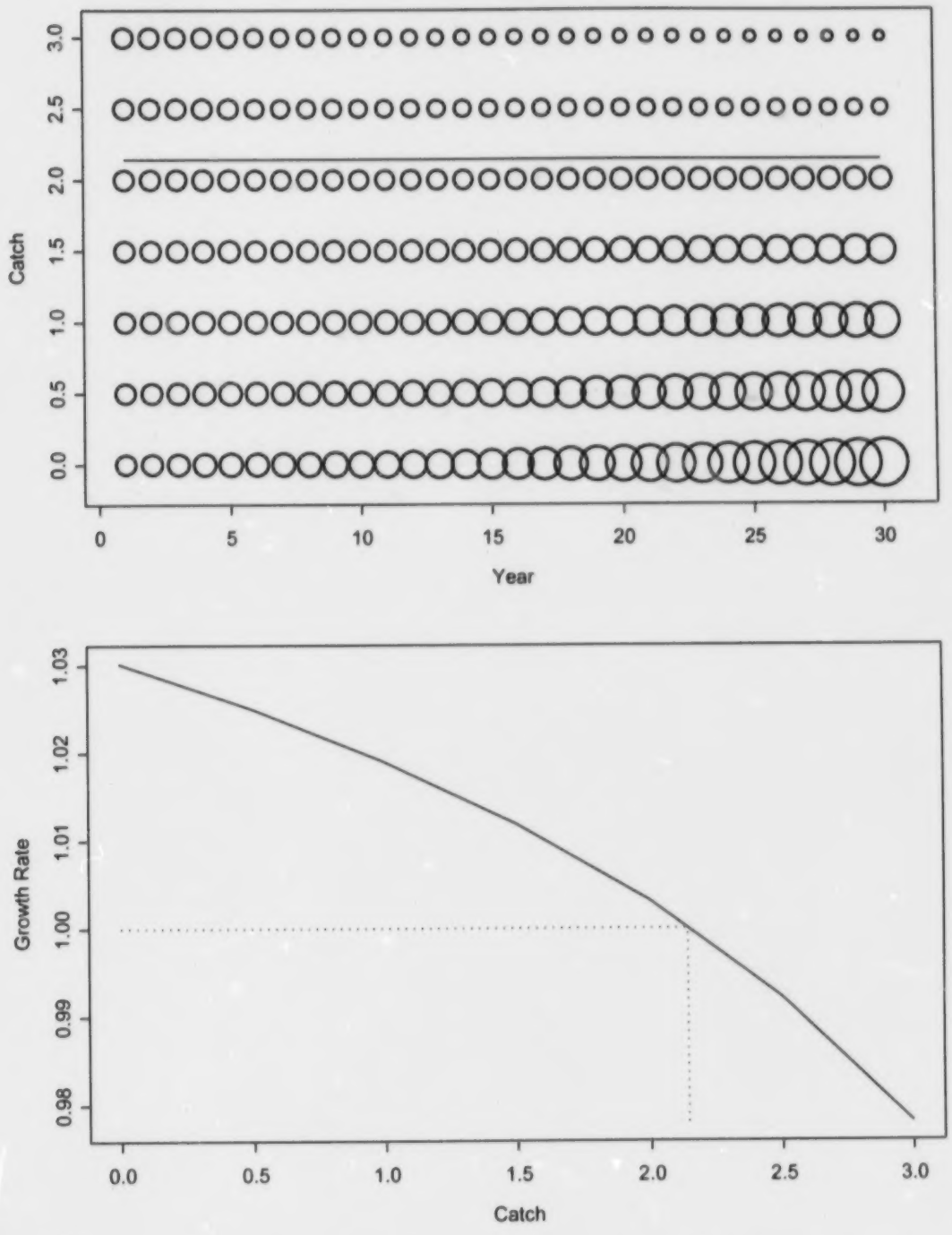

Figure 4.9. Forward simulation for 30 years with $r = 0.12$, starting from the population estimated in 2000. (Upper panel) Bubbles indicate relative biomass sizes, given a fixed catch level (10^3 t). (Lower panel) The annual growth rate (4.6) as a function of catch, with lines showing the catch biomass that allows no growth or decay.

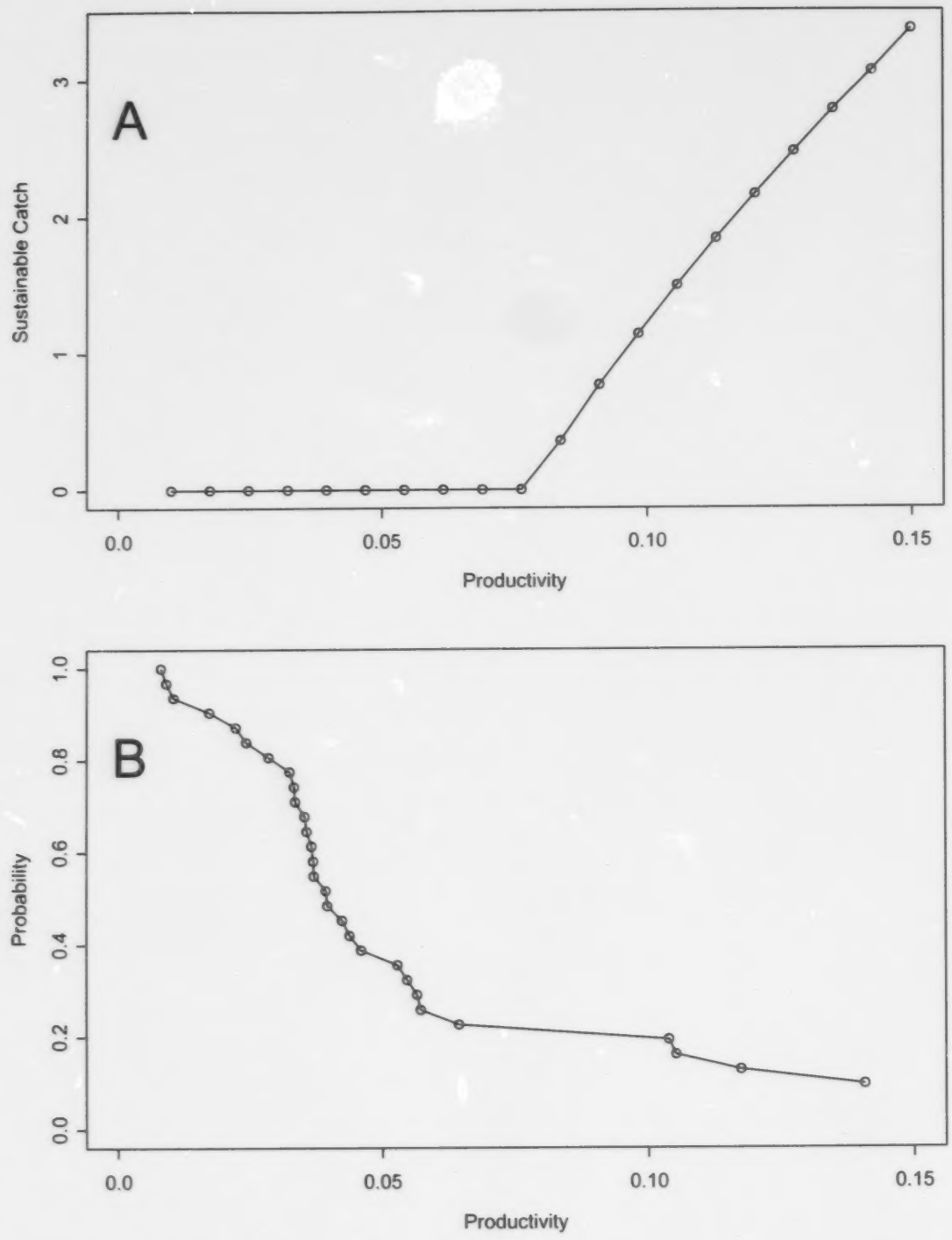

Figure 4.10. (A) Sustainable catch (kt) vs. productivity *r*, computed from simulations similar to those in Figs. 4.8–4.9. (B) Probability of achieving a given productivity level, computed from the historical record in Fig. 4.6B.

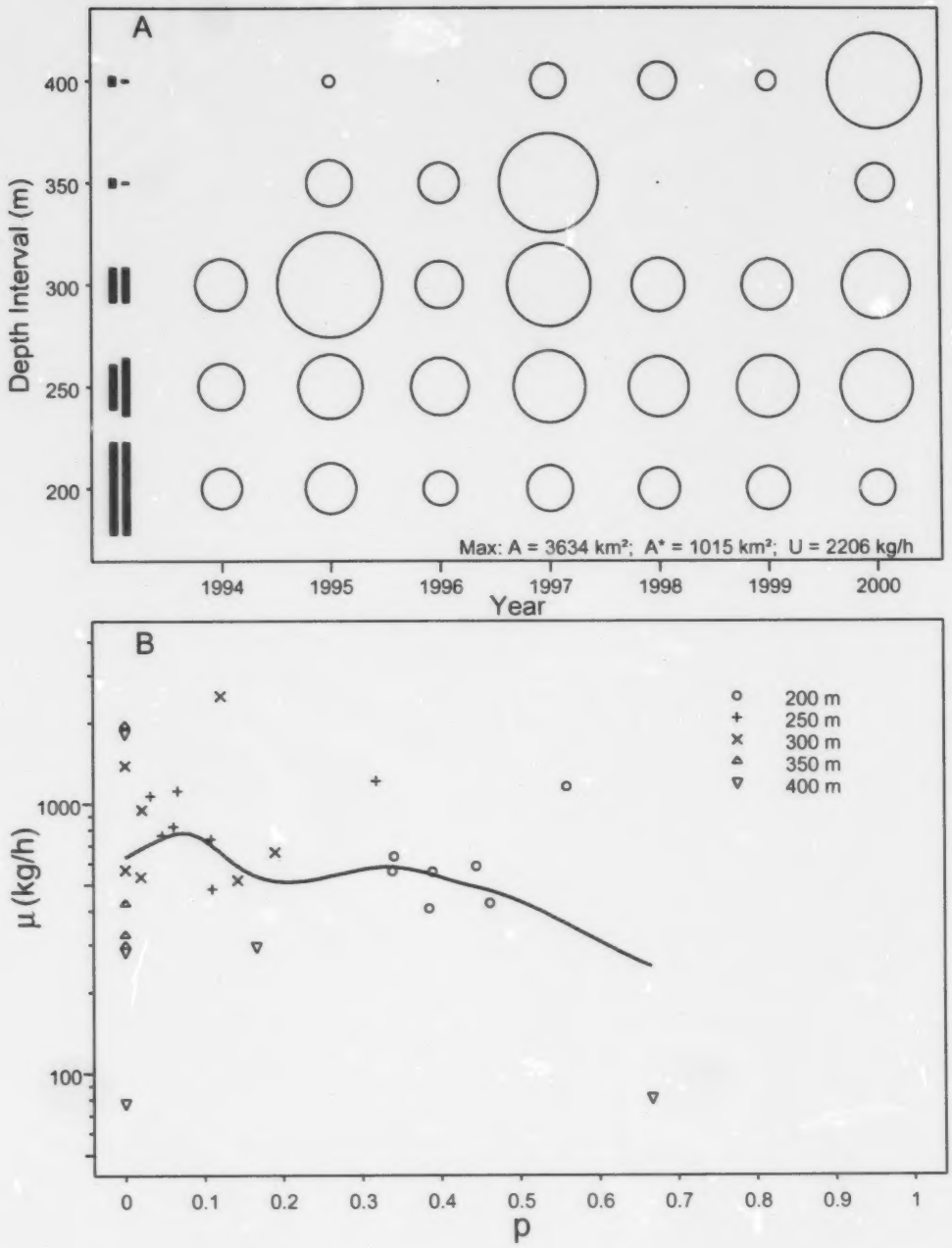

Figure 5.1. (A) Distribution of mean CPUE by 50 m-depth interval and calendar year in Goose Island Gully. CPUE values are qualified as follows: months = Jun-Oct, depths = 150-400 m, vessels in the GS fishery for 5 of the 7 years. Coloured bars to the left indicate relative bottom area A in each depth stratum – A (blue) = entire GS polygon, A^* (red) = area covered by 1 km² grid cells that contained POP catch from 1994 to Mar 2001. (B) Mean qualified CPUE μ excluding zeroes vs. the proportion of zero values p in each depth-year stratum.

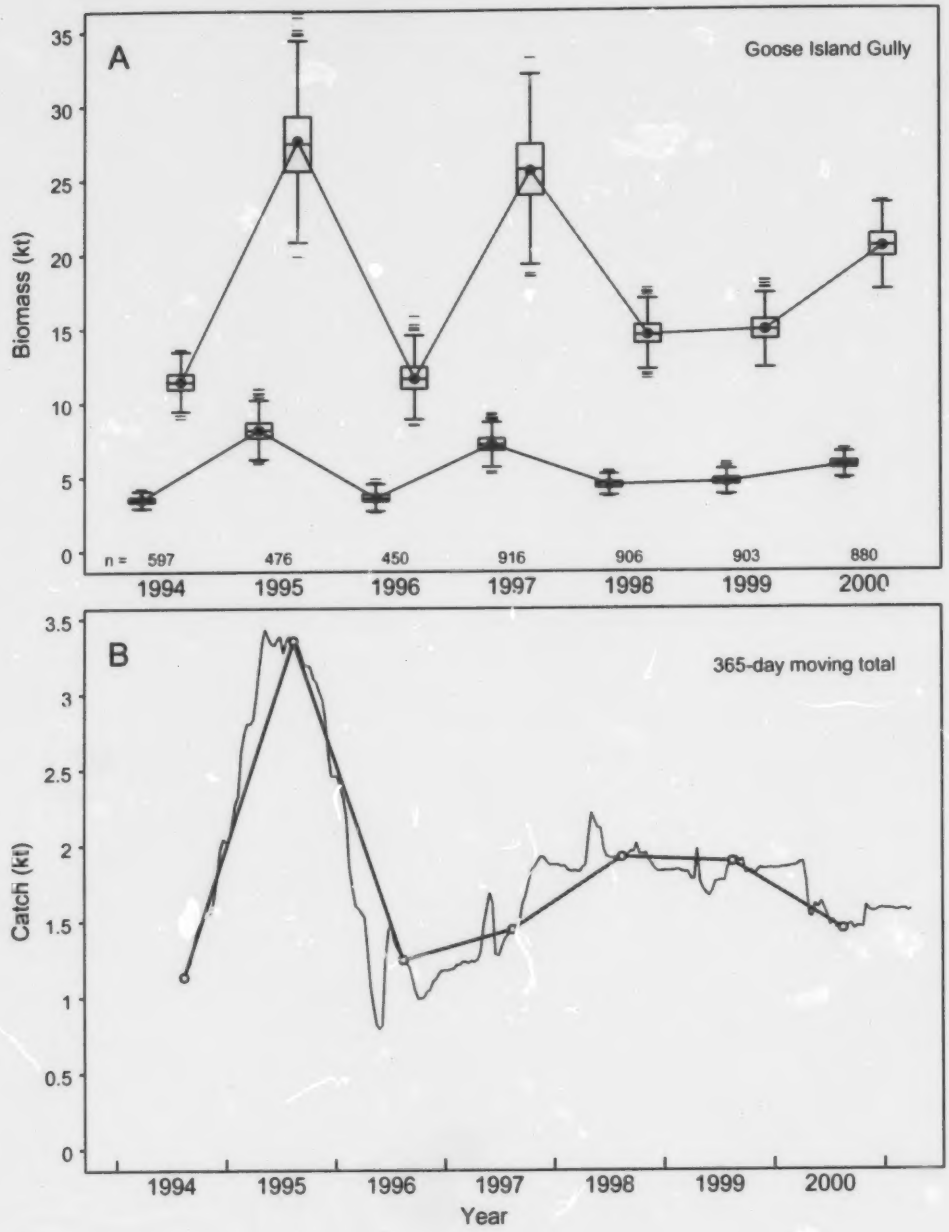

Figure 5.2. (A) Depth-stratified biomass estimates in Goose Island Gully. To derive the upper biomass estimates, we use area *A* comprising the entire GS polygon bottom area between 150 and 400 m. At identical depth limits, we derive the lower biomass estimates using area *A** comprising the bottom area covered by 1 km² grid cells containing POP catch from Jan 1994 to Mar 2001. Using 1000 bootstraps, we derive a measure of variability for each annual biomass estimate. Number of tows used in estimation is displayed at bottom of panel. (B) Running total annual catch (green line) with point values of catch for each year preceding Aug 15 (connected by red line).

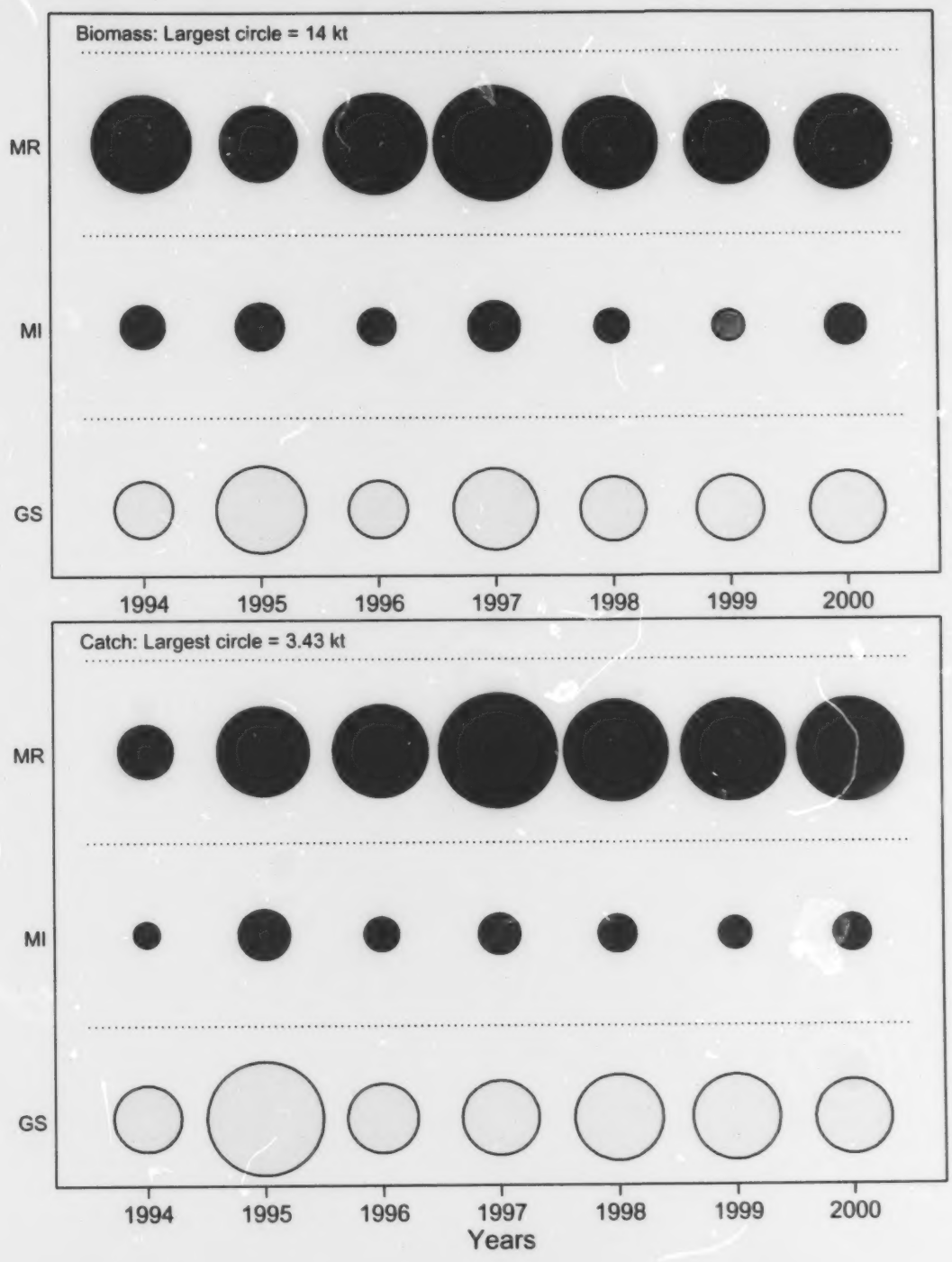

Figure 5.3. (A) Comparison of annual lower biomass estimates in the three gullies (MR = Moresby, MI = Mitchell's, GS = Goose Island). (B) Comparison of annual catches in years ending Aug 15 in the three gullies.

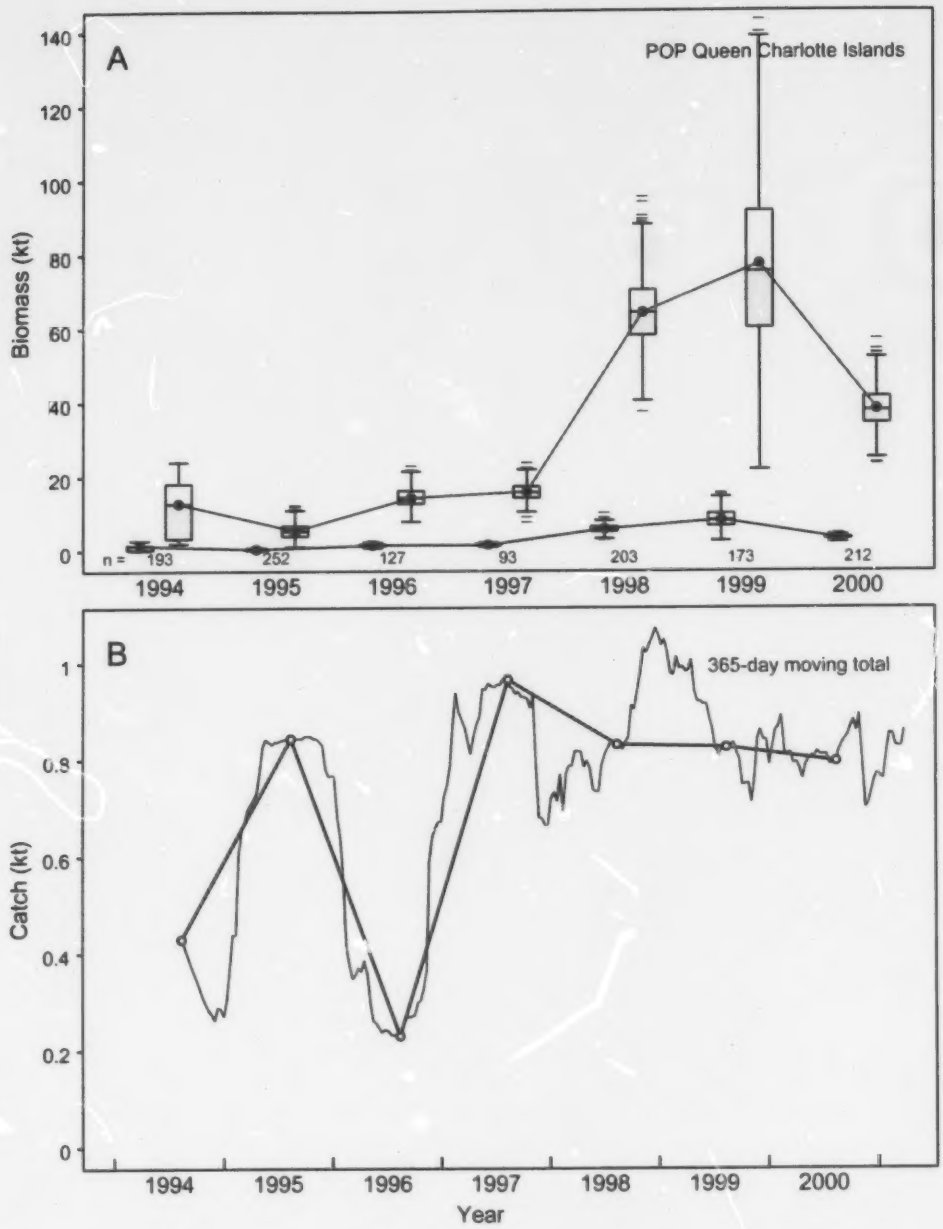

Figure 5.4. (A) Depth-stratified biomass estimates in POP area QCI. To derive the upper biomass estimates, we use area *A* comprising the entire POP-QCI polygon bottom area between 150 and 400 m. At identical depth limits, we derive the lower biomass estimates using area *A** comprising the bottom area covered by 1 km² grid cells containing POP catch from Jan 1994 to Mar 2001. Using 1000 bootstraps, we derive a measure of variability for each annual biomass estimate. Number of tows used in estimation is displayed at bottom of panel. (B) Running total annual catch (green line) with point values of catch for each year preceding Aug 15 (connected by red line).

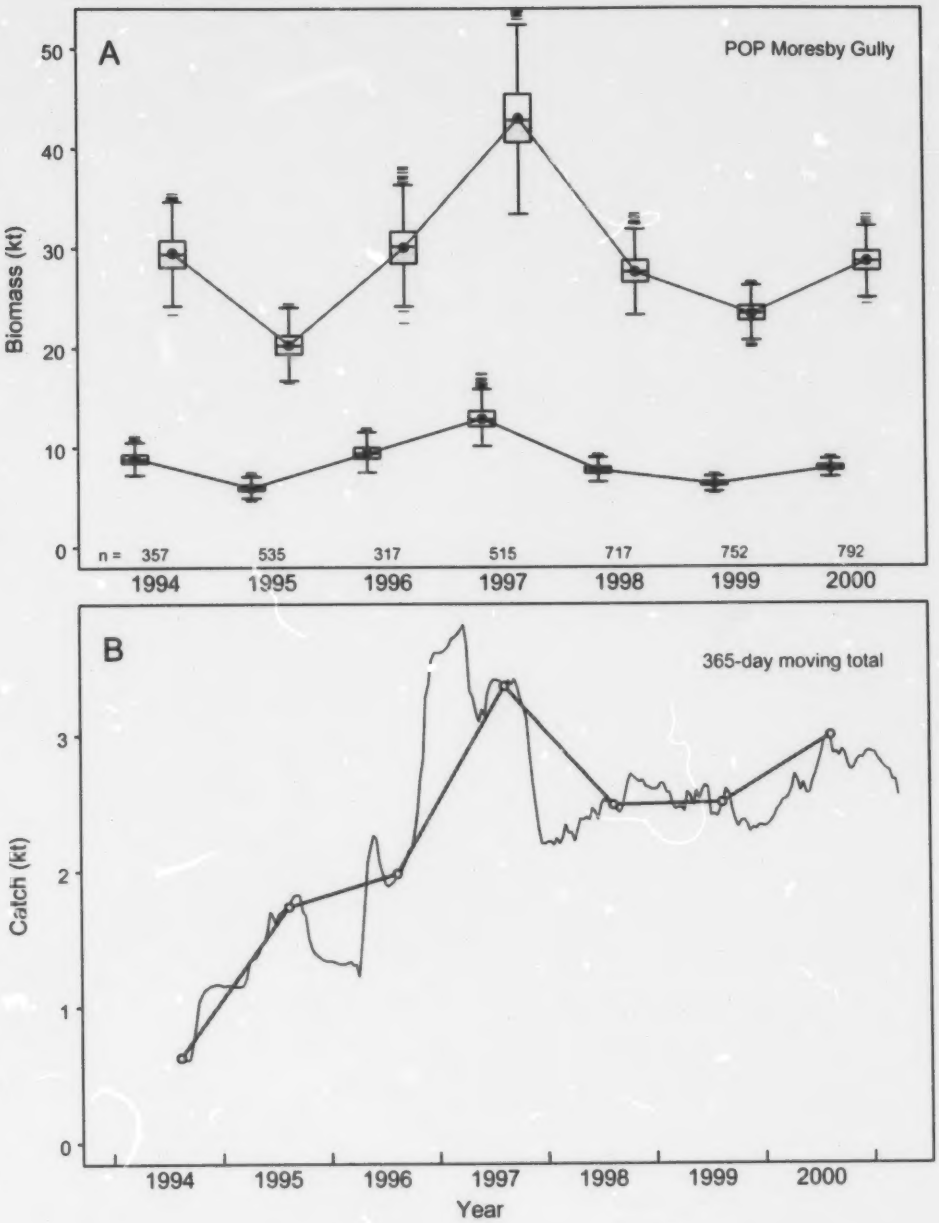

Figure 5.5. (A) Depth-stratified biomass estimates in POP area MR. To derive the upper biomass estimates, we use area *A* comprising the entire POP-MR polygon bottom area between 150 and 400 m. At identical depth limits, we derive the lower biomass estimates using area *A** comprising the bottom area covered by 1 km² grid cells containing POP catch from Jan 1994 to Mar 2001. Using 1000 bootstraps, we derive a measure of variability for each annual biomass estimate. Number of tows used in estimation is displayed at bottom of panel. (B) Running total annual catch (green line) with point values of catch for each year preceding Aug 15 (connected by red line).

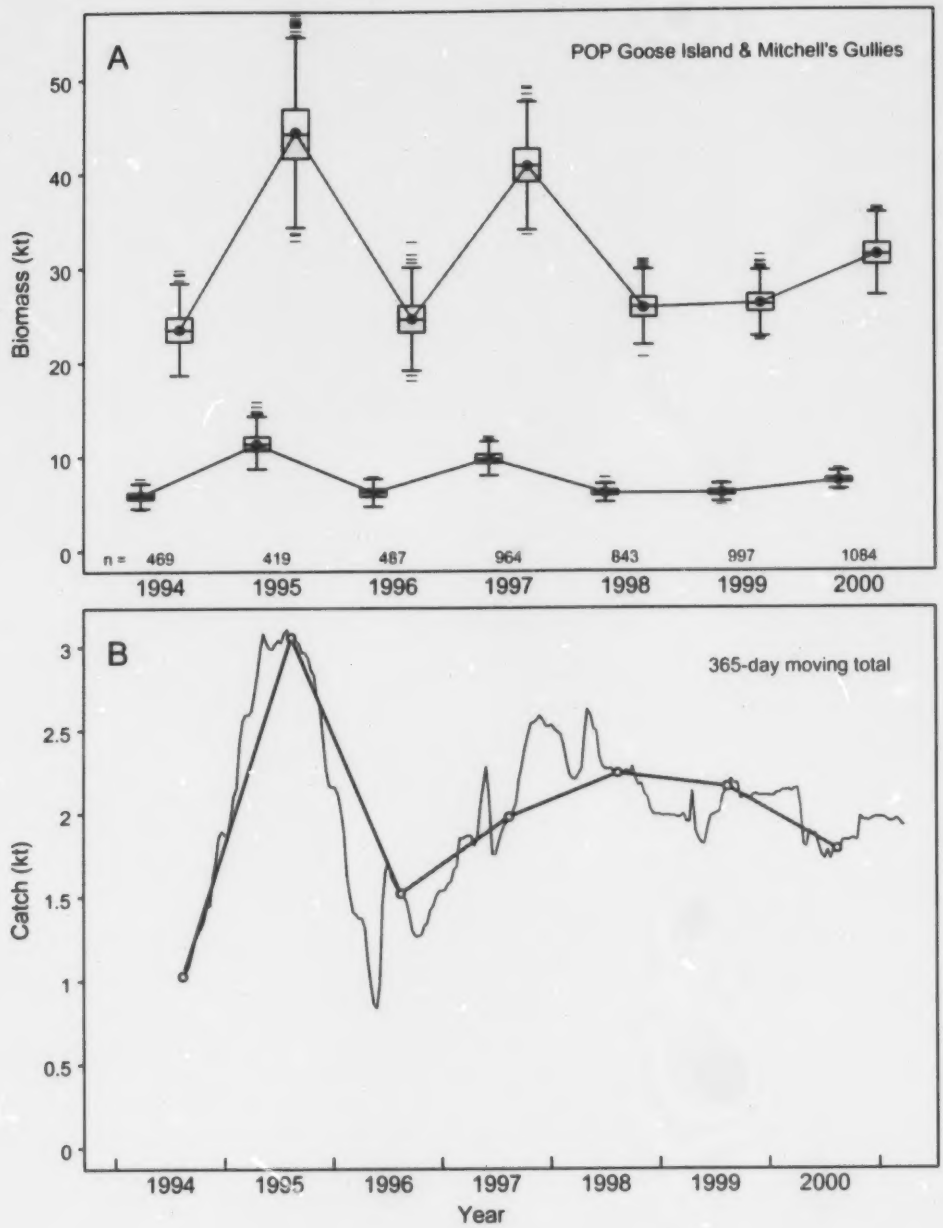

Figure 5.6. (A) Depth-stratified biomass estimates in POP area GS + MI. To derive the upper biomass estimates, we use area *A* comprising the entire POP-GSMI polygon bottom area between 150 and 400 m. At identical depth limits, we derive the lower biomass estimates using area *A** comprising the bottom area covered by 1 km² grid cells containing POP catch from Jan 1994 to Mar 2001. Using 1000 bootstraps, we derive a measure of variability for each annual biomass estimate. Number of tows used in estimation is displayed at bottom of panel. (B) Running total annual catch (green line) with point values of catch for each year preceding Aug 15 (connected by red line).

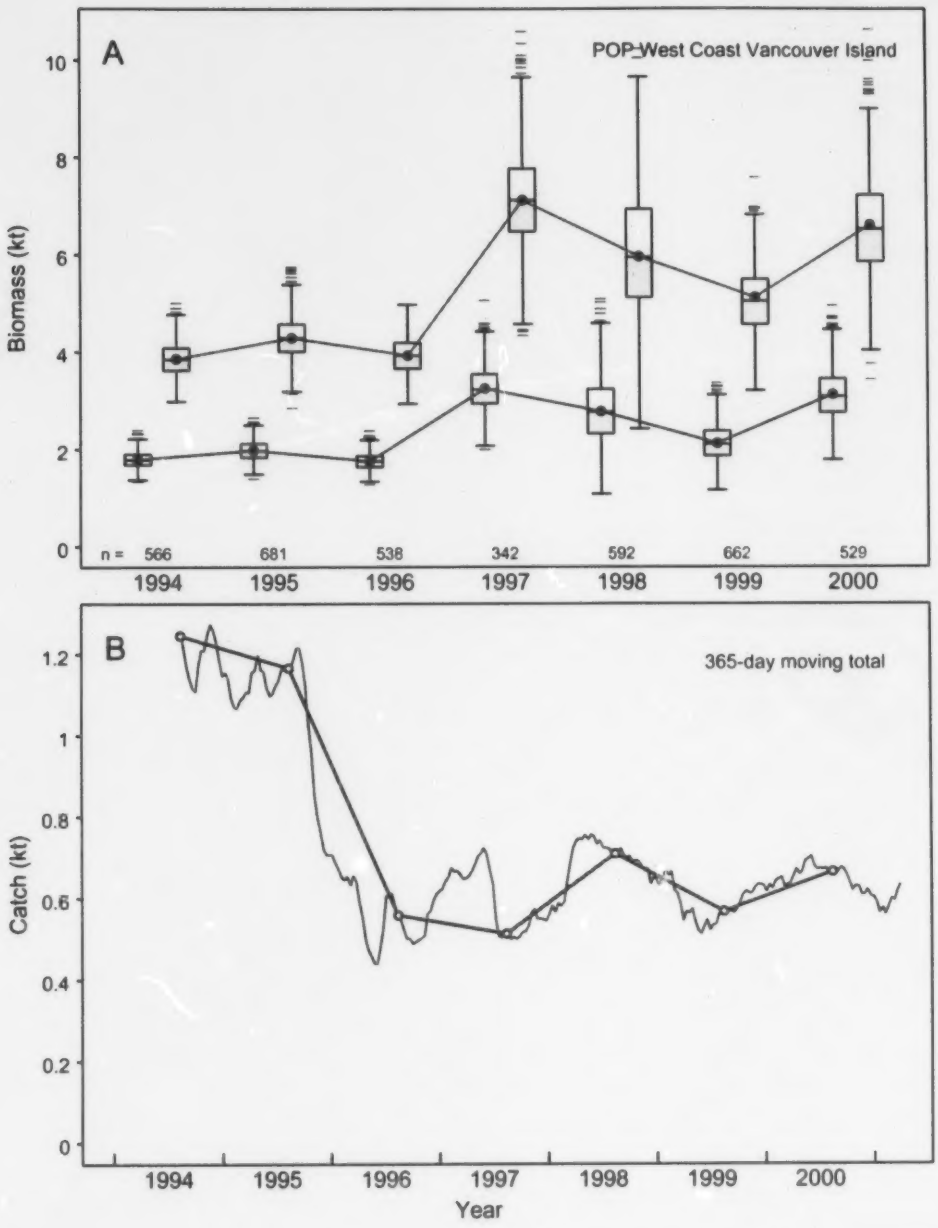

Figure 5.7. (A) Depth-stratified biomass estimates in POP area NVI + SVI. To derive the upper biomass estimates, we use area *A* comprising the entire POP-WCVI polygon bottom area between 150 and 400 m. At identical depth limits, we derive the lower biomass estimates using area *A** comprising the bottom area covered by 1 km² grid cells containing POP catch from Jan 1994 to Mar 2001. Using 1000 bootstraps, we derive a measure of variability for each annual biomass estimate. Number of tows used in estimation is displayed at bottom of panel. (B) Running total annual catch (green line) with point values of catch for each year preceding Aug 15 (connected by red line). WCVI

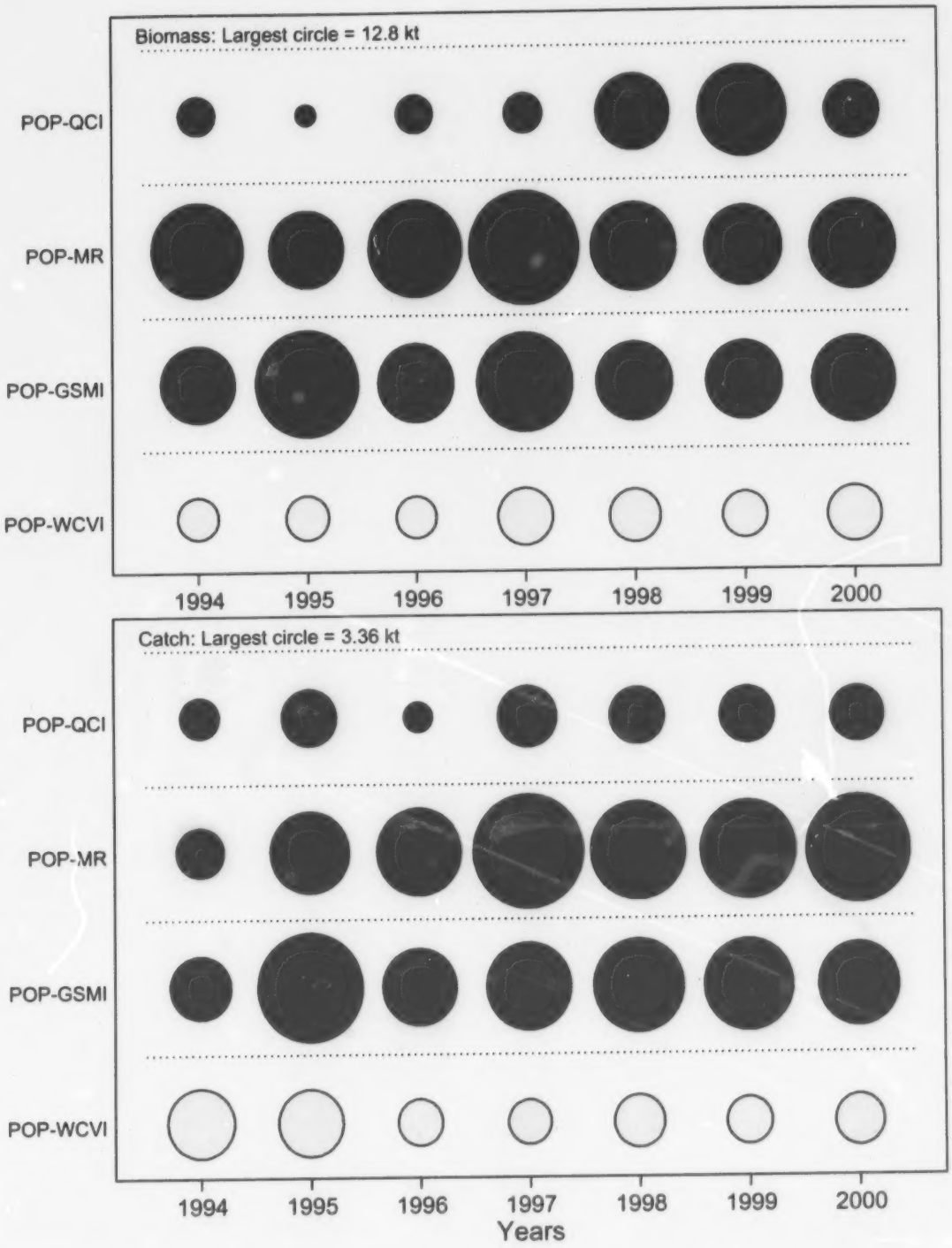

Figure 5.8. (A) Comparison of annual biomass estimates in the four POP areas (POP-QCI, POP-MR, POP-GSMI, POP-WCVI). (B) Comparison of annual catches in years ending Aug 15 in the four POP areas.

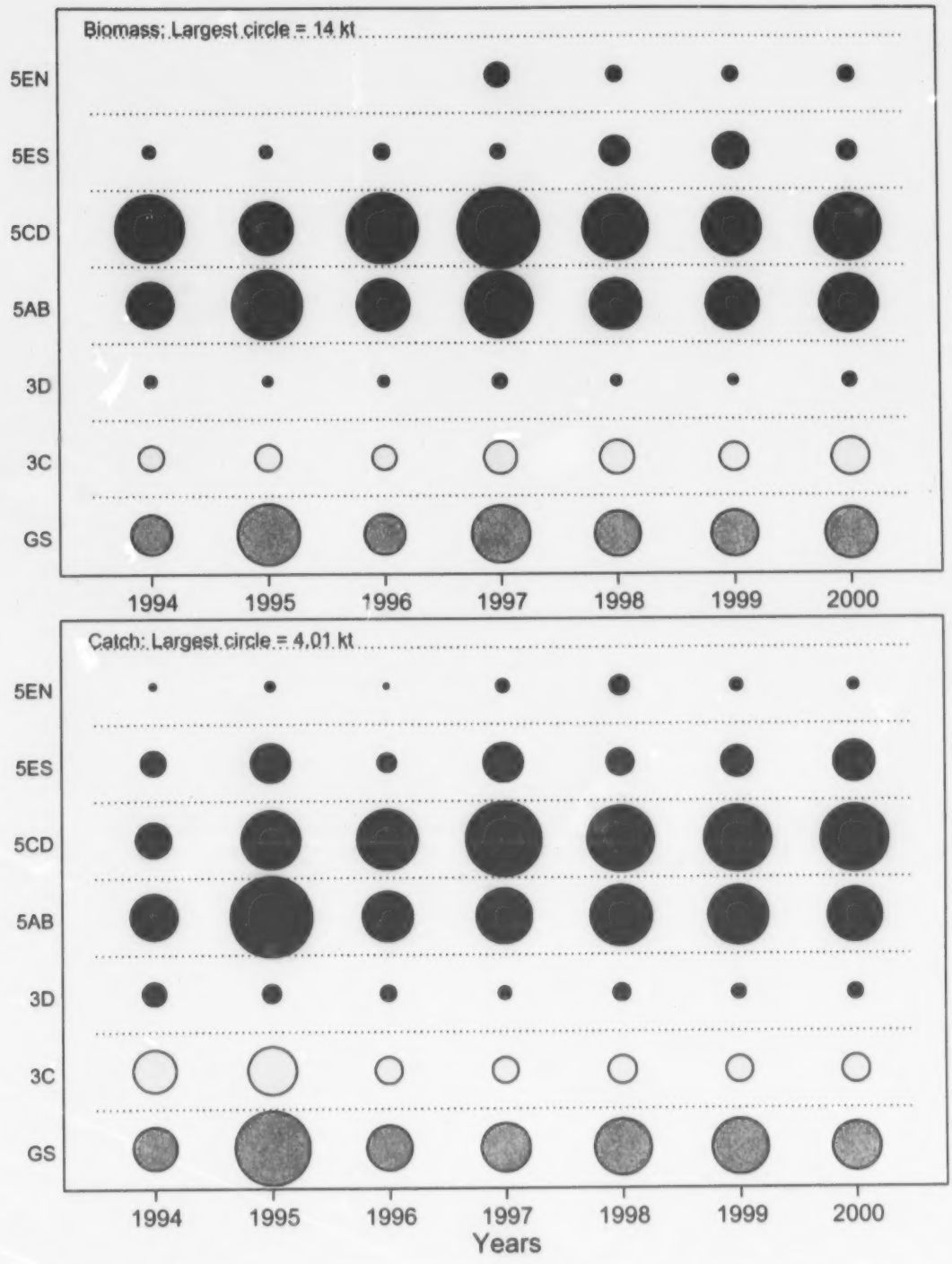

Figure 5.9. (A) Comparison of annual biomass estimates in the six SRF areas and Goose Island Gully (5EN, 5ES, 5AB, 5CD, 3C, 3D, GS). (B) Comparison of annual catches in years ending Aug 15 in the six SRF areas and GS gully.

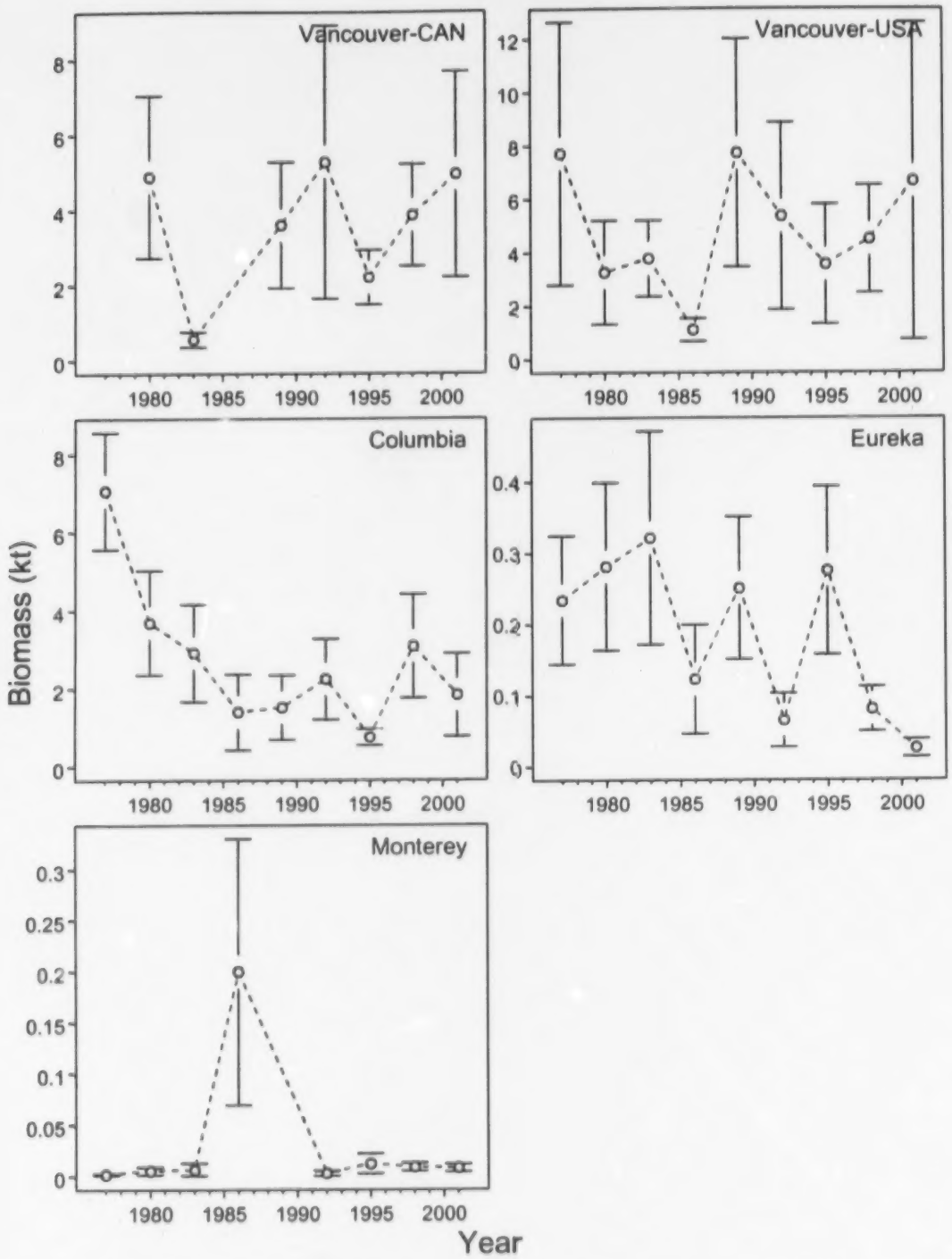

Figure 5.10. Depth-stratified biomass estimates (kt) for POP in PMFC areas along the continental U.S. coast. Data obtained from NOAA triennial surveys courtesy of Mark Wilkins. Error bars denote ±1 standard deviation.

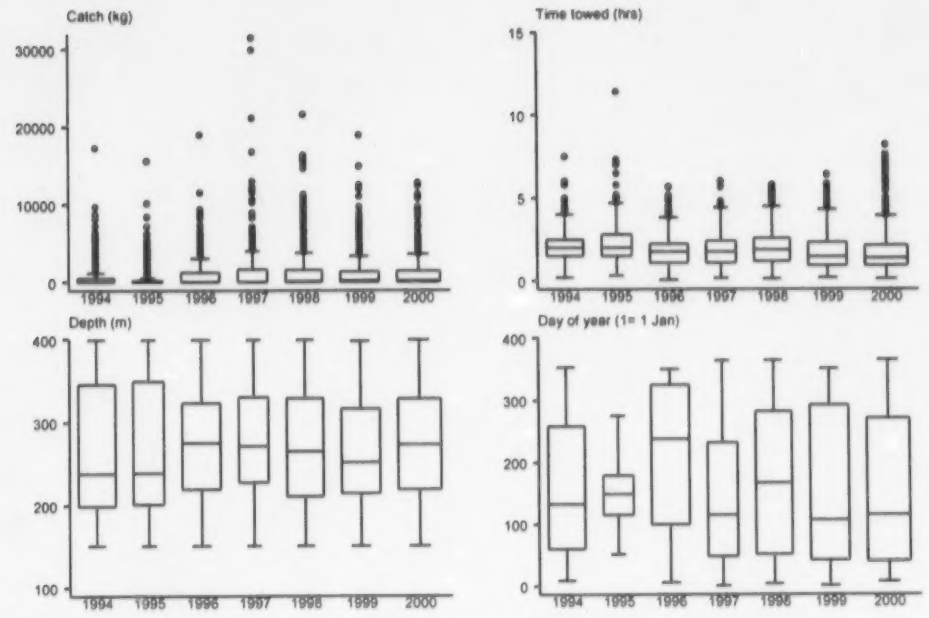

Figure 6.1a. Distribution of catch (kg), hours fished, depth and day of year for the Queen Charlotte Islands binomial model by standard fishing year. The width of the boxes is proportional to the number of tows.

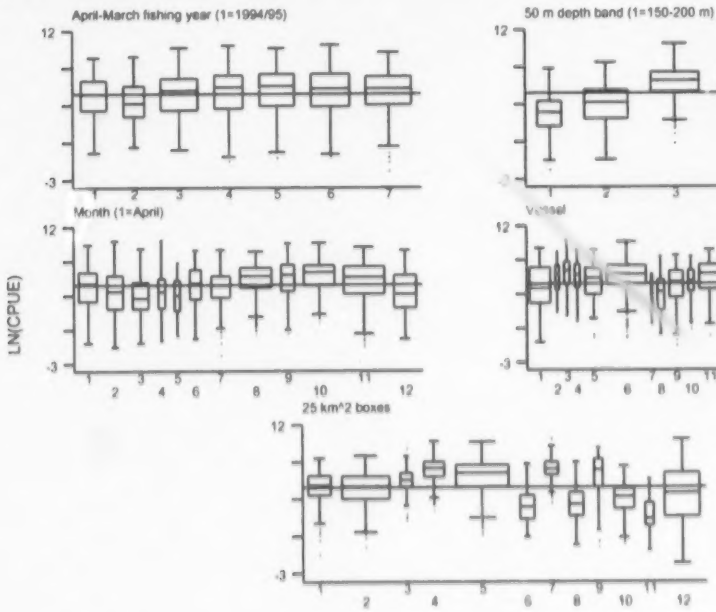

Figure 6.1b. Box plots of LN(CPUE) for each categorical variable which entered into the Queen Charlotte Island positive catch model. The width of the boxes is proportional to the number of tows in that category and the mean LN(CPUE) is plotted as a horizontal line.

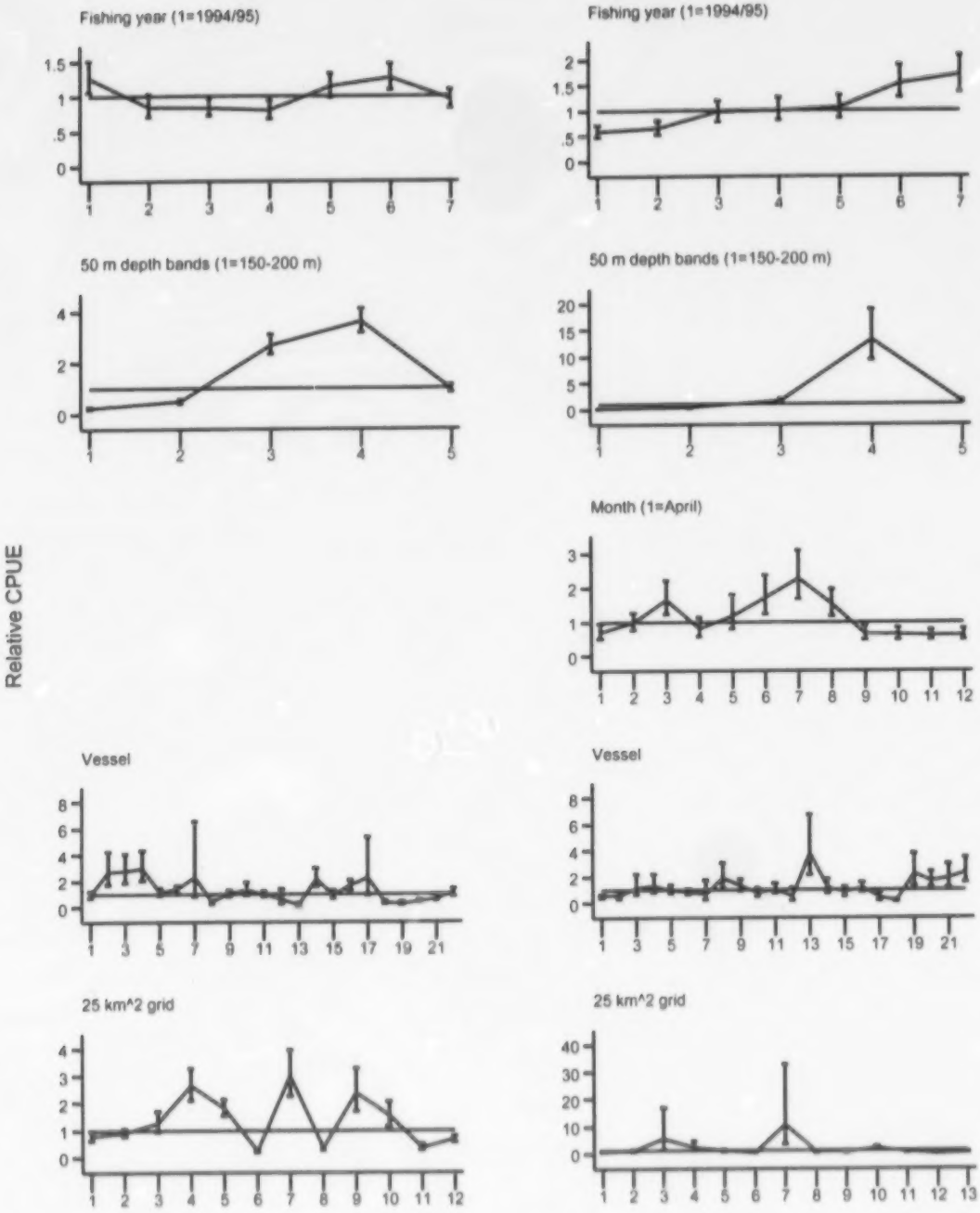

Figure 6.2. [Left column of plots]: Coefficients for the Queen Charlotte Islands positive catch model. [Right column of plots]: Coefficients for the Queen Charlotte Islands binomial model. All coefficients are plotted relative to their geometric mean, the error bars are 2*SE and the horizontal line is plotted at a coefficient value of 1.0.

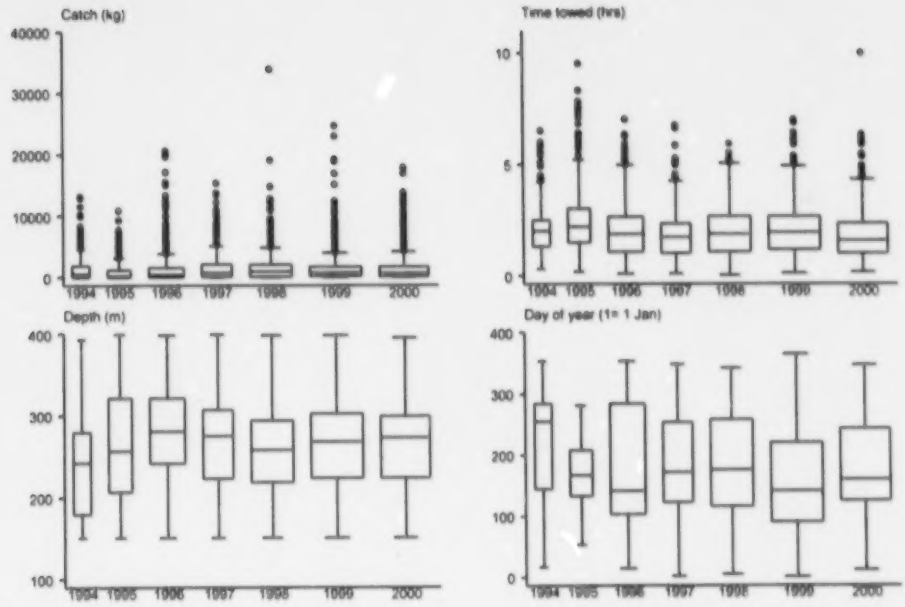

Figure 6.3a. Distribution of catch (kg), hours fished, depth and day of year for the Moresby Gully binomial model by standard fishing year. The width of the boxes is proportional to the number of tows.

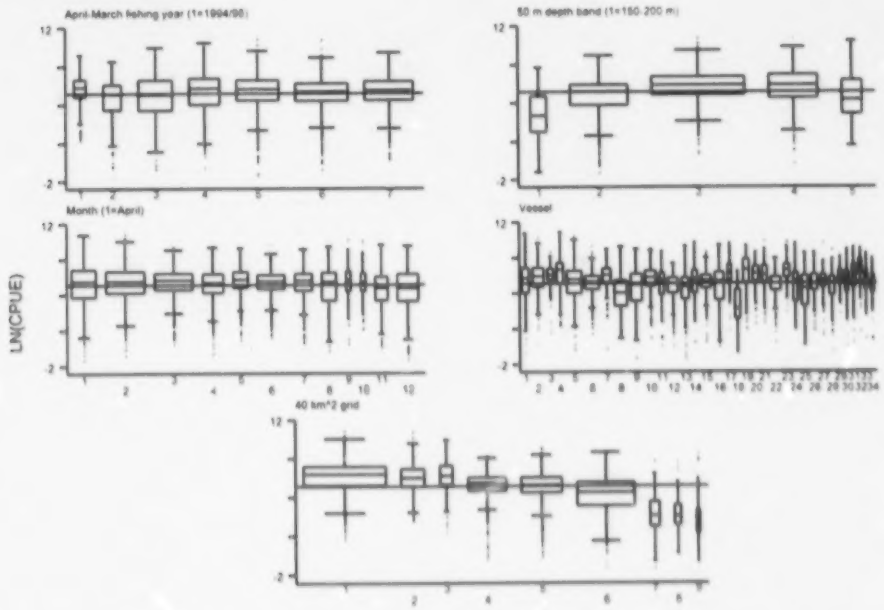

Figure 6.3b. Box plots of LN(CPUE) for each categorical variable which entered into the previous definition of the Moresby Gully positive catch model. The width of the boxes is proportional to the number of tows in that category and the mean LN(CPUE) is plotted as a horizontal line.

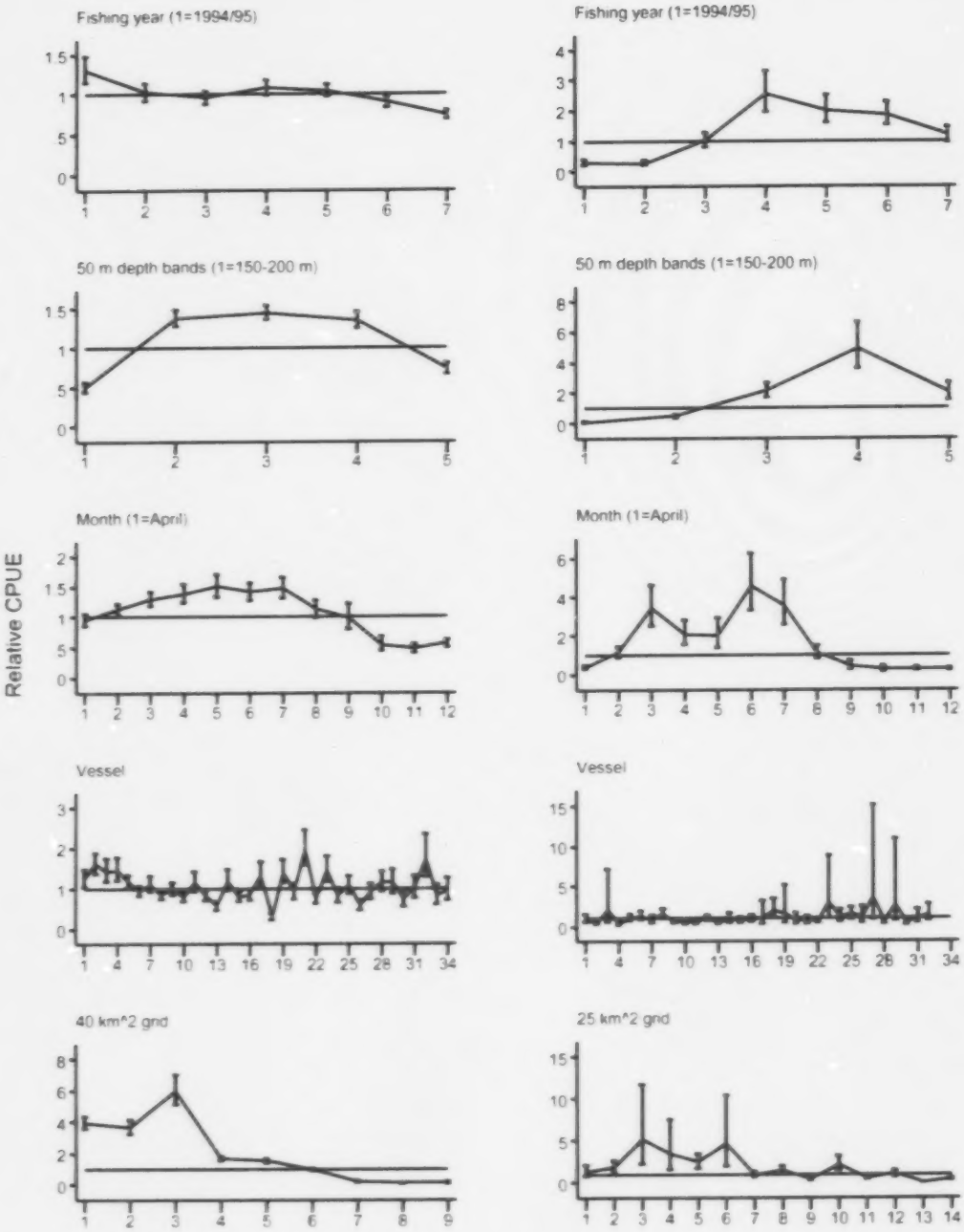

Figure 6.4. [Left column of plots]: Coefficients for the previous definition of the Moresby Gully positive catch model. [Right column of plots]: Coefficients for the Moresby Gully binomial model. All coefficients are plotted relative to their geometric mean, the error bars are 2*SE and the horizontal line is plotted at a coefficient value of 1.0.

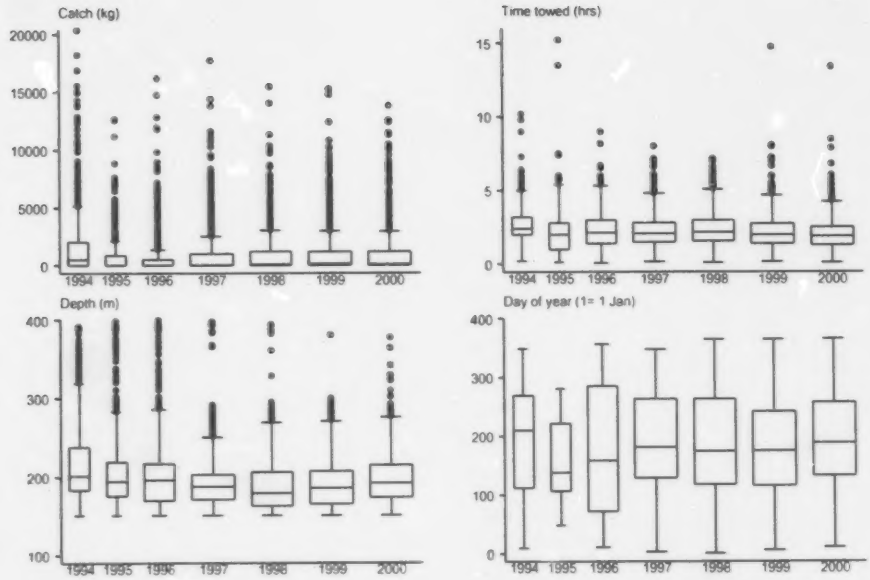

Figure 6.5a. Distribution of catch (kg), hours fished, depth and day of year for the combined Goose Island and Mitchell gullies binomial model by standard fishing year. The width of the boxes is proportional to the number of tows.

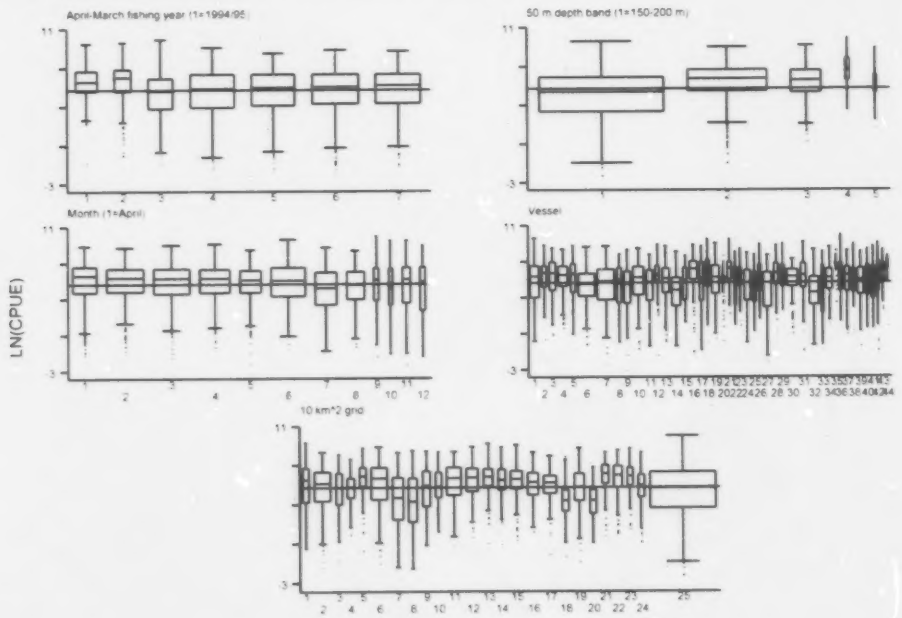

Figure 6.5b. Box plots of LN(CPUE) for each categorical variable which entered into the combined Goose Island and Mitchell gullies positive catch model. The width of the boxes is proportional to the number of tows in that category and the mean LN(CPUE) is plotted as a horizontal line.

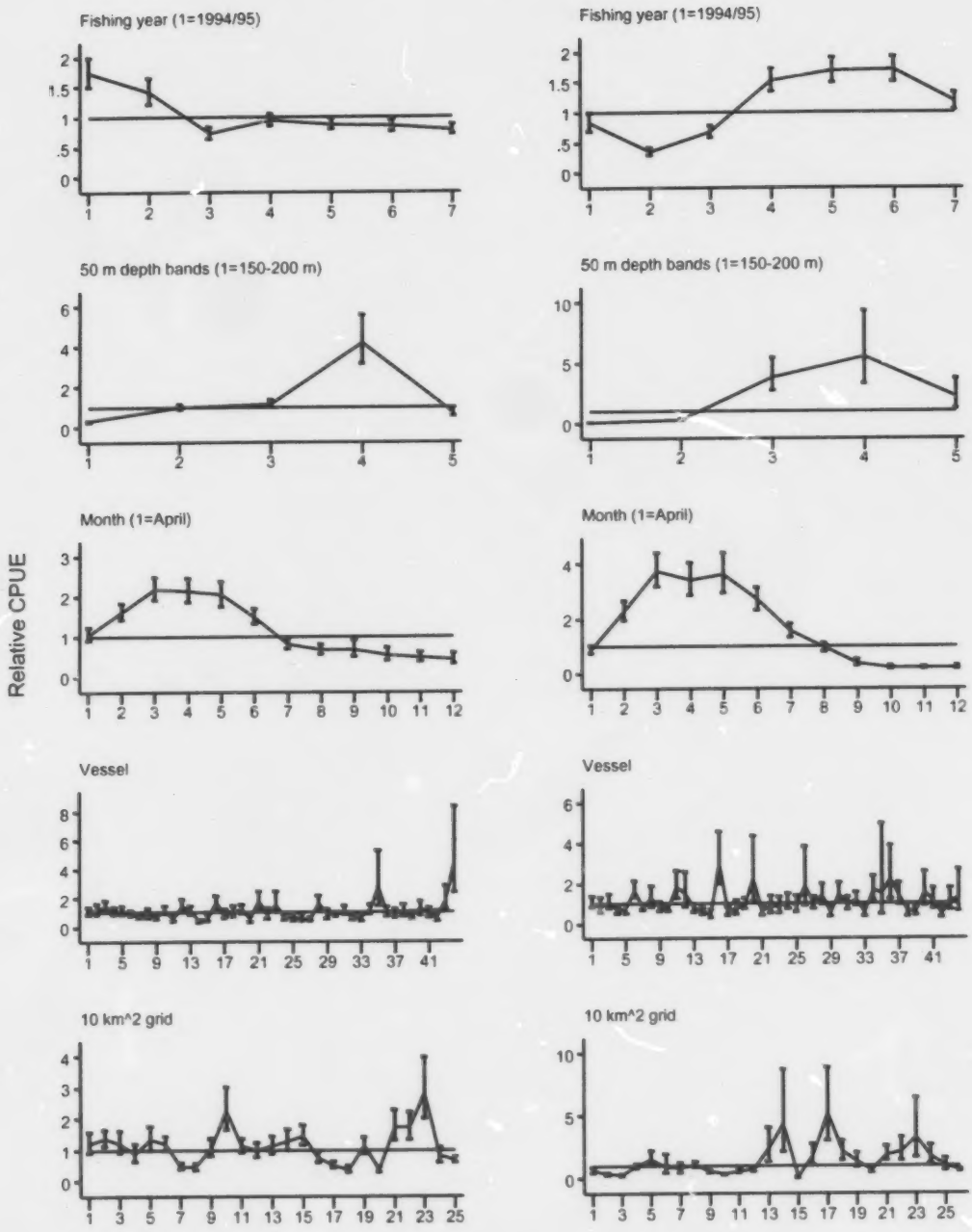

Figure 6.6. [Left column of plots]: Coefficients for the combined Goose Island and Mitchell gullies positive catch model. [Right column of plots]: Coefficients for the combined Goose Island and Mitchell gullies binomial model. All coefficients are plotted relative to their geometric mean, the error bars are 2*SE and the horizontal line is plotted at a coefficient value of 1.0.

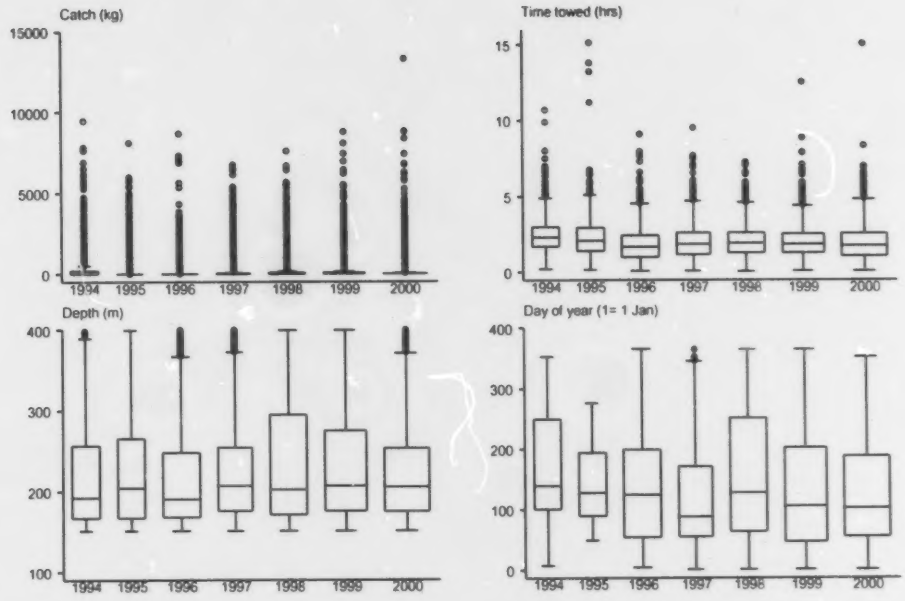

Figure 6.7a. Distribution of catch (kg), hours fished, depth and day of year for the west coast Vancouver Island binomial model by standard fishing year. The width of the boxes is proportional to the number of tows.

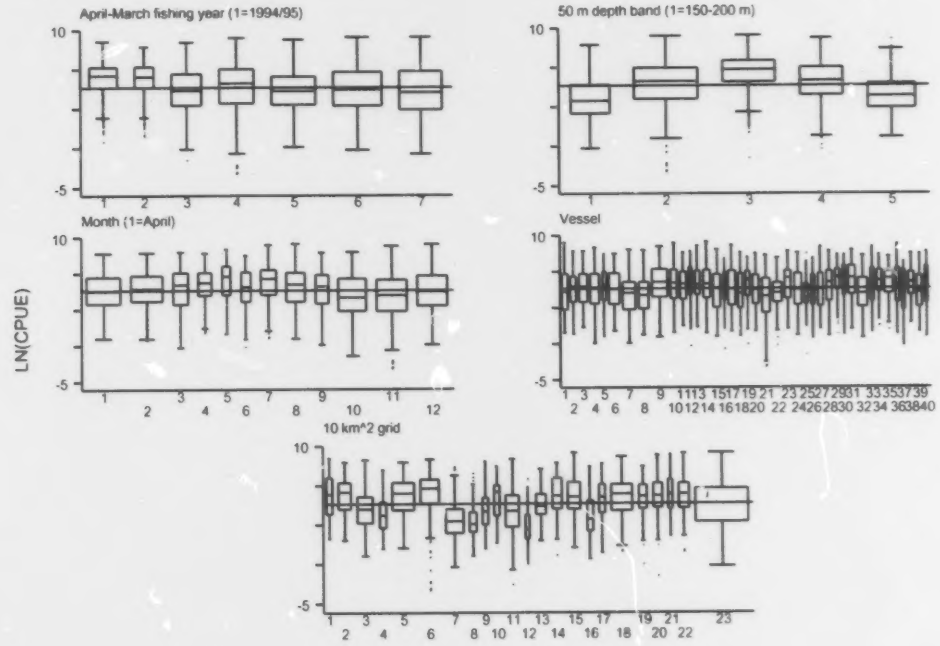

Figure 6.7b. Box plots of LN(CPUE) for each categorical variable which entered into the west coast Vancouver Island positive catch model. The width of the boxes is proportional to the number of tows in that category and the mean LN(CPUE) is plotted as a horizontal line.

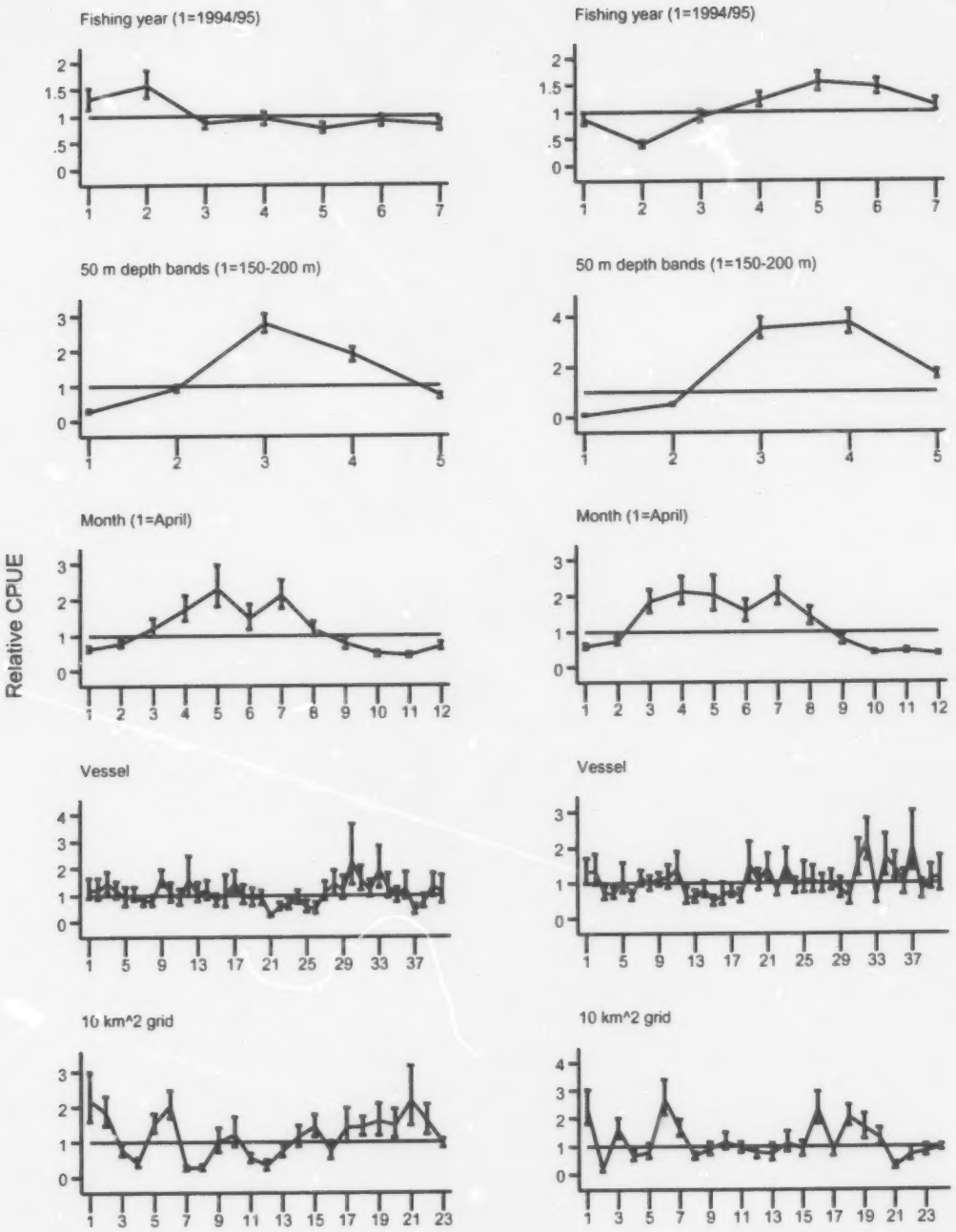

Figure 6.8. [Left column of plots]: Coefficients for the west coast Vancouver Island positive catch model. [Right column of plots]: Coefficients for the west coast Vancouver Island binomial model. All coefficients are plotted relative to their geometric mean, the error bars are 2*SE and the horizontal line is plotted at a coefficient value of 1.0.

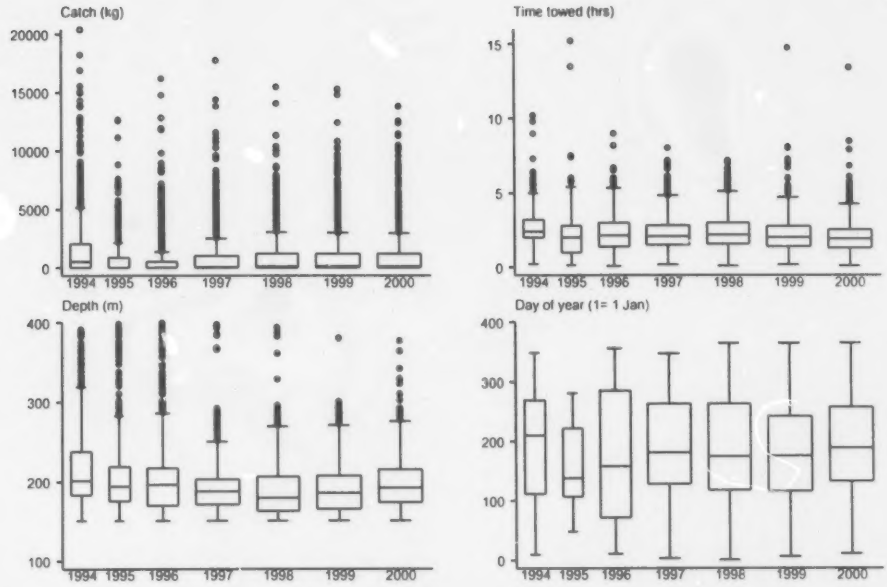

Figure 6.9a. Distribution of catch (kg), hours fished, depth and day of year for the previous definition of Goose Island Gully binomial model by standard fishing year. The width of the boxes is proportional to the number of tows.

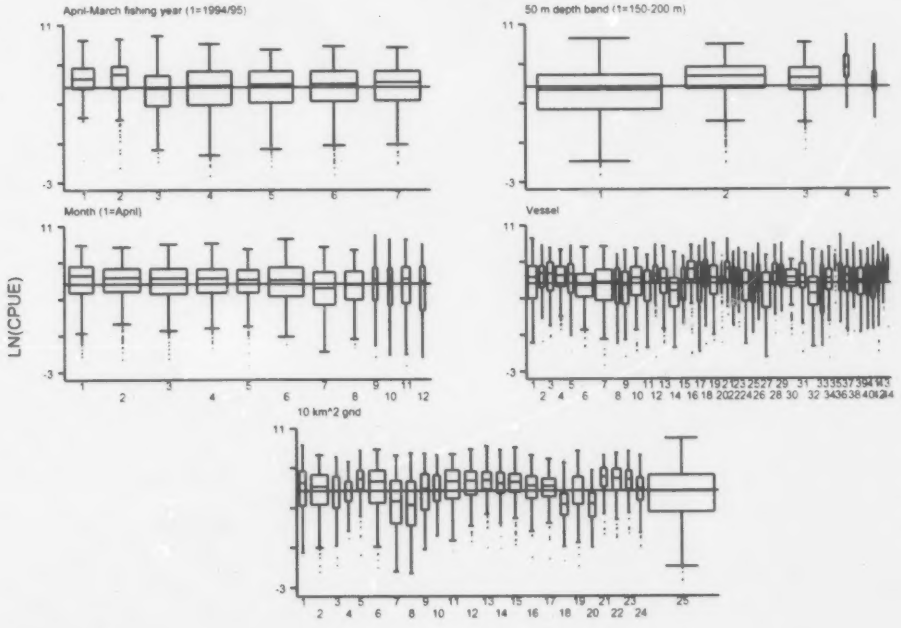

Figure 6.9b. Box plots of LN(CPUE) for each categorical variable which entered into the previous definition of Goose Island Gully positive catch model. The width of the boxes is proportional to the number of tows in that category and the mean LN(CPUE) is plotted as a horizontal line.

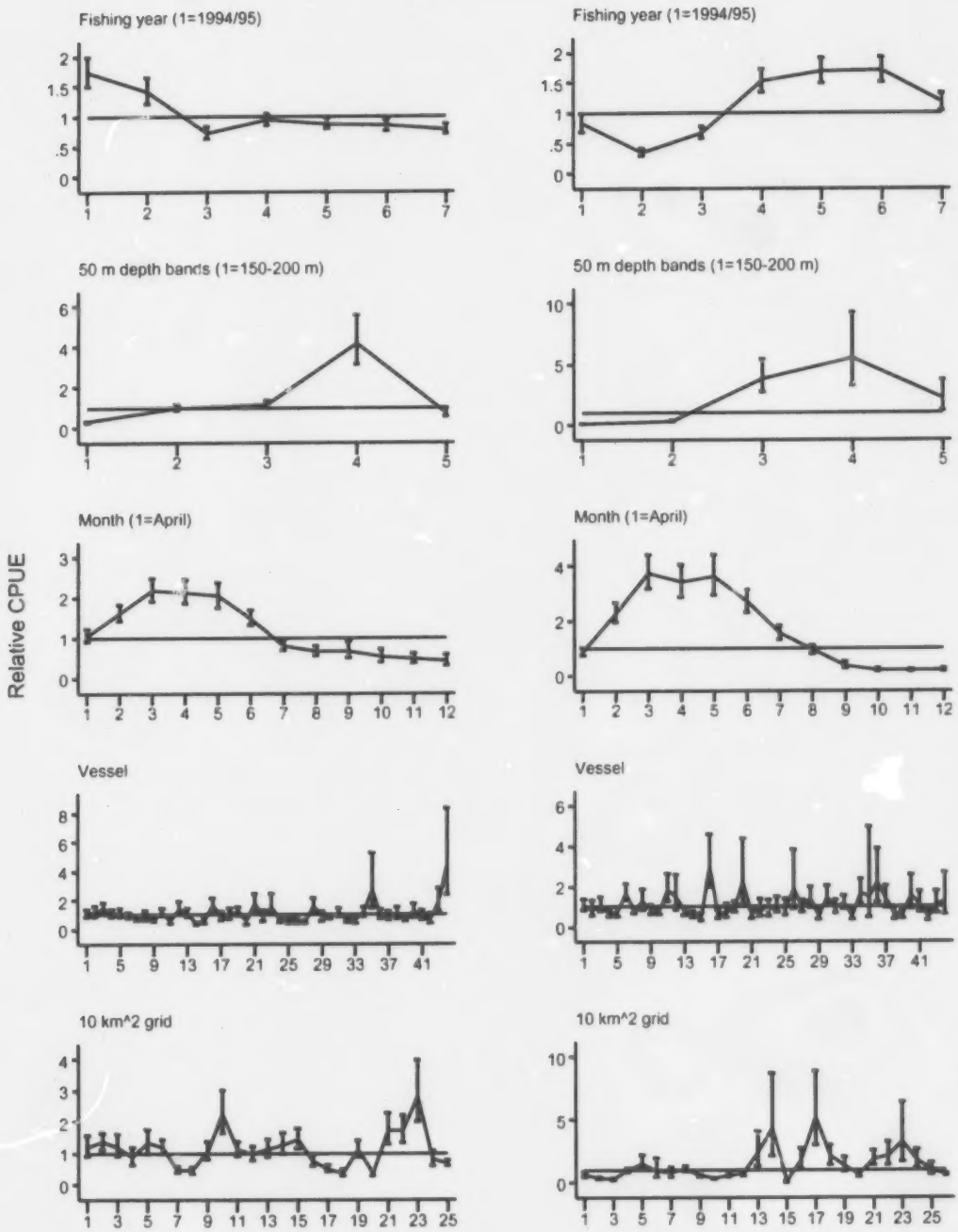

Figure 6.10. [Left column of plots]: Coefficients for the previous definition of Goose Island Gully positive catch model. [Right column of plots]: Coefficients for the previous definition of Goose Island Gully binomial model. All coefficients are plotted relative to their geometric mean, the error bars are 2*SE and the horizontal line is plotted at a coefficient value of 1.0.

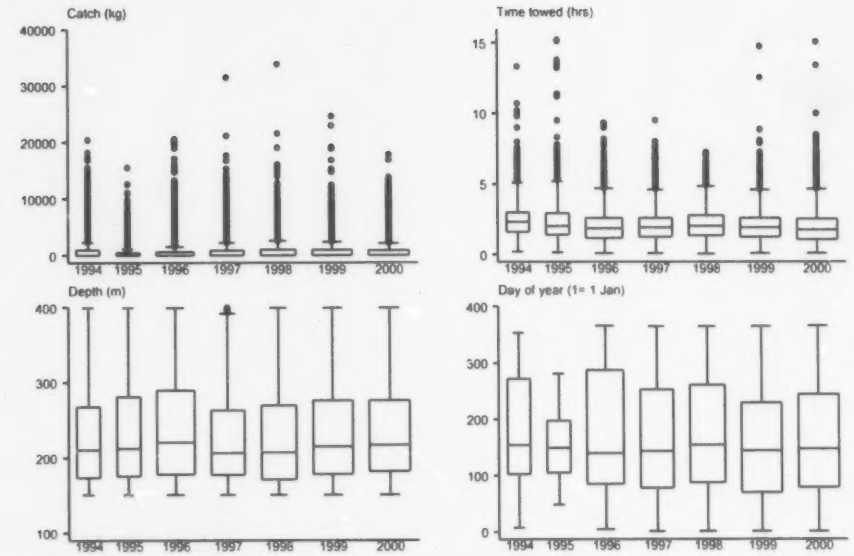

Figure 6.11a. Distribution of catch (kg), hours fished, depth and day of year for the Total B.C. binomial model by standard fishing year. The width of the boxes is proportional to the number of tows.

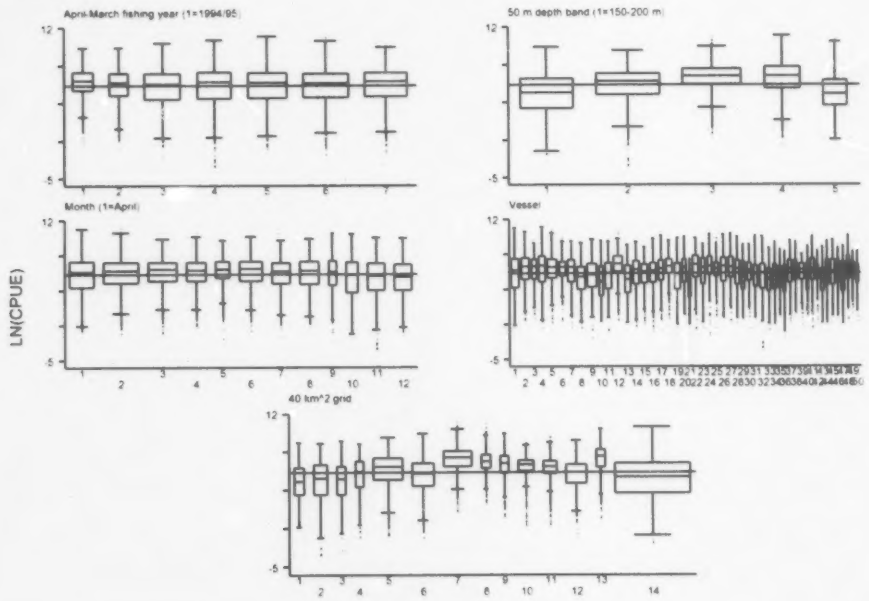

Figure 6.11b. Box plots of LN(CPUE) for each categorical variable which entered into the previous definition of the Total B.C. positive catch model. The width of the boxes is proportional to the number of tows in that category and the mean LN(CPUE) is plotted as a horizontal line.

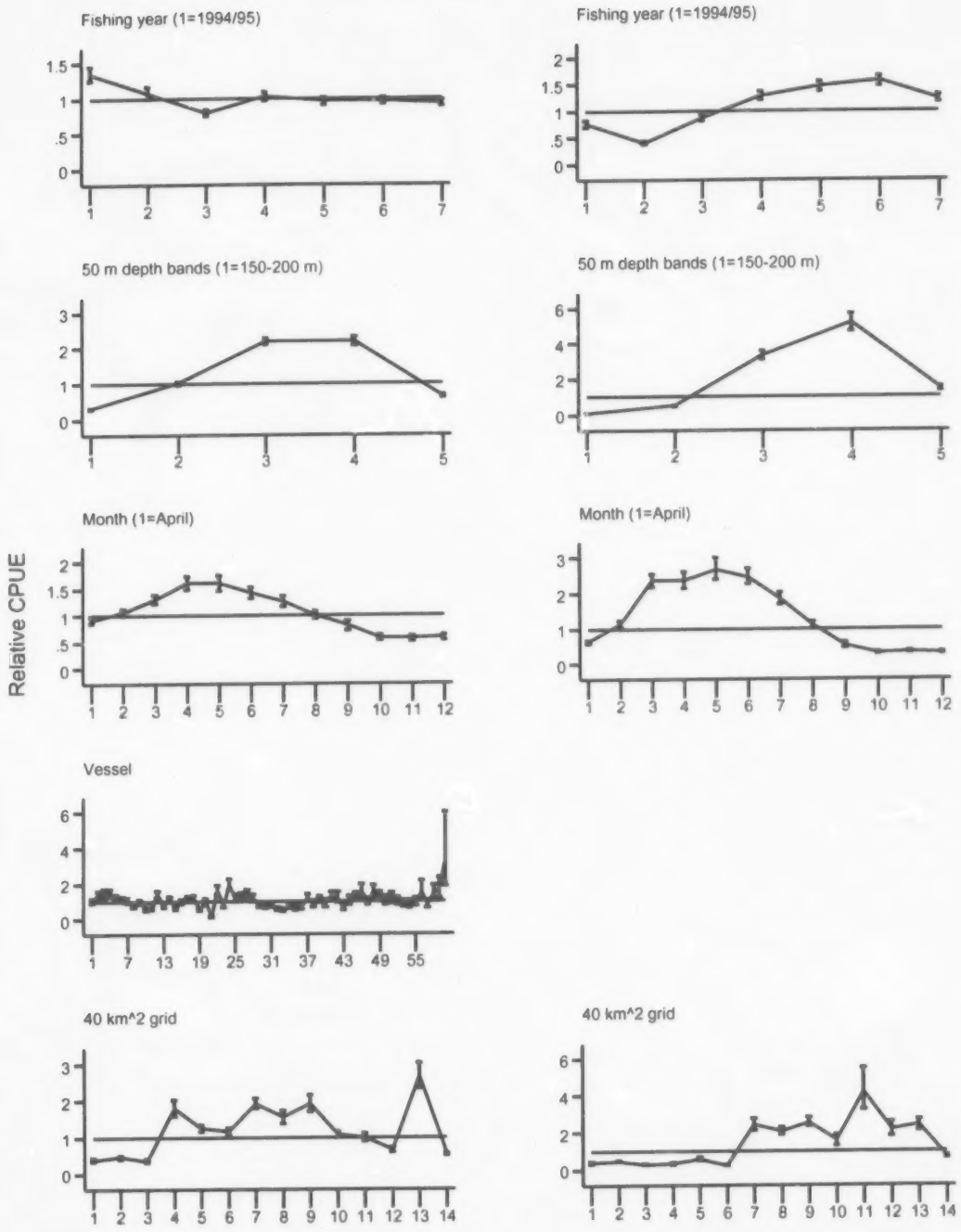

Figure 6.12. [Left column of plots]: Coefficients for the previous definition of the Total B.C. positive catch model. [Right column of plots]: Coefficients for the Total B.C. binomial model. All coefficients are plotted relative to their geometric mean, the error bars are 2*SE and the horizontal line is plotted at a coefficient value of 1.0.

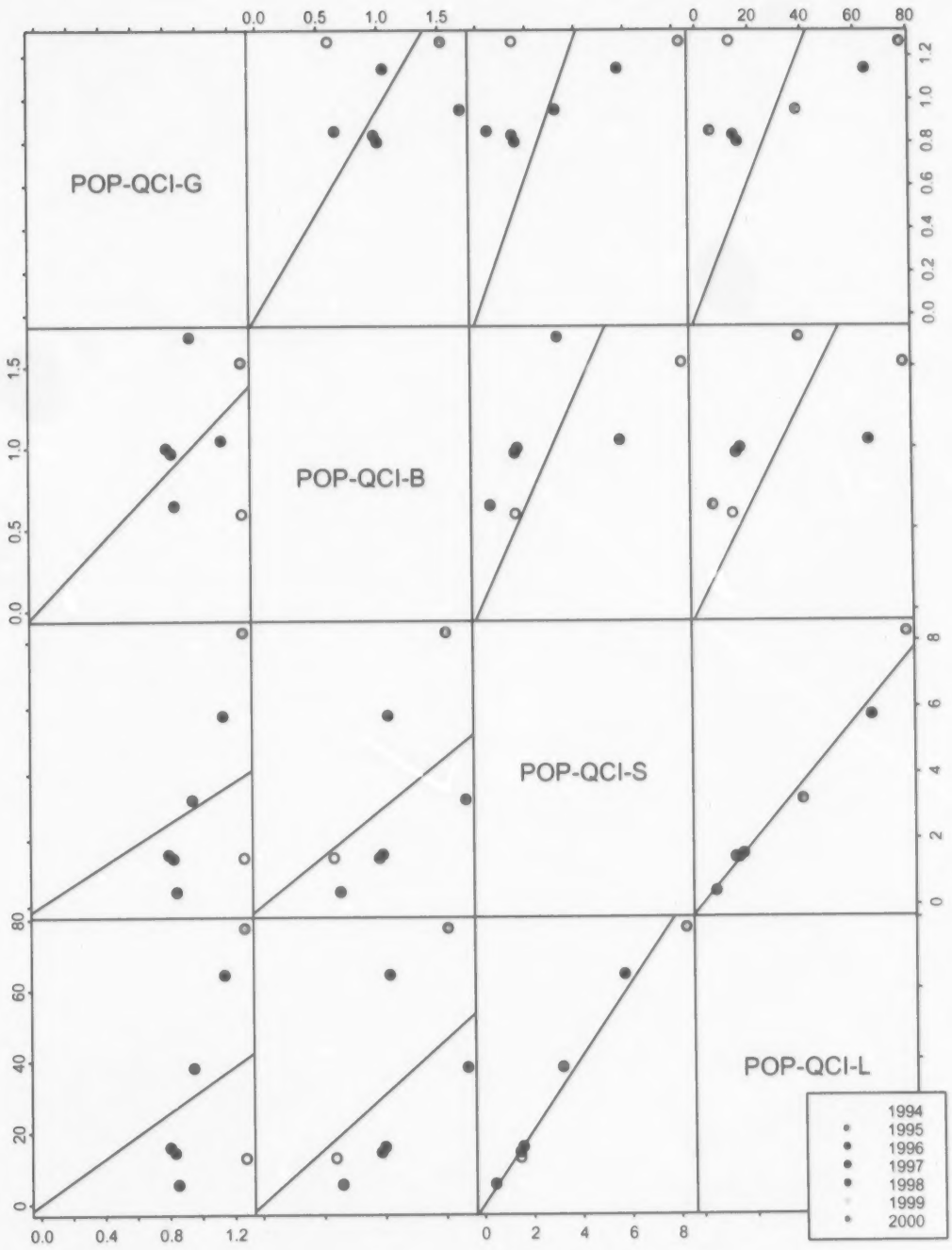

Figure 7.1. Pairs plot comparing various biomass indices in POP-QCI. Indices: G = positive catch model, B = binomial model, S = swept-area model using small area A^*, L = swept-area model using large area A. Annual estimates are colour-coded as per the legend in lower right panel. Line runs through (0,0) and the centroid.

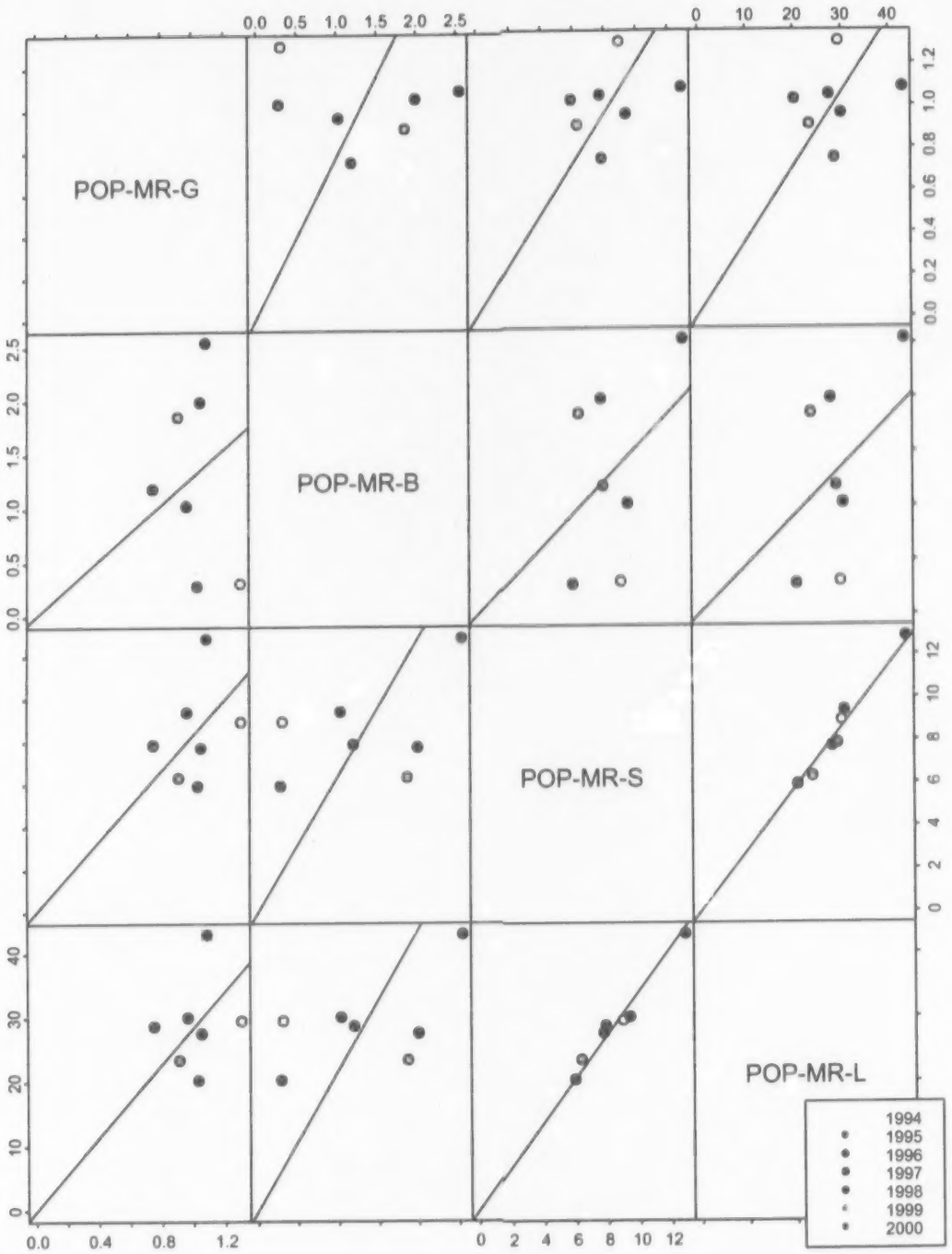

Figure 7.2. Pairs plot comparing various biomass indices in POP-MR. Indices: G = positive catch model, B = binomial model, S = swept-area model using small area A^*, L = swept-area model using large area A. Annual estimates are colour-coded as per the legend in lower right panel. Line runs through (0,0) and the centroid.

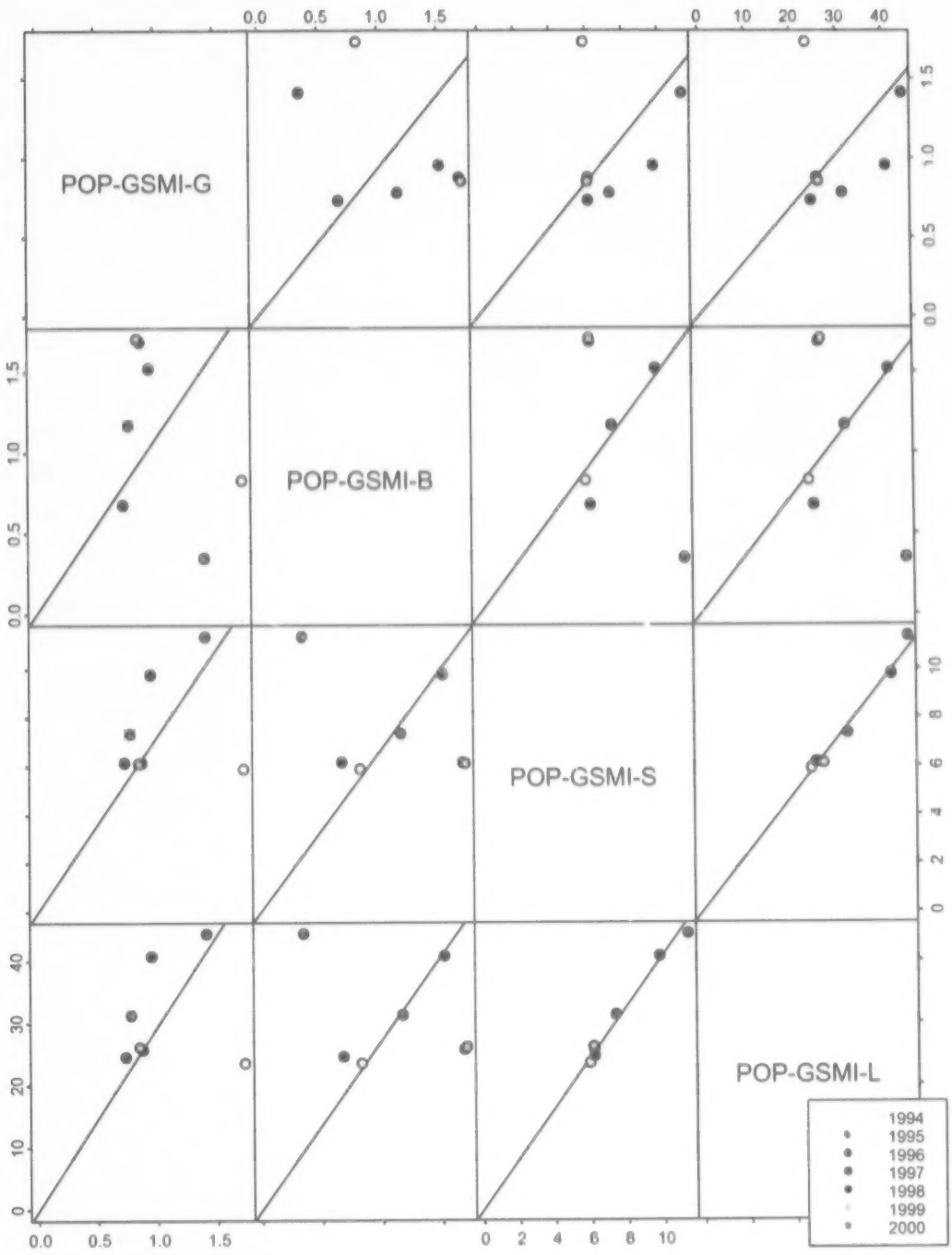

Figure 7.3. Pairs plot comparing various biomass indices in POP-GSMI. Indices: G = positive catch model, B = binomial model, S = swept-area model using small area A^*, L = swept-area model using large area A. Annual estimates are colour-coded as per the legend in lower right panel. Line runs through (0,0) and the centroid.

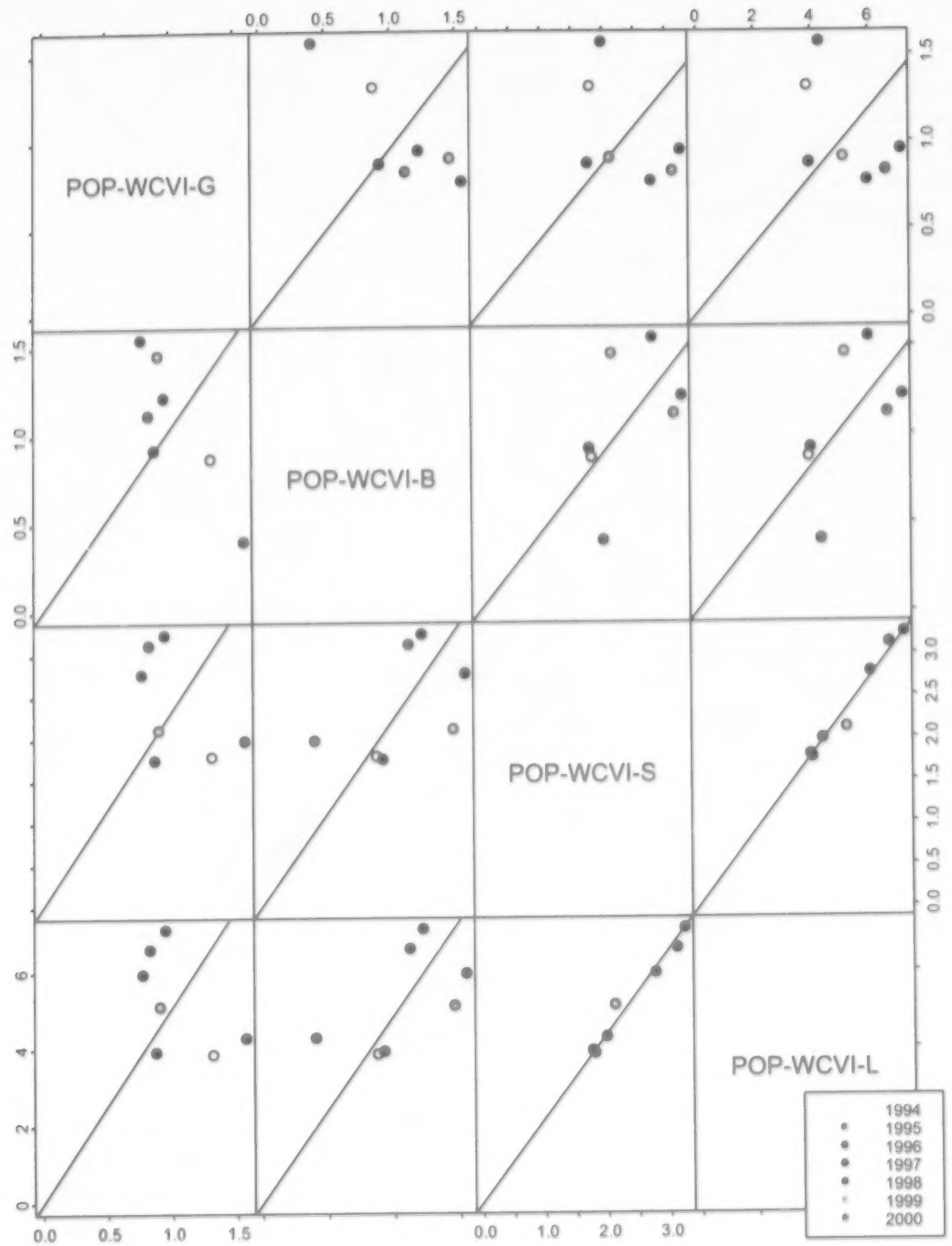

Figure 7.4. Pairs plot comparing various biomass indices in POP-WCVI. Indices: G = positive catch model, B = binomial model, S = swept-area model using small area A^*, L = swept-area model using large area A. Annual estimates are colour-coded as per the legend in lower right panel. Line runs through (0,0) and the centroid.